UNIVERSITI
TEKNOLOGI
PETRONAS

Aerodynamics Optimization of the Universiti Teknologi PETRONAS 'PERODUA Eco-Challenge 2011' Car

By

MUHAMMAD SHAFIQ BIN ROSLAN
10860

Dissertation submitted in partial fulfillment of
The requirements for the
Bachelor of Engineering (Hons)
(Mechanical Engineering)

Sept 2011

Universiti Teknologi Petronas
Bandar Seri Iskandar
31750 Tronoh
Perak Darul Ridzuan

SUPERVISOR'S DECLARATION

I hereby declare that I have checked this project and in my opinion this project is satisfactory in terms of scope and quality for the award of the degree of

Bachelor of Mechanical Engineering

Signature: .....

Name of Supervisor: Ir. Dr. Masri bin Baharom

Position: Head of Mechanical Engineering Department

Date: 16th January 2012

STUDENT'S DECLARATION

I hereby declare that the work in this report is my own except for quotations and summaries which have been duly acknowledged. The report has not been accepted for any degree and is not concurrently submitted for award of other degree.

Signature: .....

Name: Muhammad Shafiq Bin Roslan

ID Number: ME 10860

Date: 16th January 2012

ABTRACT

This is the construction and report on the experimentation of a shape-optimization method applied to aerodynamic design of a car. The scopes of study areas are in research, designing and analysis in computational fluid dynamics tool. The significance of this research would be important to evaluate the condition of the final model that posses the best drag coefficient. This research starts by searching for any other relevant journal or article published by other researches and from there, the design would be review and useful information will be summarize and taken as an information to this research. From the data available from the model, the drag coefficient will be calculated manually and also by using software. CATIA v5, GAMBIT v2.2.30 and FLUENT v6.3.26 software are then used to design analyze the air flow behavior. The result from the computational fluid dynamics software will be compare with the result from wind tunnel experiment.

ACKNOWLEDGEMENTS

I am grateful and would like to express my sincere gratitude to my supervisor, Ir. Dr. Masri bin Baharom for his brilliant ideas, invaluable guidance, continuous encouragement and constant support in making this research possible. He has always impressed me with his outstanding professional conduct, his strong conviction for science, and his belief that a Bachelor program is only a start of a life-long learning experience.

I am grateful for his progressive vision about my work progressing, his tolerance of my naive mistakes, and his commitment to my future career. I also would like to express special thanks again to my supervisor for his suggestions and co-operation throughout the study. I also sincerely thanks for the time spent proofreading and correcting my many mistakes. My sincere thanks go to all lecturers, technologies and technicians of the Mechanical Engineering Department, Universiti Teknologi PETRONAS who helped me in many ways and made my stay in this university pleasant and unforgettable. Many special thanks go to my fellow friends for their excellent cooperation, inspirations and supports during this study.

I acknowledge my sincere indebtedness and gratitude to my parents for their love, dream and sacrifice throughout my life. I cannot find the appropriate words that could properly describe my appreciation for their devotion, support and faith in my ability to attain my goals. Special thanks should be given to my fellow members. I would like to acknowledge their comments and suggestions, which was crucial for the successful completion of this study.

TABLE OF CONTENTS

CHAPTER 1- INTRODUCTION

1.1 Project Background.....1

1.2 Problem Statement.....2

1.3 Objective.....2

1.4 Scope of Works.....3

CHAPTER 2-LITERATURE REVIEW

2.1 Analysis of Literature.....4

CHAPTER 3- METHODOLOGY

3.1 Design Standard 14

3.2 Identify and Understanding Equipments.....14

3.3 Predicting the aerodynamics characteristics.....15

3.4 Software Features 16

3.5 Numerical Simulation.....17

3.6 Identify Design and Safety Specifications 18

3.7 Develop the Model.....19

3.8 Reducing Drag Calculation.....21

3.9 Validate the Model.....23

3.10 Flow Chart.....25

3.11 Project Planning.....26

CHAPTER 4– RESULTS AND DISSCUSION

4.1 Data Gathering and Analysis..... 28

4.1.1 X-Tron I Model.....28

4.2 Result and Discussion.....38

4.2.1 Software.....38

4.2.2 Design.....42

4.3 Result.....43

4.4 Model Prototype and Wind Tunnel Experiment.....45

CHAPTER 5-CONCLUSION AND RECOMMENDATION.....48

REFERENCES.....49

APPENDIXES.....50

LIST OF FIGURES

Figure 2.1: History of vehicle dynamic in passenger car

Figure 2.2: Induced vortices

Figure 2.3: Highly streamlined body

Figure 2.4: The aerodynamic optimization of different types of car roof

Figure 2.5: The Perodua research and development team car

Figure 3.1: The model test simulation in a rectangular box

Figure 3.2: The boundary conditions consist of inlet, outlet and four walls

Figure 3.3: X-Tron

Figure 3.4: X-Tron II

Figure 3.5: Stream I

Figure 3.6: Stream II

Figure 3.7: Alpha

Figure 3.8: Beta

Figure 3.9: Omega

Figure 3.10: Probe I

Figure 3.11: Probe II

Figure 3.12: Probe III

Figure 3.13: Open circuit wind tunnel

Figure 3.14: Flow chart of research processes

Figure 4.1: The grid shape of the Perodua Eco-Challenge 2011 Model after meshed in Gambit

Figure 4.2: Contours of dynamic pressure

Figure 4.3: Contours of total pressure

Figure 4.4: Path lines sequence flow color by velocity magnitude (m/s)

Figure 4.5: The path lines colored by velocity magnitude isometric view (m/s)

Figure 4.6: The path lines colored by velocity magnitude back view (m/s)

Figure 4.7: The path lines colored by velocity magnitude top view (m/s)

Figure 4.8: Path lines sequence flow color by total pressure magnitude (Pascal)

Figure 4.9: The path lines colored by total pressure magnitude (Pascal)

Figure 4.10: The path lines colored by total pressure magnitude (Pascal)

Figure 4.11: The path lines colored by total pressure magnitude (Pascal)

Figure 4.12: Optimized total pressure distribution contour for X-Tron I (left) to optimal X-Tron II (right)

Figure 4.13: The Probe I model being place in wind tunnel

Figure 4.14: The Probe I model in simulation

LIST OF TABLES

Table 3.1: Gantt chart for FYP 1

Table 3.2: Gantt chart for FYP 2

Table 4.1: Drag coefficients for all models at 40m/s

Table 4.2: The drag force data from wind tunnel experiment (refer appendix)

LIST OF GRAPHS

Graph 2.1: Forces and moment with the change of α

Graph 2.2: Forces and moment with the change of R

Graph 4.1: The residual shows the energy residual converges after 50 iterations while continuity residuals converge after 300 iterations

LIST OF CHARTS

Chart 2.1: Consumer reports city cycle

Chart 2.2: Consumer reports highway cycle

Chart 4.1: Histogram of dynamic pressure

Chart 4.2: Histogram of total pressure

LIST OF SYMBOLS

ρ Density

p Pressure

v Vehicle speed

D Drag force

L Lift force

DA Aerodynamic Drag force

CD Drag Coefficient

A Frontal Area

LA Aerodynamic lift force

CL Lift coefficient

Pr Air temperature

Re Reynold number

LIST OF ABBREVIATIONS

CAD Computer-aided design

CFD Computational fluid dynamic

3-D Three dimensional

Re Reynolds number

Ma Mach number

Fr Froude number

ε/l Relative roughness

BLM Base-line model

CHAPTER 1

INTRODUCTION

1.1 Project Background

This is the construction and report on the experimentation of a shape-optimization method applied to aerodynamic design of a car. The scopes of study areas are in research, designing and analysis in computational fluid dynamics tool.

Automotive aerodynamics is the study of the aerodynamics of road vehicles. The main concerns of automotive aerodynamics are reducing drag (though drag by wide wheels is dominating most cars), reducing wind noise, minimizing noise emission, and preventing undesired lift forces and other causes of aerodynamic instability at high speeds [1]

Computational fluid dynamics (CFD) is playing a key role in helping to understand the flow along the car body surface. The CFD has been used in the last two decades to devise solutions and gain insight of the air flow around the car body and CFD, together with experimental validation, has been able to improve the design of cars. [2]

In this work, a simulation of energy and viscous model (Spalart-Allmaras) to evaluate the model behavior in the airflow is to be performed using Computational fluid dynamics (CFD). The Spalart–Allmaras model is a one equation model for the turbulent viscosity. It solves a transport equation for a viscosity-like variable. The Spalart-Allmaras model will be used along with the vorticity-based production to simulate the turbulent air flow behavior.

1.2 Problem Statement

The Universiti Teknologi PETRONAS 'PERODUA Eco-Challenge 2011' car has several design problems in term of aerodynamic efficiency. The open cockpit design of the car body can cause high resistance force by wind. The cross section area (characteristic area) is also wide and broad. The tires width area also can be reduce. After all, the improvement model in term of drag coefficient has to be investigated such as the characteristic shape and ratio between of the length, height and width of the car. At the end, the best model will be selected and the wind tunnel experiment needs to be done to validate the result from the software.

1.3 Objective

The main objective of this project is to choose the best model that has lowest drag coefficient with engineering design value. The focus of this project is to analyst the maximum dynamic pressure and drag force of the model in order to calculate the drag coefficient. The development and basic understanding of this final year project topic entitled 'Aerodynamics Optimization of the Universiti Teknologi PETRONAS 'Perodua Eco-Challenge 2011'car should be revise by the incoming participants to design the new car model thus improve the achievement.

The objectives of this project are:

i. To simulate the flow behavior based on the model design:
    a) Shape/design
    b) Speed
ii. To acquire the result and select the best car design for the next competition.
iii. To study the correlation between velocity, pressure and type of flow (laminar and turbulence).

1.4 Scope of Works

Scope of works is a division of works needs to be performed in order to maintain good management, protocol and safety. It is typically broken out into specific tasks with deadlines. This research starts by searching for any other relevant journal or article published by other researchers and from there, the design would be review and useful information will be summarize and taken as an information to this research.

The model will be design in Catia. The design will be analyzed in computational fluid dynamics package, Gambit and Fluent software to study the air flow behavior. The data available from the model will be used to calculate the drag coefficient based the output data gain from the software. The result from the computational fluid dynamics software will be compare with the result from wind tunnel experiment. The method consist of using the computer aided engineering software and also experimental in wind tunnel.

The Computational Fluid Dynamics (CFD) will be used to save time and money. The CFD can reveal the behavior of air flow, where there is going in an internal space, and how fast. The capital cost of a large well-equipped wind-tunnel is high, but unlike computers, wind tunnels never become obsolete. Wind-tunnel models are expensive, and setting them up may take a few days, but once this has been done, a great deal of high-quality data can be collected in a very short time; one run may take only a matter of seconds. The geometry can be rapidly modified and the model retested immediately.

Thus, for low-accuracy quick results, CFD modeling is relatively cheap, but if large quantities of more reliable data are required, then the wind-tunnel is currently the better source. Wind-tunnels and computers both have relative advantages, and even in the longer term they are likely to be used as complementary rather than alternative tools. [3] The significance of this research would be important to evaluate the condition of the final model that posses the best drag coefficient.

CHAPTER 2

LITERATURE REVIEW

2.1 Analysis of literature

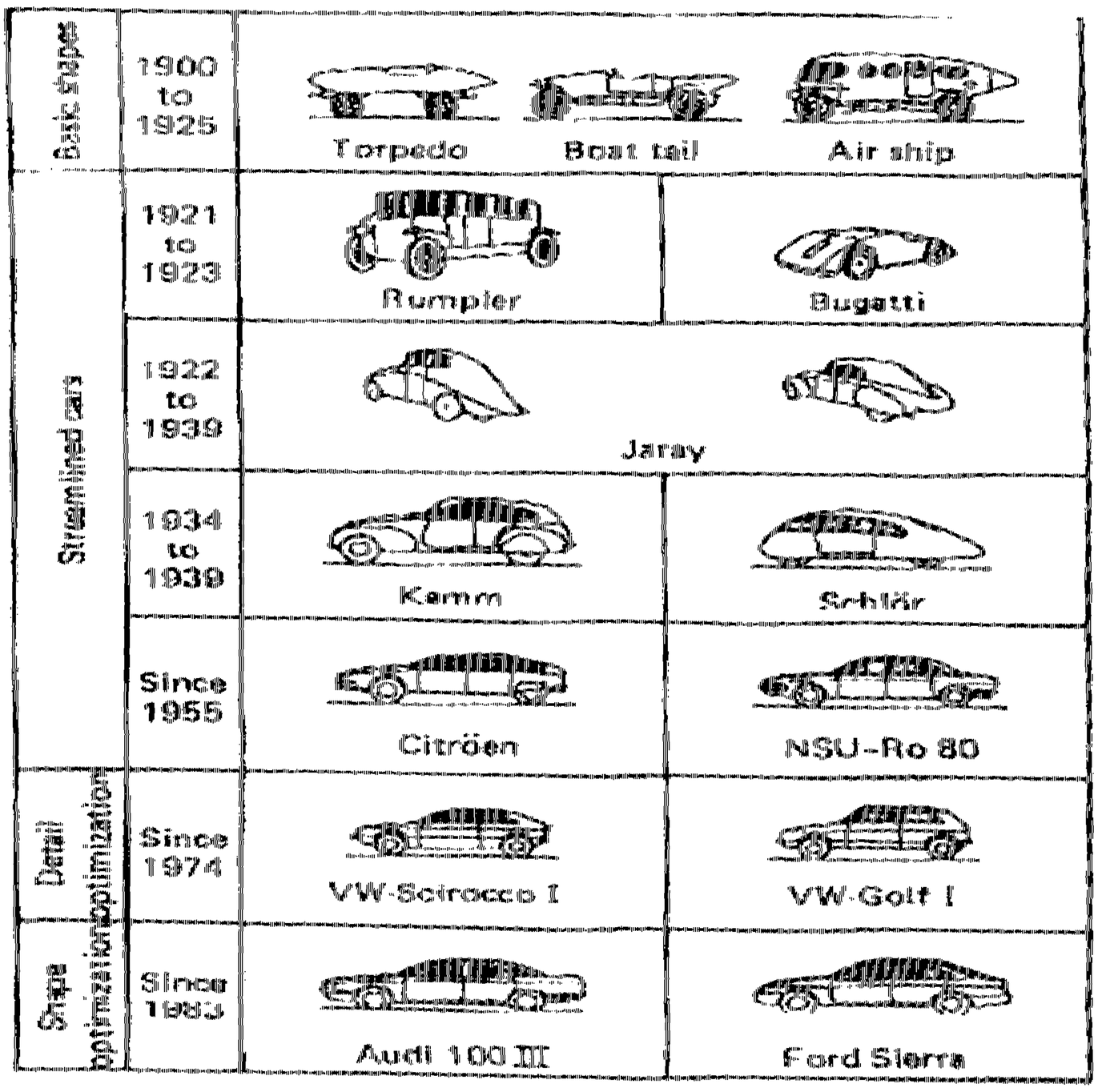

Figure 2.1: History of vehicle dynamic in passenger car

The first automobile to be developed according to the aerodynamic principles was a torpedo-shaped vehicle that had given it a low drag coefficient but the exposed driver and out of body wheels must have certainly disturbed its good flow properties. However they ignored the fact that the body was close to the ground in comparison to aircrafts and underwater ships flown in a medium that encloses the body. [4] In a car like this, the ground along with the free-standing wheels and the exposed undercarriage causes disturbed flow. As the years pass the studies on aerodynamic effects on cars increase and the designs are being developed to accommodate for the increasing needs and for economic reasons. The wheels developed to be designed within the body, lowering as a

result the aerodynamic drag and produce a more gentle flow. The tail was for many years long and oddly shaped to maintain attached the streamline. The automobiles became developed even more with smooth bodies, integrated fenders and headlamps enclosed in the body. The designers had achieved a shape of a car that differed from the traditional horse drawn carriages. They had certainly succeeded in building cars with low drag coefficient. [5] Form drag results from the generation of vortices as the projectile displaces the air around it. Figure 2.2 illustrates this:

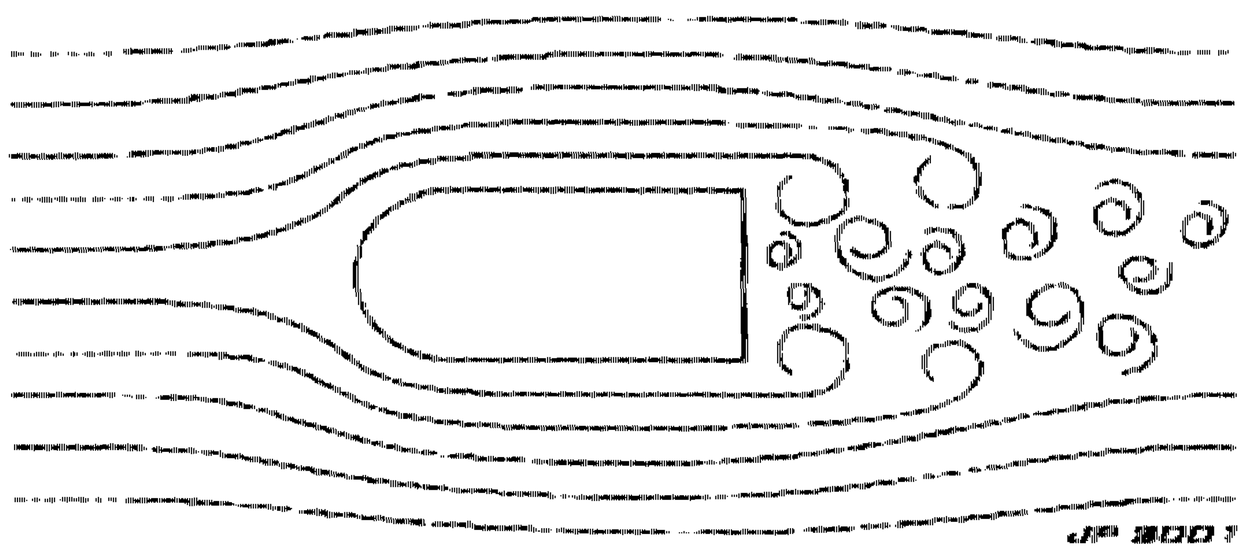

Figure 2.2: Induced vortices

The formation of vortices requires energy and this comes from the kinetic energy of the projectile. The vortices eventually dissipate behind the projectile and the streamlines return to a smooth profile. In order to minimize the form drag the projectile needs to be 'streamlined'. [6] The best general streamlined shape is shown in figure 2.3:

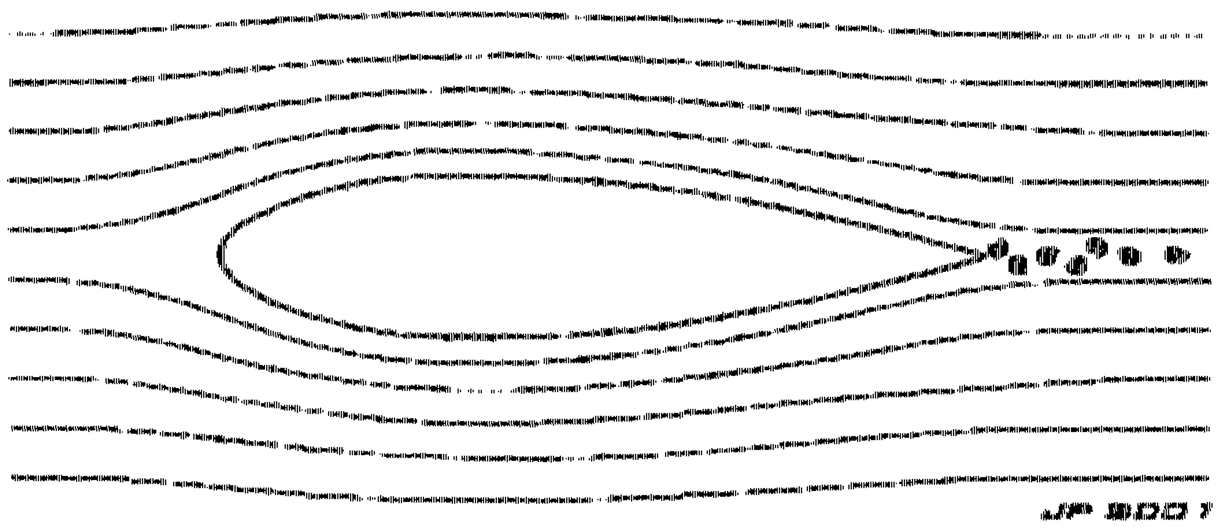

Figure 2.3: Highly streamlined body

For a streamlined body to achieve a low drag coefficient the boundary layer around the body must remain attached to the surface of the body for as long as possible, causing

the wake to be narrow. A high form drag results in a broad wake. The boundary layer will transition from laminar to turbulent providing the Reynolds number of the flow around the body is high enough. Larger velocities, larger objects, and lower viscosities contribute to larger Reynolds numbers. It is important that the pressure should be allowed to rise as much as possible towards the rear of the vehicles, and this means that the cross-sectional area should preferably reduce gradually towards the rear, as the teardrop shape. The gradual reduction is necessary in order to prevent separation due to strongly adverse pressure gradients. Below is the aerodynamic optimization based on effects of car roof angle α and effects of Arc-roof radius R. [7]

The experiment for effects of car roof angle, α. The roof angle α of P64 Box Car is 162°. The approach is by getting different situations through changing triangular angle α of car roof, and analyzing them by analog computing. Graph 2.1 demonstrates the figures of air side force, air lift force and air overturning moment, when the angle are 124°, 136°, 140°, 144°, 148°, 152°, 156°, 168° and 180°.

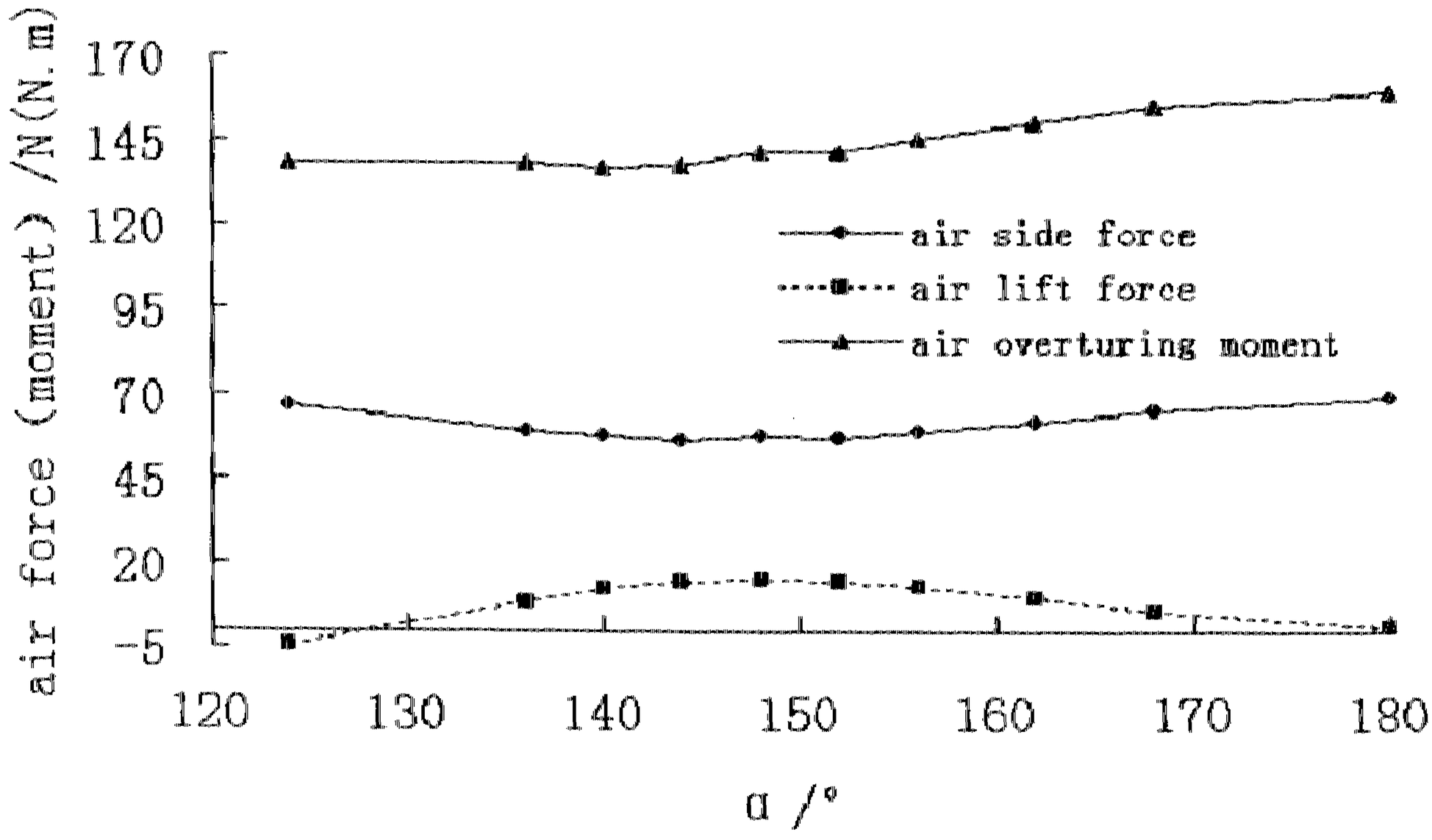

Graph 2.1: Forces and moment with the change of α

Specifically, with the increase of angle in the given range, the curve of air side force falls from 124° to 144° and increases from 144° to 180°. When the angle is 144°, air side force reaches the bottom(56.2N), which is 9.1% lower than that of P64 Box Car. With the raise of angle in the given range, the line of air lift force increases from 124° to 148° and falls from 148° to 180°. When the angle is 124°, air lift force is negative. Besides, when the angle is 180°, air lift force is the minimum (1.3N), which is 86.5% lower than that of P64 Box Car. When the angle changes from 124° to 144°, the curve of air overturning moment almost maintains the same, since the drop of air side force is equal to the increase of air lift force. After that, there is a gradual rise from 144° to 180°, in which region the air overturning moment is obviously determined by air side force. When the angle is from 140° to 144°, air overturning moment reaches the bottom(137N·m), which is 9.0% lower than that of P64 Box Car. From the statistics shown in the graph, we can see that the aerodynamic performance of car with angle in range of 124° to 162° is better than that of P64 Box Car. While, when the angle changes from 162°to 180°, the aerodynamic performance is worse than that of P64 Box Car. In addition, the aerodynamic performance of cars with triangular roof varying from 140 ° to 144° are best, since they have the lowest air overturning moment of car, which is the main factor to aerodynamic performance.

Then, the effects of arc-roof radius, R. The roof is changed from triangle to arc-shape. The approach is by changing radius of car roof R to get different situations, and analyzing them by analog computing. Graph 2.2 reflects the curves of air side force, air lift force and air overturning moment, when the radius are 1410mm,1600mm, 1800mm, 1900mm, 2000mm, 2100mm, 2200mm and 3000mm.

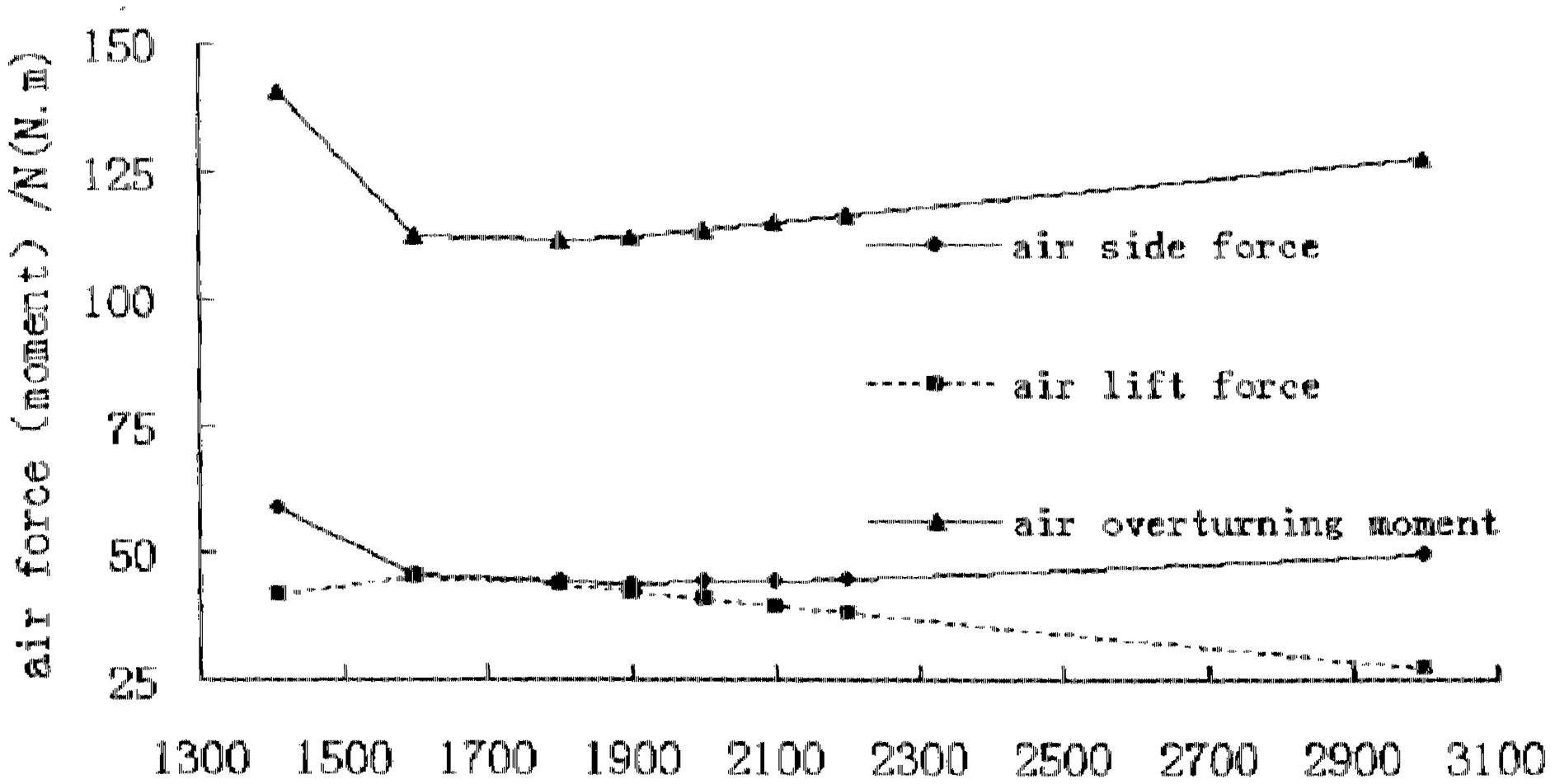

Graph 2.2: Forces and moment with the change of R

When the radius changes from 1410mm to 3000mm, the aerodynamic performance is better than that of P64 Box Car. With the increase of radius from 1410mm, this means the roof changes from drum to flat regularly, the trends of air force and air overturning moment are similar, but the trend of air lift force is opposite. Beside, the line of air overturning moment is always above the curve of air side force, which is in turn above the curve of air lift force. So air overturning moment is the synthesis of air side force and air lift force and its trend is mainly depend on the trend of air side force. Specifically, with the increase of radius, the figure of air side force descends from 1410mm to 1600mm and rises gradually from 1600mm to 3000mm. When the radius is 1900mm, air side force reaches its minimum (44.0N), which is 28.9% lower than that of P64 Box Car. With the raise of radius, the number of air lifts force climbs from 1410mm to 1600mm and drops from 1600mm to 3000mm. When the radius is 1600mm, air lift force is the maximum (45.3N), which is 373.4% higher than that of P64 Box Car.

The curve of air overturning moment the same as line of air side force in the whole range. When the radius is 1800mm, air overturning moment reaches its bottom (111.4N·m), which is 26.0% lower than that of P64 Box Car. The graph above reveals that the aerodynamic performance of car with arc-roof varying from 1600mm to 1800mm is best, which has the lowest air overturning moment. In conclusion, the optimization results as according to the aerodynamic performance of different cars simulated numerically above, the angle α from 140° to 144° is a better choice for triangular roof. Besides, the radius R from 1600 to 1800mm is a better choice for arc-shaped roof, which has the best aerodynamic performance in the study. While, when the car roof is flat, it has the worst aerodynamic performance. Contours of velocity above and under the car with flat roof are almost symmetrical. The maximum velocity is in the areas of the convergence at the body and the roof and the convergence at the body and the car bottom. The pressure around car roof and the pressure around car bottom are also symmetrical in this condition, so its air lift force is small. But because of its sharp angular appearance, there are a vortex above the roof and two big vortexes in the field of leeward side of car body under cross wind, in which region pressure is so small that air side force is strong and positive pressure is distributed near the top of windward side of car body. As a result air overturning moment is great.

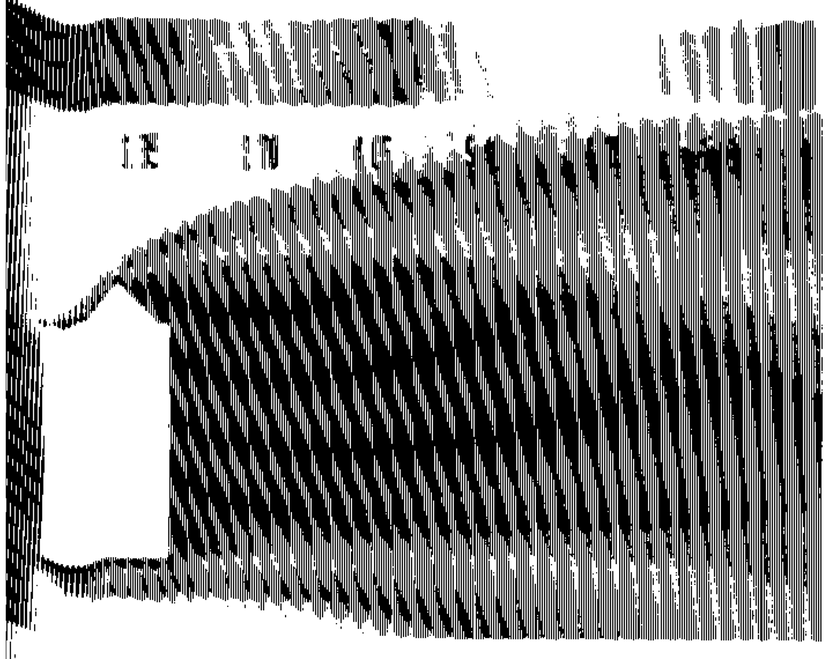

Velocity contours of car with α 140°

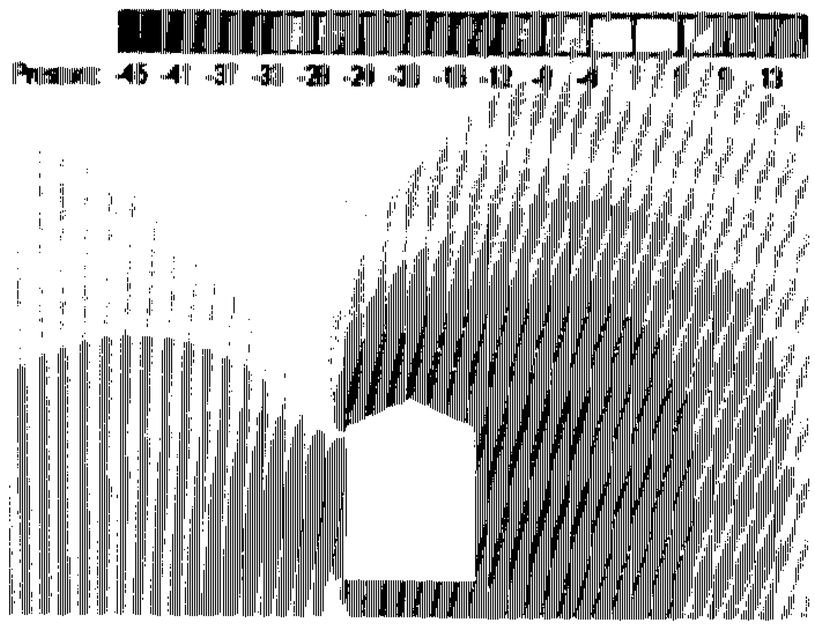

Pressure contours of car with α 140°

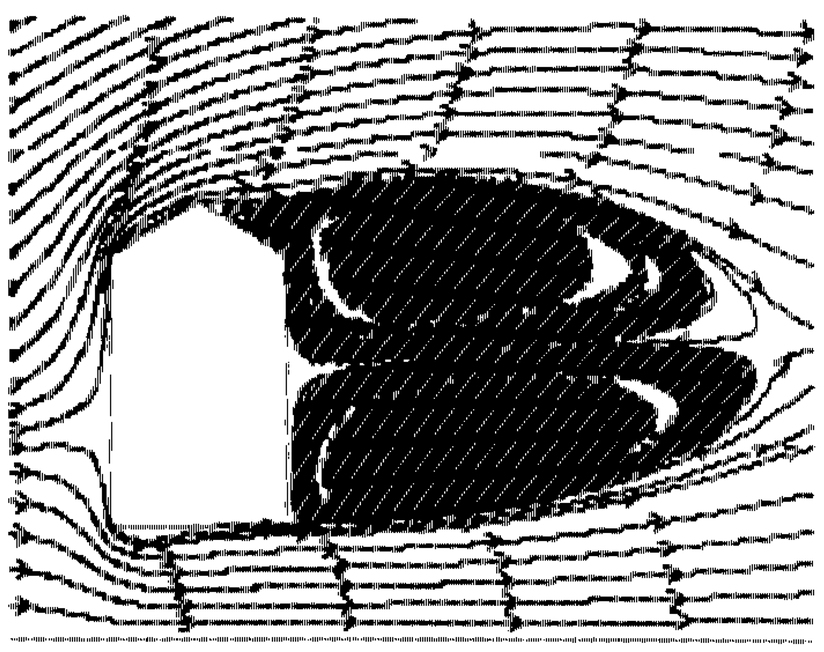

Streamlines of car with α 140°

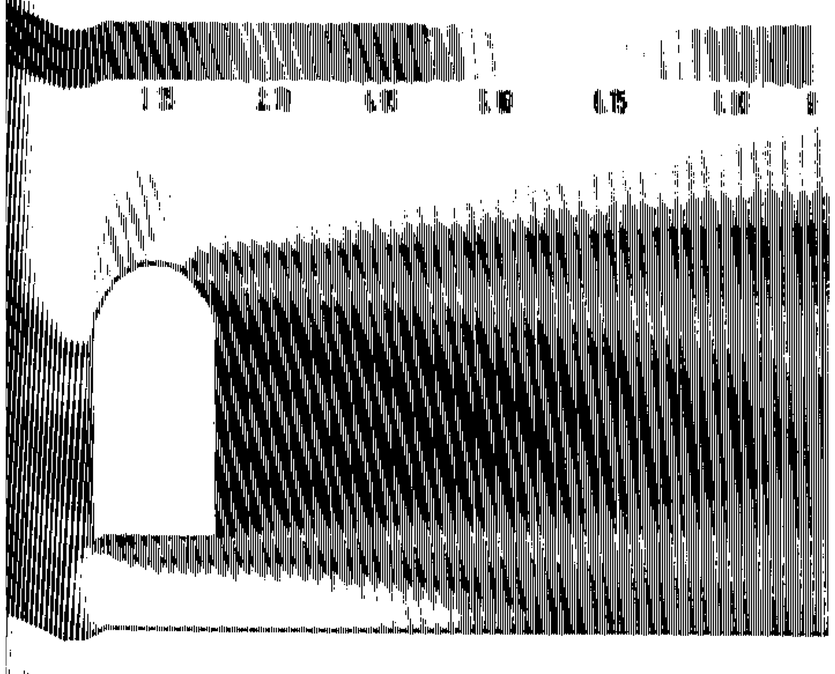

Velocity contours of car with R 1800mm

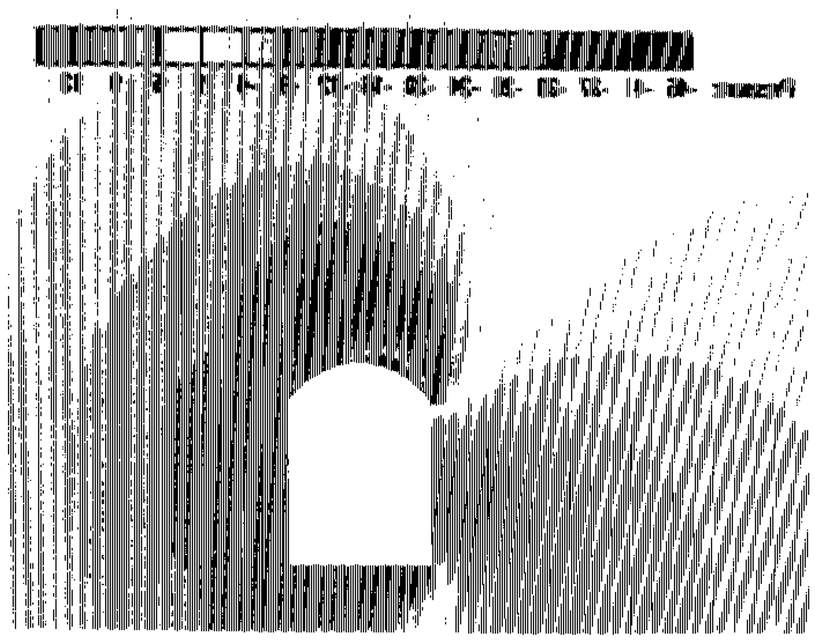

Pressure contours of car with R 1800mm

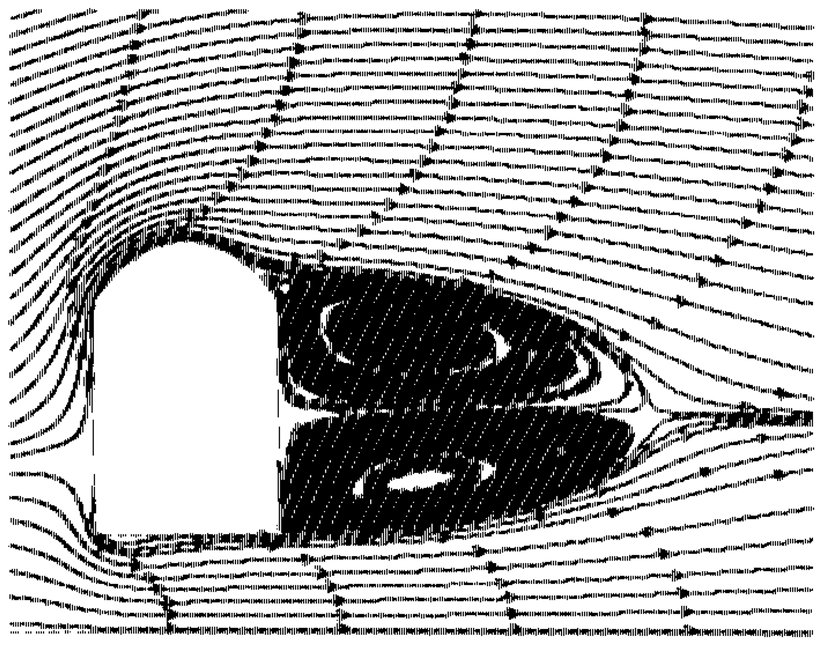

Streamlines of car with R 1800mm

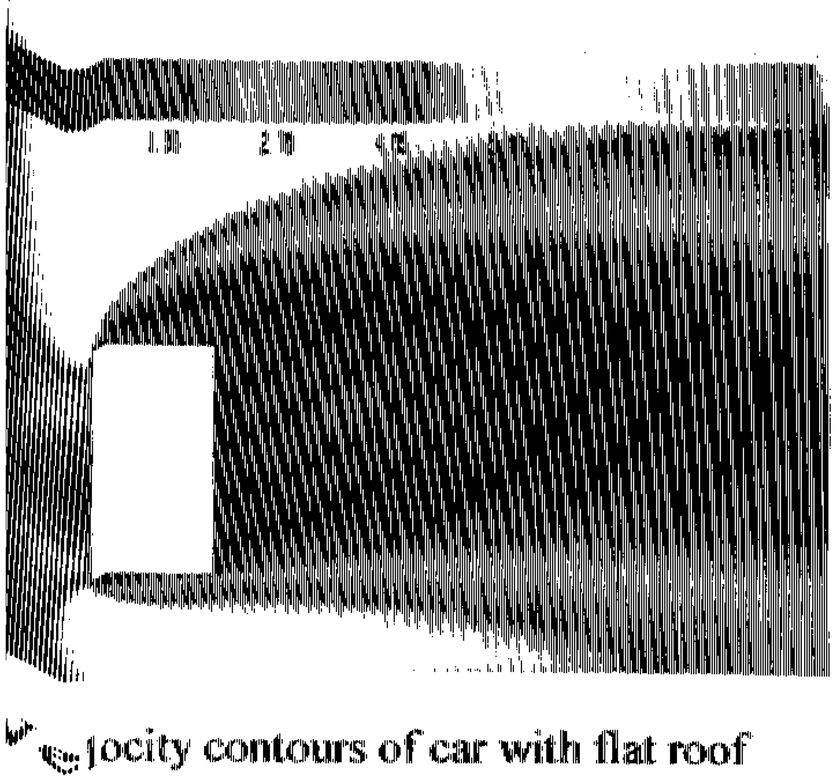

Velocity contours of car with flat roof

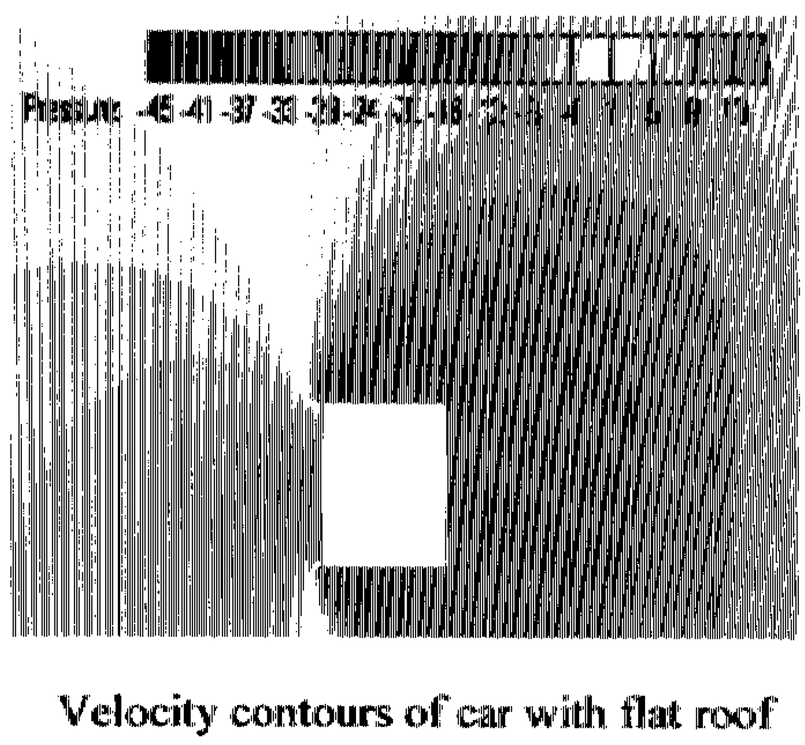

Velocity contours of car with flat roof

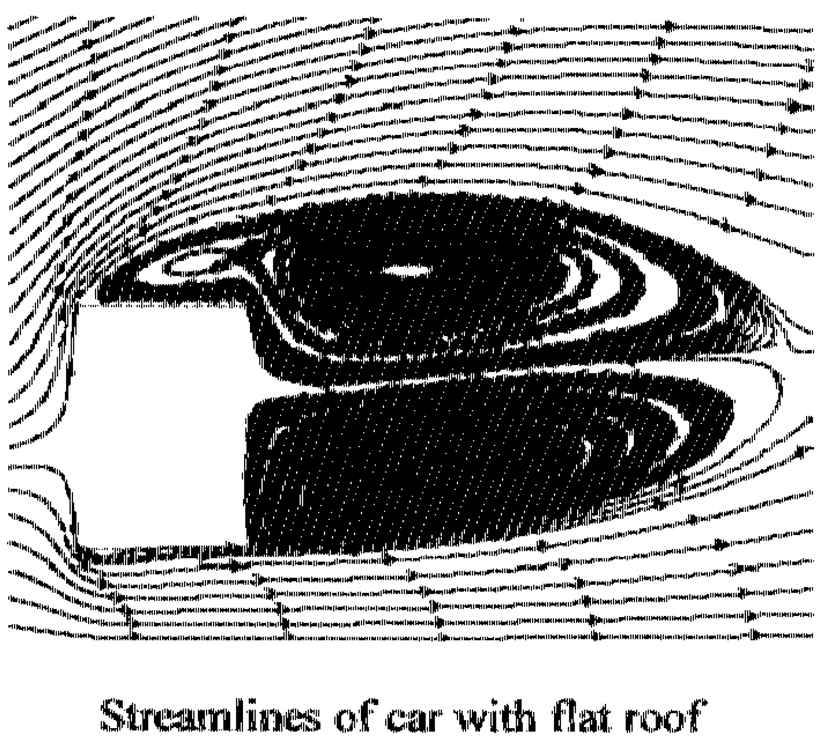

Streamlines of car with flat roof

Figure 2.4: The aerodynamic optimization of different types of car roof

1) Air overturning moment of car can be obtained by resultant force consisted of air side force and air lift force acting on the train, which is based on the top of track. Besides,with the increase of angle α (or radius R), the trend of air overturning moment is mainly depend on the trend of air side force.

2) With the increment of roof angle α from 124° to 180°, aerodynamic performance of car becomes better before becoming worse. With other dimension remain unchanged; the angle (α) from 140° to 144° is a better choice for triangular roof.

3) With the increment of roof radius (R) from 1410mm to infinite, aerodynamic performance of car becomes better before being worse. With other dimension remain unchanged, the radius R from 1600mm to 1800mm is a better choice for arc-shaped roof car, and in that condition the aerodynamic performance is best in the study.

Perodua also sent their team to compete with the student through their research and development team. Even though they not manage to become the champion, but their design is excellent to reduce aerodynamics drag. It due to the speed of around 60km/h, thus aerodynamics drag is not significant. This is the aerodynamics features to reduce the drag coefficient.

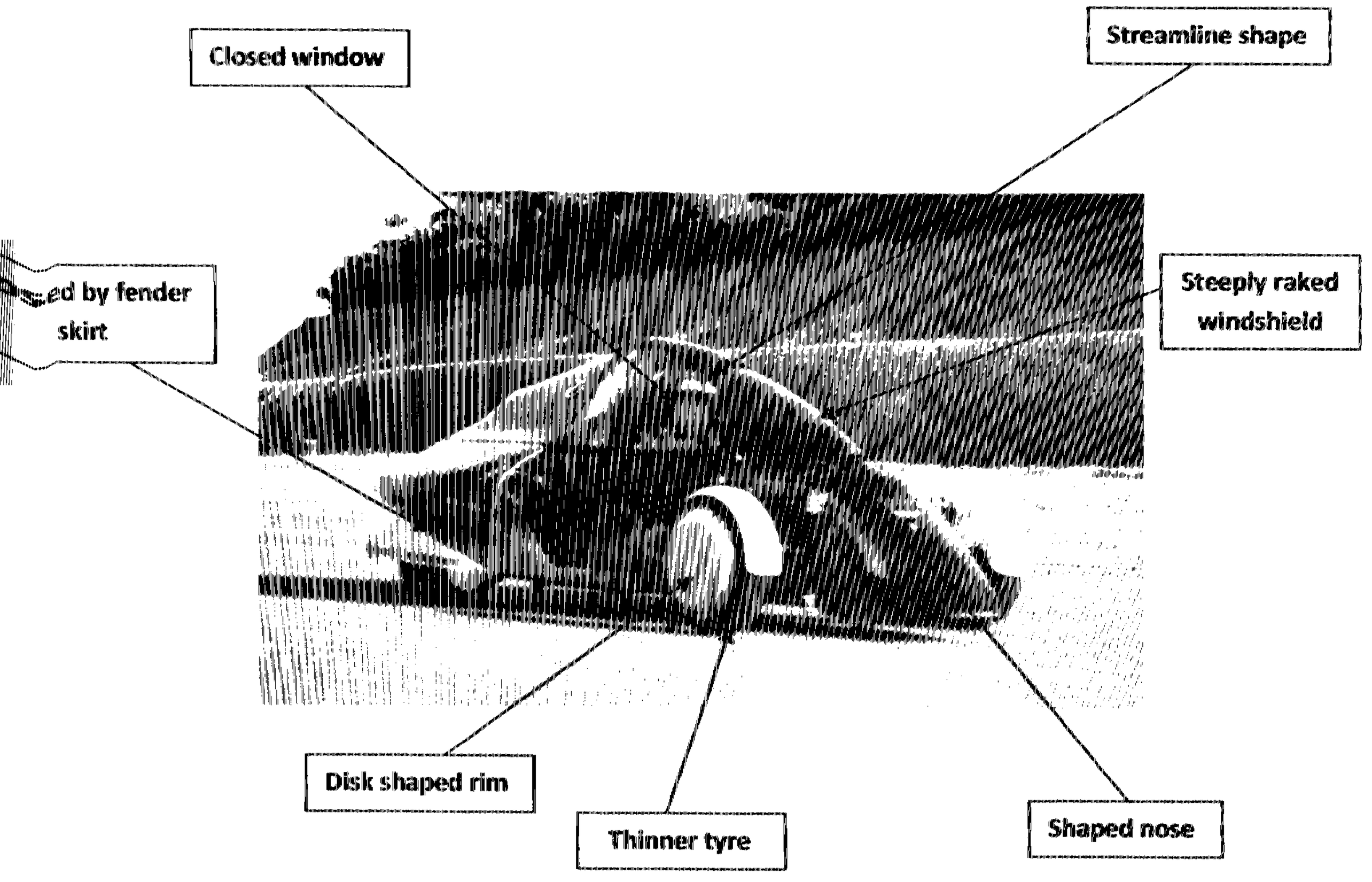

Figure 2.5: The Perodua research and development team car

The Perodua research and development team car will become the benchmark for designing the new models as it set a good example of aerodynamics features.

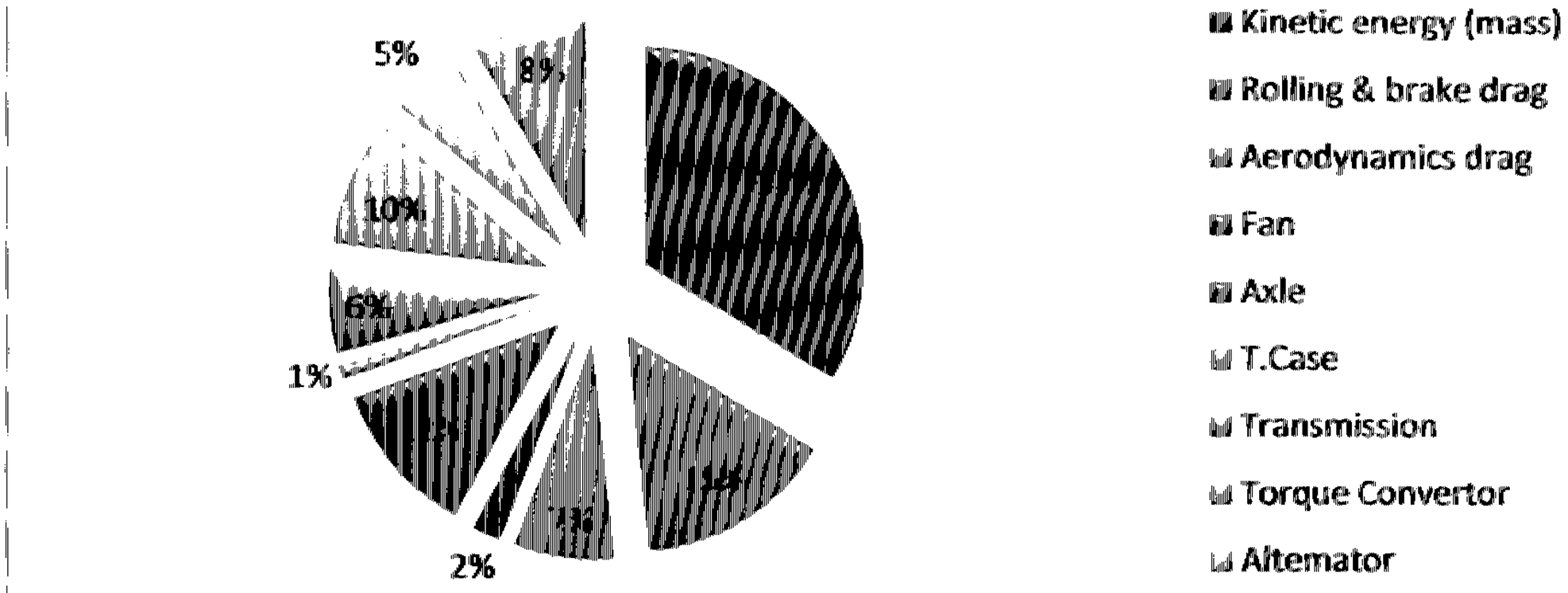

Chart 2.1: Consumer reports city cycle

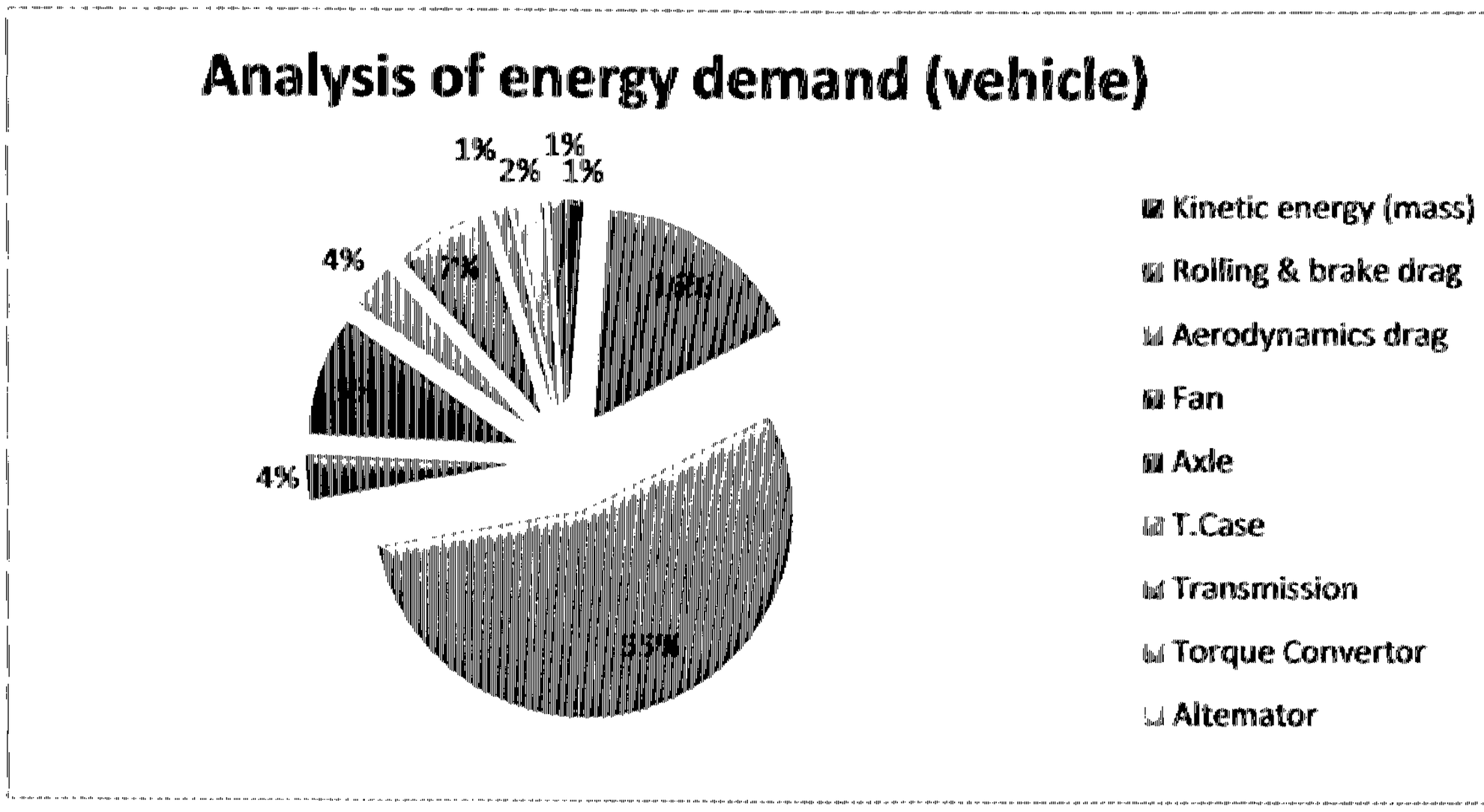

Chart 2.2: Consumer reports highway cycle

From the pie chart 2.1, at low speed the aerodynamics drag only consumes about 7% of vehicle energy while at high speed is about 55%. The kinetic energy has major influence in the low speed. Hence, the car should be built as lightest as possible while also complying with the regulation. **[8]**

CHAPTER 3

METHODOLOGY

3.1 Design Standard

The design standard of the car body must comply with the Perodua Eco Challenge 2011 Rules and Regulations. The vehicle seated vehicle, design and build by students. The engine and transmission will be provided by Perodua. The vehicle basic configuration are such as single seated vehicle, space frame body structure design with body shell design (driver and engine must be covered), use steel or aluminum as the body structure and 3 to 4-tire configuration. The body may be made from carbon fiber due to its light properties. The dimensions of the car are specified in term of overall height, overall width, wheelbase and ground clearance. The overall height except for the structural roll bar, no part for the car can be higher than 900mm from the ground. The overall width of the car including complete wheels shall not exceed 1500mm when the steered wheels are in straight position. The wheelbase of the car should have minimum of 1500mm. The ground clearance of the car should have minimum of 100mm from the ground with the driver onboard. The outer shell parts should have aerodynamic and aesthetic purposes.

3.2 Identify and Understanding Equipments

Wind tunnels allow test conditions to be well controlled and in independent of external atmospheric conditions. Next is the installation of the model in the test section. The process of matching a particular vehicle model with a wind tunnel raises three important issues:

- Model size and the blockage it creates in the test section
- Simulation of the moving road
- Mounting of model and its rotating wheels in the test section[9]

The primary benefits from using a computational tool would be the quick response and the ability to improve and modify a vehicle's shape before it was built. Computational methods also can be serving as a diagnostic tool for improving existing vehicles. When compared to other form of experiment, computations have the advantage that generated results can be used over and over to study new parts of the problem. Most computational methods for the solution of airflow over vehicle shapes are based on solving the equations of continuity and momentum. Current codes differ primarily in the way they model the forces acting on the fluid particle (pressure and viscous forces), and in the numerical representation of the governing partial-differential equations.

The simplest model (complexity of geometry) will not have the effect of viscosity. Therefore, drag due to friction and flow separation cannot be predicted. These codes, sometimes called potential problem solvers, are now well developed and can be compute the flow over a complex body usually in a few minutes. Consequently, from the availability point of view, they are suitable for race car application. The computed results over a prototype race car depicting streamlines and surface pressure contours (shown by different colors). The most complex computer codes include the effect of viscosity, and in principle should be capable of predicting surface friction and flow separation. **[10]**

3.3 Predicting the aerodynamics characteristics

There are two different overall configuration of wind-tunnel exists, which are the closed-return type of tunnel and the open-return type of tunnel. In UTP, there is one open-return form of tunnel. The open-return arrangement consists essentially of a tube open at both ends. Air is drawn from and returned to the surroundings.

The advantage of the open-return type is that it is relatively compact, and normally makes use of the open space of the enclosing buildings as its return circuit. Another advantage is that because the air is drawn from and discharged into a relatively large space, it does not tend to heat up.

The open-return tunnel does however have two disadvantages; firstly, as the air is simply exhausted to the surroundings, its kinetic energy is wasted, and therefore more

power is required than for a closed-return configuration. A second problem is that since the air starts from rest in the surrounding room at atmospheric pressure, the pressure in the working section must be lower than atmospheric (following the Bernoulli relationship). The working section interior must therefore be well sealed from the surroundings.

Wind-tunnel testing would produce totally reliable results due to vast experience from aeronautical work. However, the precaution steps should be taken during the test. There are three primary source s of error in wind tunnel-testing:

1) Scale or Reynolds number effect
2) Errors due to the fact that the road moves relative to the car, whereas the floor of the tunnel is normally stationary.
3) Error due to blockage

Other important sources of error are

4) Failure to model fine detail accurately
5) Failure to model the effects of the through the cooling and ventilating systems.
6) Difficulties in measuring forces when the wheels are in contact with the road. [11]

3.4 Software Features

Recently, with the latest technology, some companies have take advantages by creating computer aided design software. The software is available to aid the engineers to do design with lesser time. In modeling a new body/shell for the car, the researcher needs to consider the design tool and material that should be used. The suitable design tools for this study such as:

i) Catia – Design
ii) Gambit and Fluent – Computational Fluid Dynamics

At the end of the day, because of all these standard requirements, the engineers have to redefine the input into the software with regard to the standard. Note that, to obey the

standards is very important because small mistakes will break down the whole system in operating big machinery.

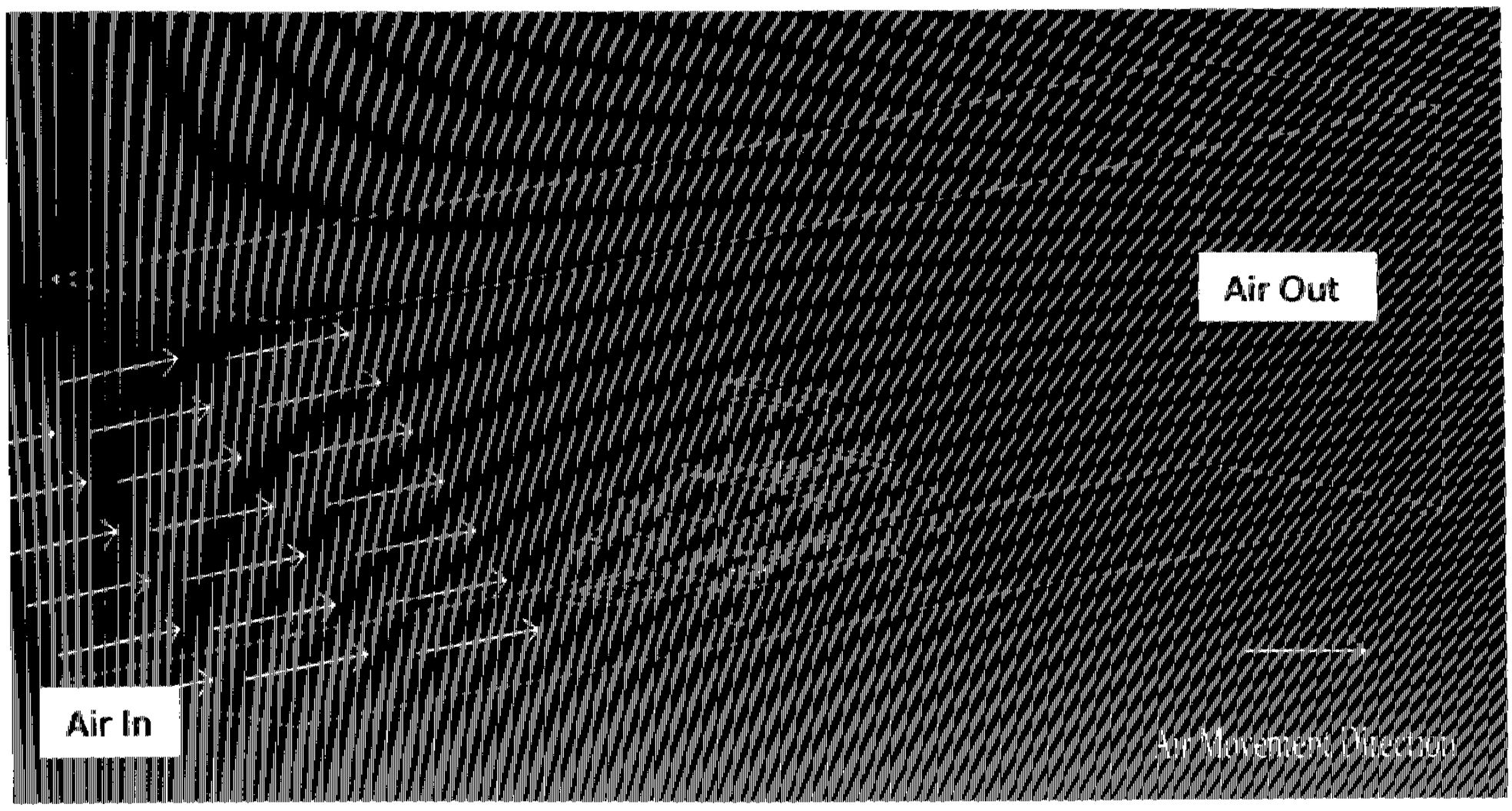

Figure 3.1: The model test simulation in a rectangular box

3.5 Numerical Simulation

The three-dimensional geometry model of the car is generated using a 3D modeling software package (Gambit, v2.2.60, Fluent Inc., Lebanon, NH, USA). The computational domains include the inlet, outlet, wall of air and the wall of car model. Then the geometry is meshed in 3D Tet/Hybid elements. An unstructured-mesh finite-volume-based commercial CFD package, Fluent (v6.2.16,Fluent) is used to solve the incompressible steady Naiver-Stokes equations.

The Navier–Stokes equations, named after Claude-Louis Navier and George Gabriel Stokes, describe the motion of fluid substances. These equations arise from applying Newton's second law to fluid motion, together with the assumption that the fluid stress is the sum of a diffusing viscous term (proportional to the gradient of velocity), plus a pressure term. The Navier–Stokes equations in their full and simplified forms help with the design of cars as the model used to model the air flow around a body. The incompressible continuity equation and Reynolds averaged the Naiver-Stokes equations are employed to simulate the steady turbulent flow through the car

body, and the Spalart-Allmaras single equation turbulence model is adopted to make the equations closed. [12]

The rectangular dimension is 11.6m (l) x 2.6m (h) x 3.0m (w).The analysis uses tetrahedral and hybrid elements with 1,928,963 numbers of elements. Thus, the interval size being used are 60 which are appropriate in order to prevent overload in number of element will be produced.

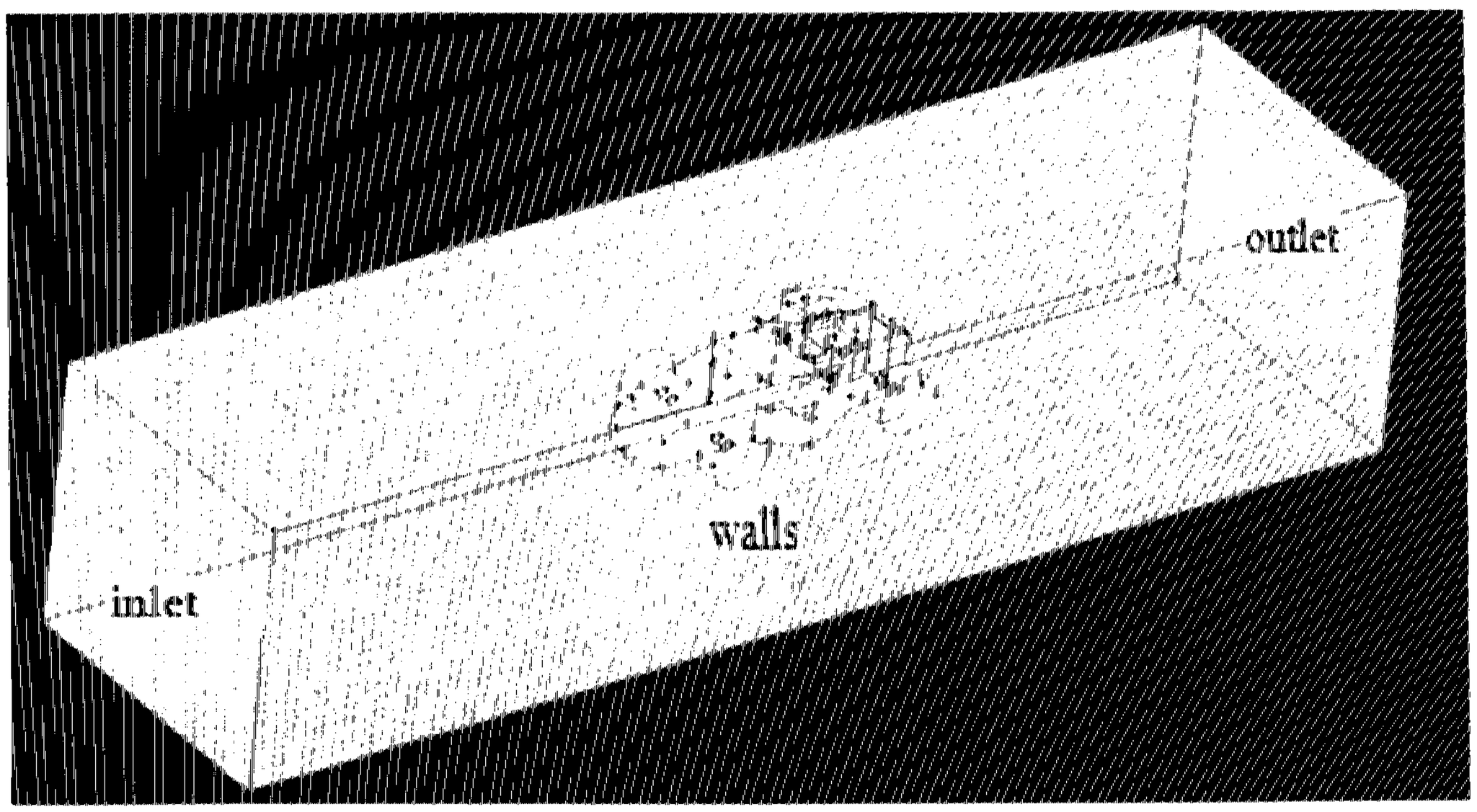

Figure 3.2: The boundary conditions consist of inlet, outlet and four walls.

The boundary names of the rectangular consist of wall, inlet velocity/vi and outlet velocity/vo. The continuum type is air/fluid. The inlet velocity will be set at 40 m/s which is about 144 km/h. For all the repetition experiment, the velocity magnitude will be 40 m/s.

3.6 Identify Design and Safety Specifications

The aerodynamics design should consider the aerodynamics of the complete vehicle, flow over wheel, sliding seals and skirts, underbody channels, fender skirt, disk shaped rim, sharp nose, steeply raked windshield, streamline shape, thinner tire, closed window, and also internal flow. Aerodynamic long tail improves fuel efficiency 15 percent.

3.7 Develop the Model

The (X-Tron I) datum should be analyzed in the software to get the drag coefficient as the early reference. Then, the new models will be developed in the software. The model that posses the lowest drag coefficient will be chosen as the prototype model. The prototype will be made in scale model to undergo a few series of test in the wind tunnel as it is more accurate. The wind tunnel result will be compared with the Computational Fluid Dynamics result to study its variance. The models are classified into four platforms which are X-Tron, Stream, Code and Probe. The models are:

X-Tron

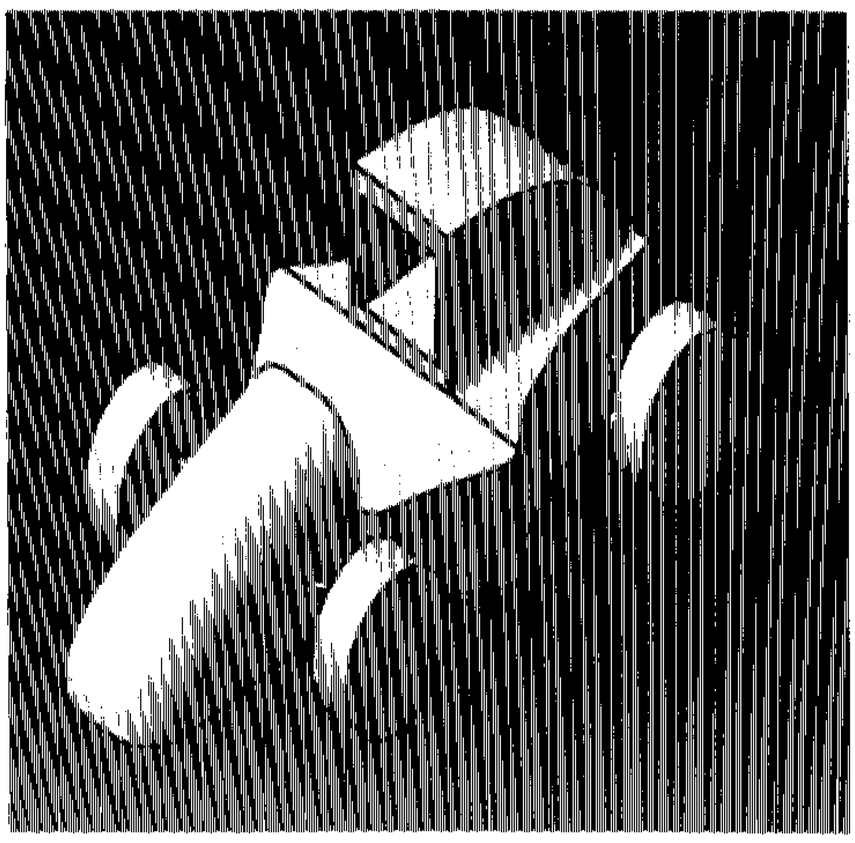

Figure 3.3: X-Tron

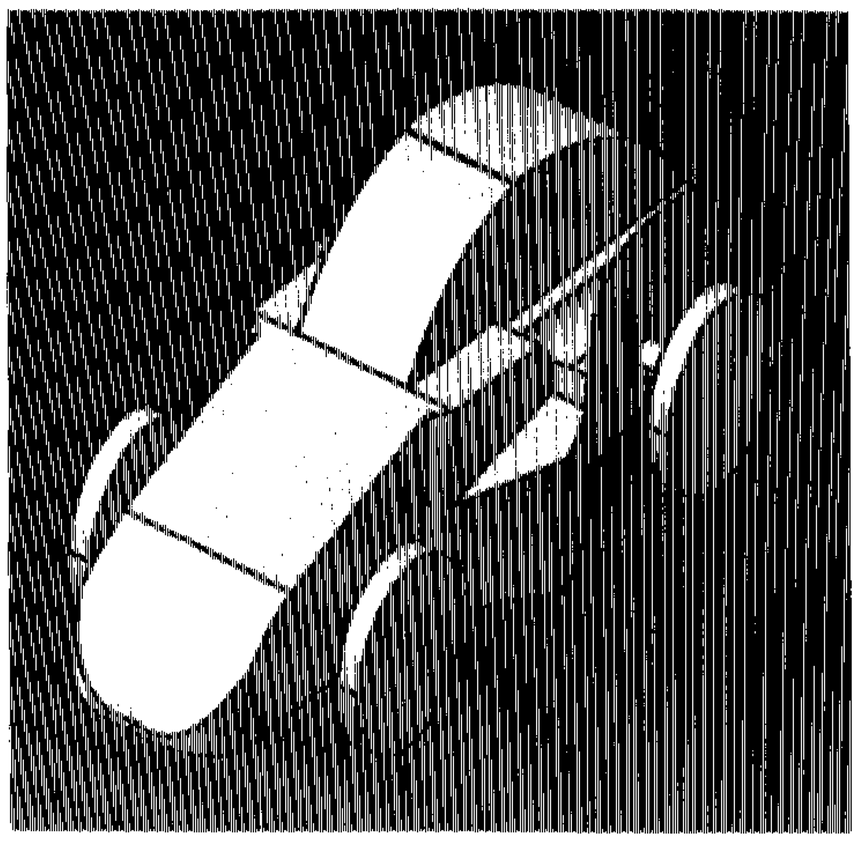

Figure 3.4: X-Tron II

Stream

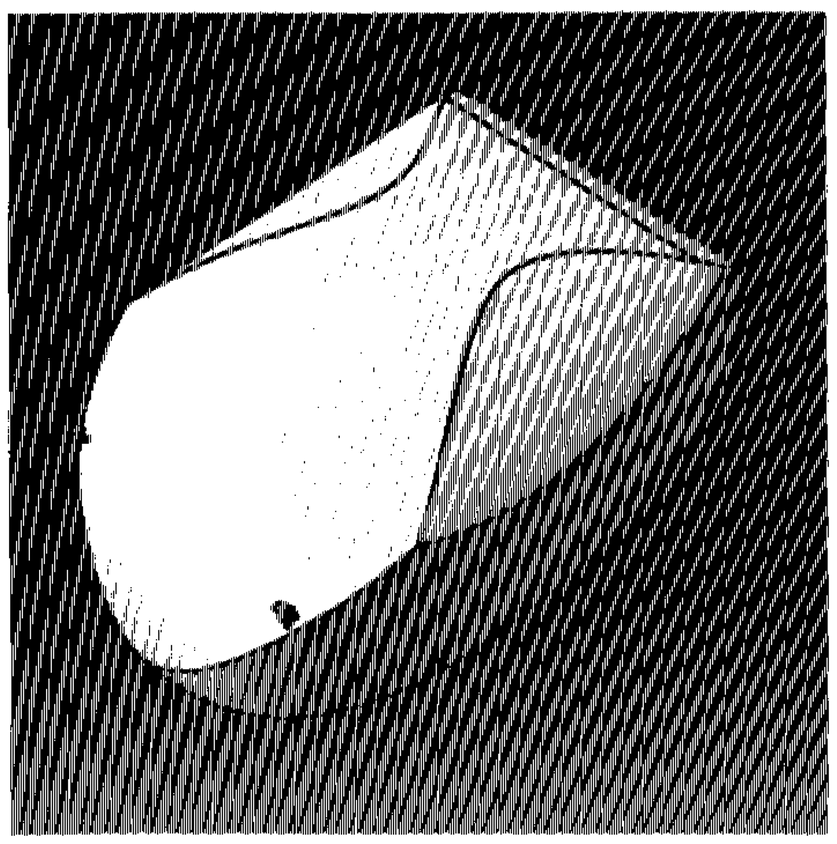

Figure 3.5: Stream I

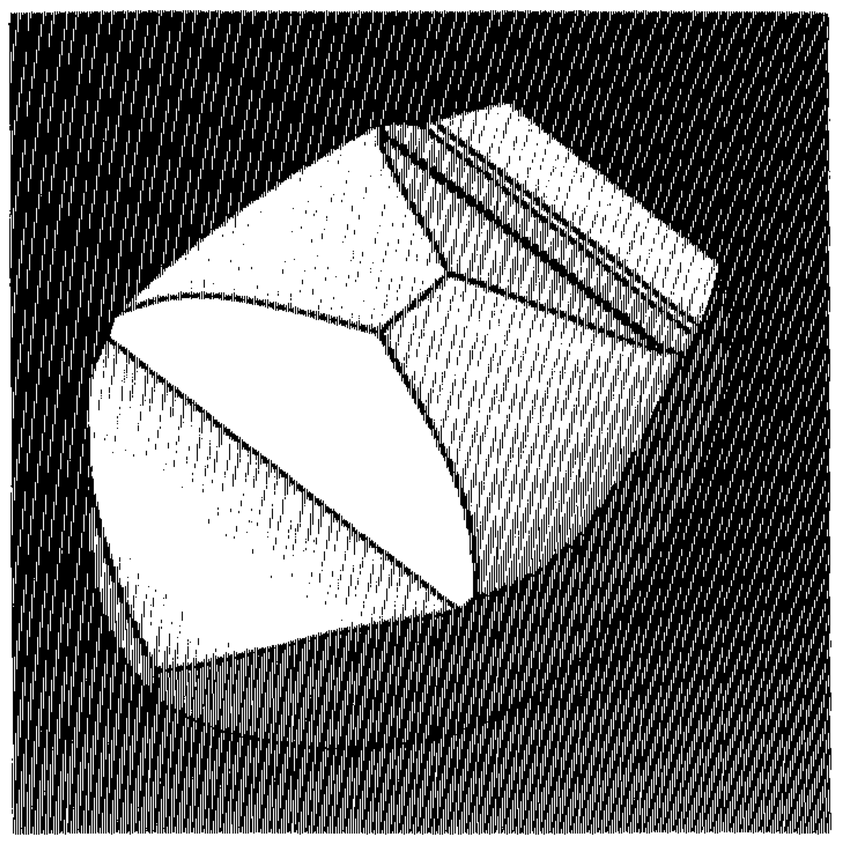

Figure 3.6: Stream II

Model Development Progress

Code

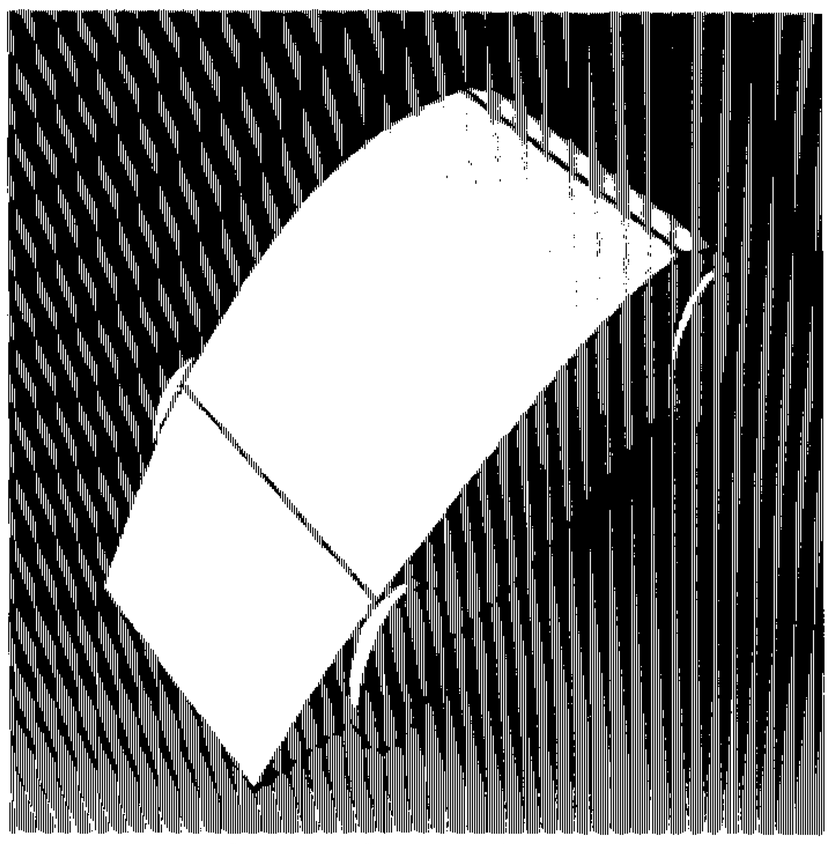

Figure 3.7: Alpha

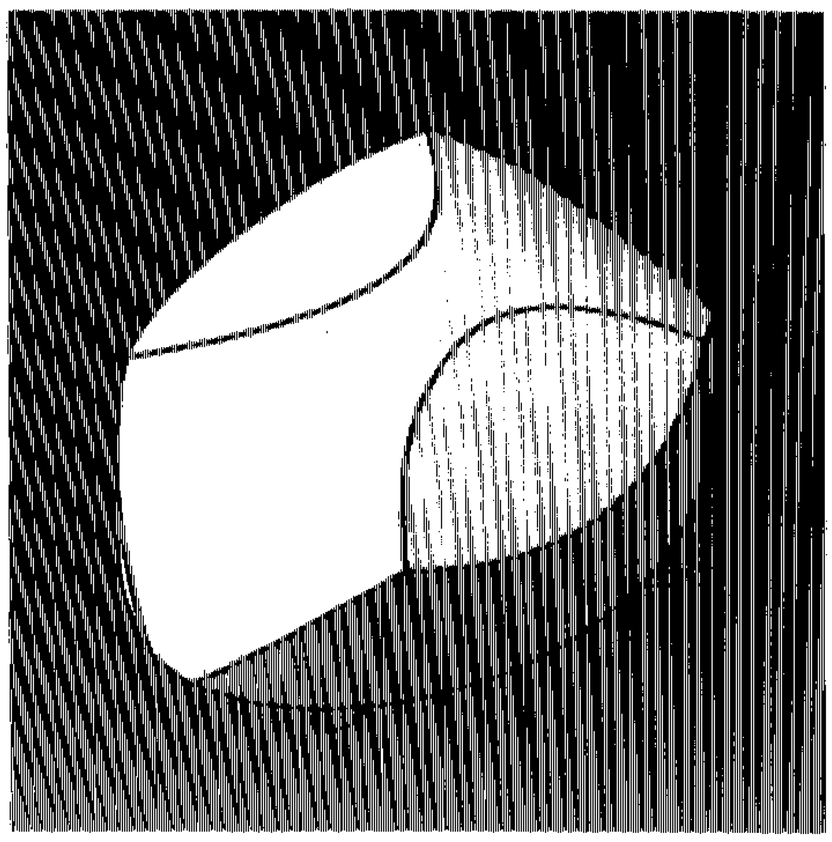

Figure 3.8: Beta

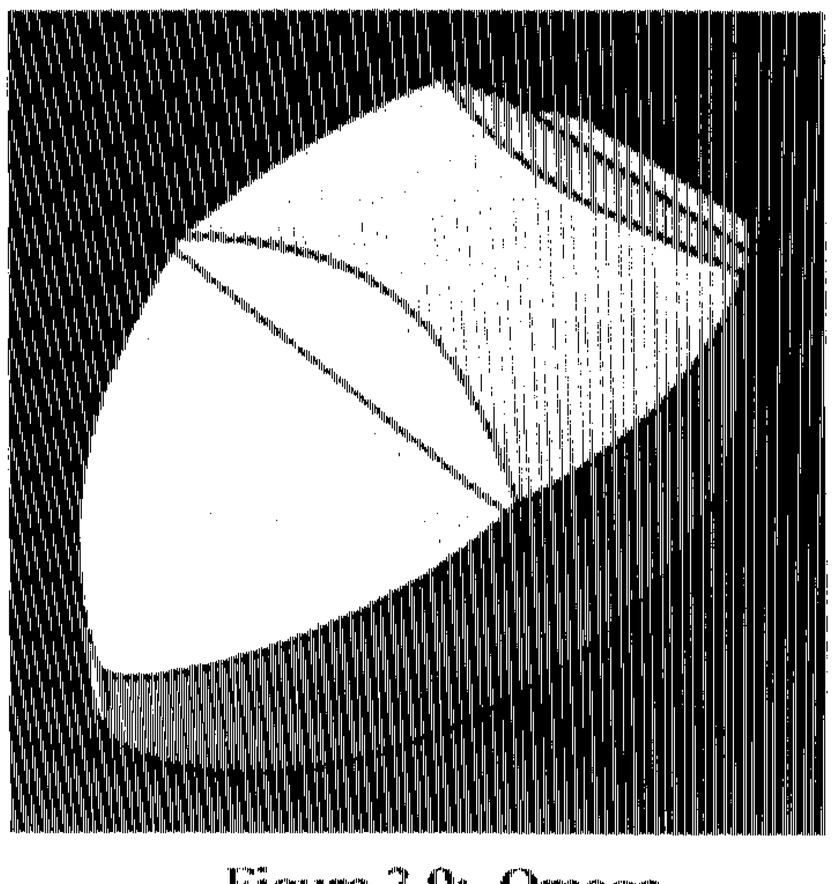

Figure 3.9: Omega

Model Development Progress

Probe

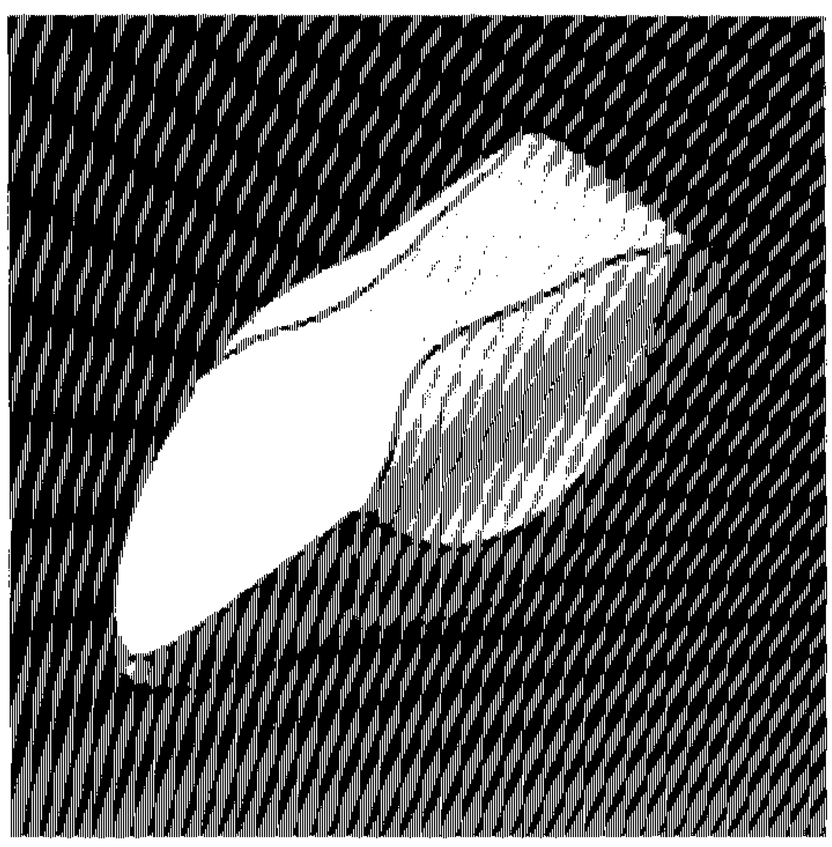

Figure 3.10: Probe I

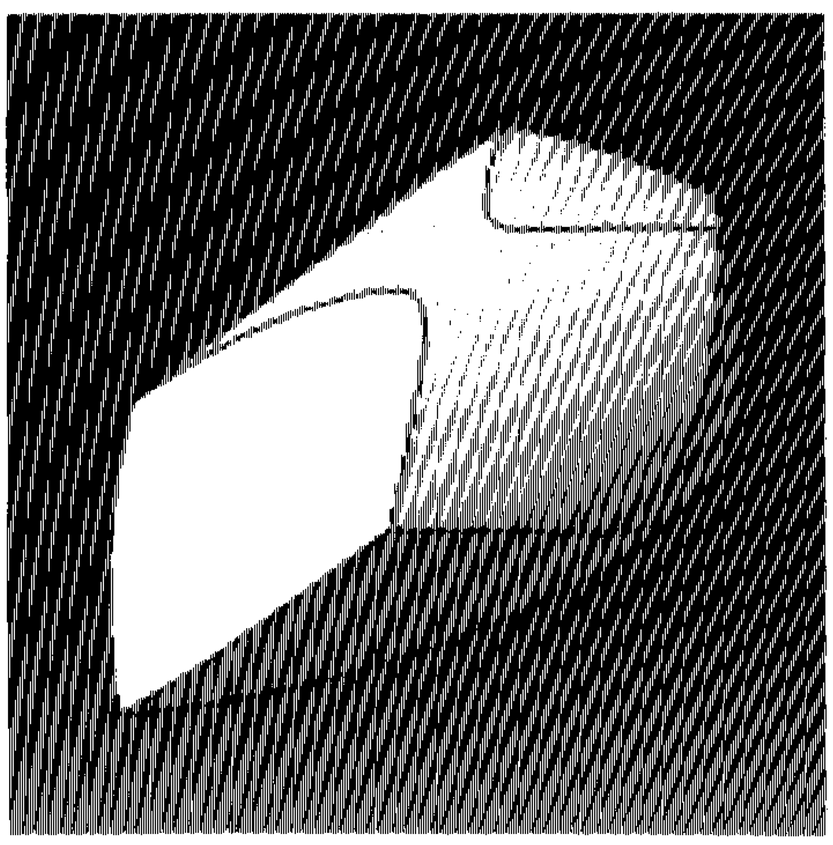

Figure 3.11: Probe II

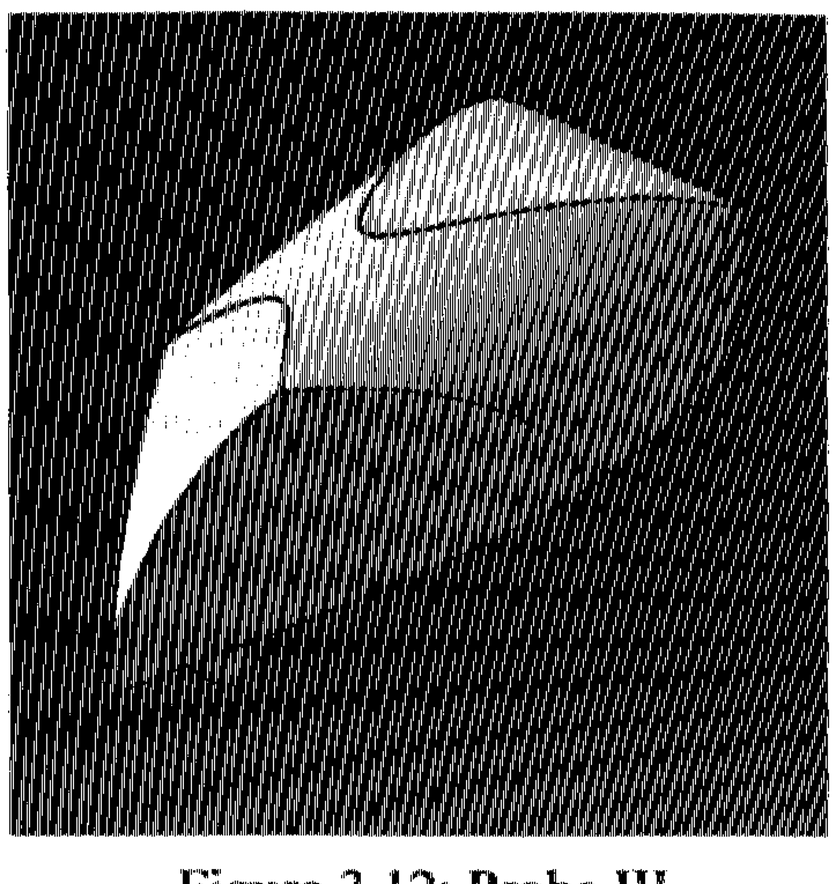

Figure 3.12: Probe III

3.8 Reducing Drag Calculation

The drag coefficient is a common metric in automotive design pertaining to aerodynamic effects. The drag force is a reactive force that tends to slow an object down as it falls through a medium. The drag coefficient is a value for a particular object that describes the ratio of the drag force to the factors that influence the drag force. The drag coefficient depends on the size, shape, and weight of the object but it is usually associated with the extent to which the object is streamlined. Generally, the larger the drag coefficient, the more a drag force it will produce while falling, and therefore, the slower it will fall.

The drag force (F_D) is related to the density (ρ) of the medium in which the object is located, the planar area (A) perpendicular to the movement, and the velocity (V) of the object relative to the velocity of the medium. If the object were a sphere, the planar area is that of a circle of the same radius. If the object were a cube, then the planar area is a square. If an object was moving at a velocity of 4 m/s into a wind speed of 6 m/s, then the relative velocity would be 10 m/s. If the wind speed of 6 m/s was in the same direction as the velocity of the object of 4 m/s, then the relative velocity would be 2 m/s. The drag force is related to these variables and the drag coefficient (C_D) by:

$$F_D = C_D \frac{1}{2} \rho A V^2$$

The value of the drag coefficient is quite variable and may vary with the relative velocity. Modern cars have drag coefficients from 0.2 to 0.3, with some sports cars having a lower value. A neighborhood bicyclist who is drafting might have a coefficient of 0.5. A dolphin may have a coefficient of 0.004, which helps it swim long distances with little drag resistance. **[13]**

The Reynold's number R is a dimensionless quantity that is important in drag coefficient analyses. It is computed as:

$$R = \frac{\rho VD}{\mu} = \frac{\rho D}{\upsilon}$$

Where; ρ is the fluid density, μ is the dynamic viscosity, υ is the kinematic viscosity, V is the velocity, and D is the length parameter such as the diameter of the object.

Coefficient of drag is influenced by substitution of drag force and free stream velocity into the drag equation. To achieve the flow similarity between real and model, Reynolds number has to be equal respectively.

$Re_M = Re_R$

Where M denotes the model, R denotes the real car

Theoretical definition of Reynolds number is a ratio between inertia force over friction force.

Re = (Inertia Force) / (Friction Force)

Where laminar flow, Re < 2300

Another definition of Reynolds number is

Re = (V.L) / (v)

Where V is the free stream velocity and v is the kinematic viscosity.

Final relationship between Re (model) and Re (real) can be expressed in the following equation

$$V\infty, m = \frac{V\infty, r \; x \; Lr \; x \; vm}{vr \; x \; Lm}$$

The ratio of Lr : Lm is the scale of the model. For example, to find relationship between free stream velocity @ 40 m/s of real and model car travel velocity from a model with a scale 1:43,

$$\frac{Lr}{Lm} = \frac{43}{1}$$

The model car travel should be at 1720 m/s.

3.9 Validate the Model

To validate the model, the wind tunnel test should be done before the fabrication process of the actual model. Universiti Teknologi PETRONAS owns an open circuit wind tunnel in the Mechanical Department. Open circuit wind tunnels do not directly re-circulate air. Rather, air is drawn in from the laboratory environment, passes through the test section and is returned back to the lab through the tunnel exhaust. Wind tunnel is equipped with smoke fume in order to have clear indication of aerodynamic profile of tested models. It is important to have deep understanding about aerodynamic as designing vehicle with efficient aerodynamic profile is crucial in reducing the drag force for less power and fuel consumption.

This drag force is generated by vortices at the back of moving vehicles. Vortices are generated because of the abrupt change of air flow momentum resulting wake at the rear that produces the drag force effect. Thus, the bigger the boot space area, the higher generated drag force of a vehicle.

Meanwhile, lift force is caused by the difference of air flow velocity between top and bottom section of vehicle. Higher air flow velocity produces lower pressure at the section. Lift force is experienced when the air flow velocity is higher at the top section compared to the bottom section. The high velocity air flow at top section generates lower pressure than the lower air flow velocity at the bottom which is lower air flow velocity and higher pressure.

This experiment is mainly about Bernoulli's principles and by putting the models to the test, better understanding can be gained thus applying theoretical knowledge into practical use.

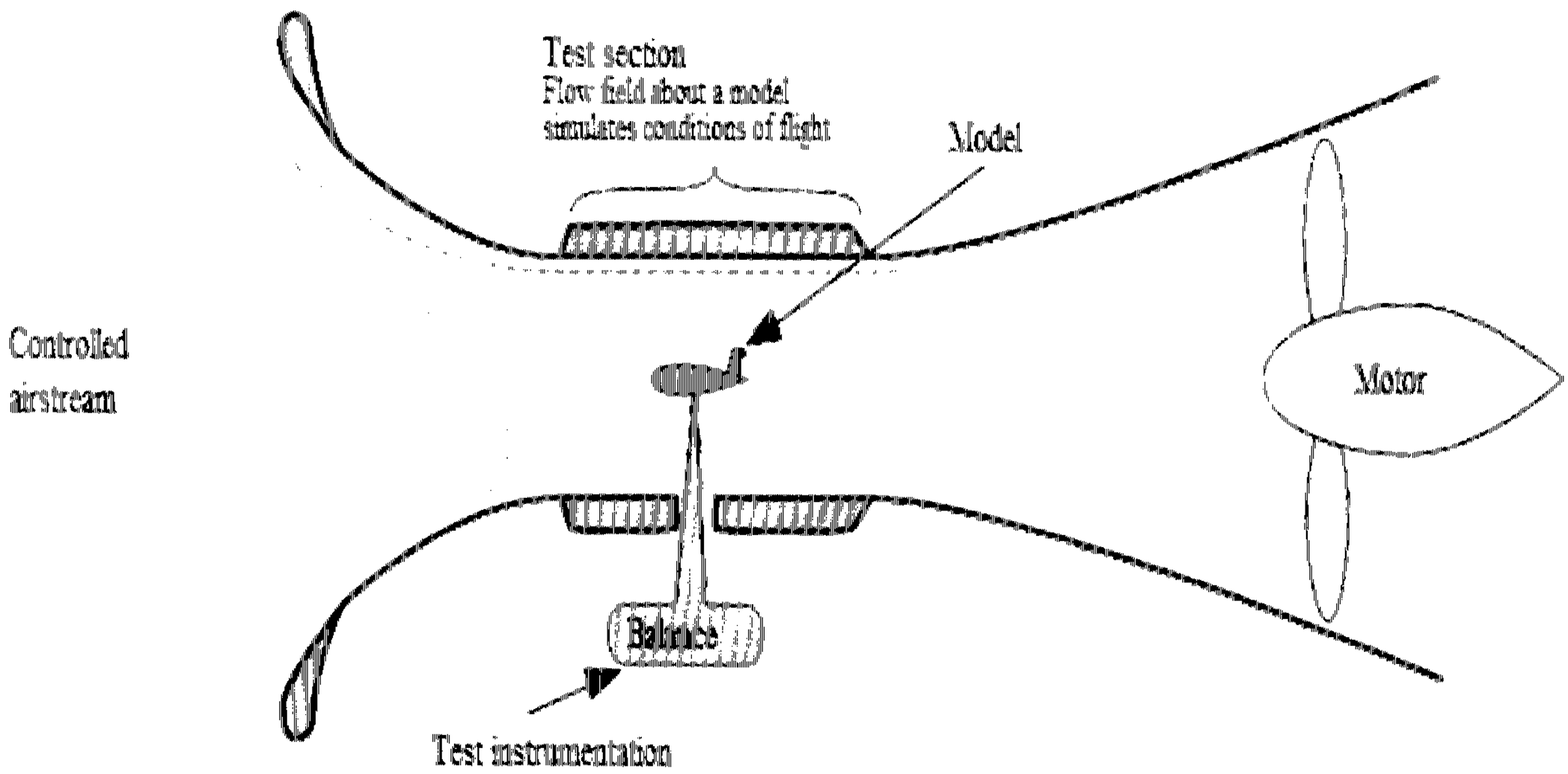

Figure 3.13: Open circuit wind tunnel

The wind tunnel testing is done to obtain all the parameters such as the value of drag, lift, and pitch that varies with the air stream velocity. Drag coefficient can be obtained using the following formula, [14]

$$F_{drag} = C_d . A . \frac{\rho_L}{2} . v_\infty^2$$

$$\text{Thus, } C_d = \frac{F_d}{\frac{1}{2} A . \rho_L v_\infty^2}$$

Where:

A = cross sectional area exposed to flow

ρ_L = fluid density (density of air 1.2 kg/m^3)

3.10 Flow Chart

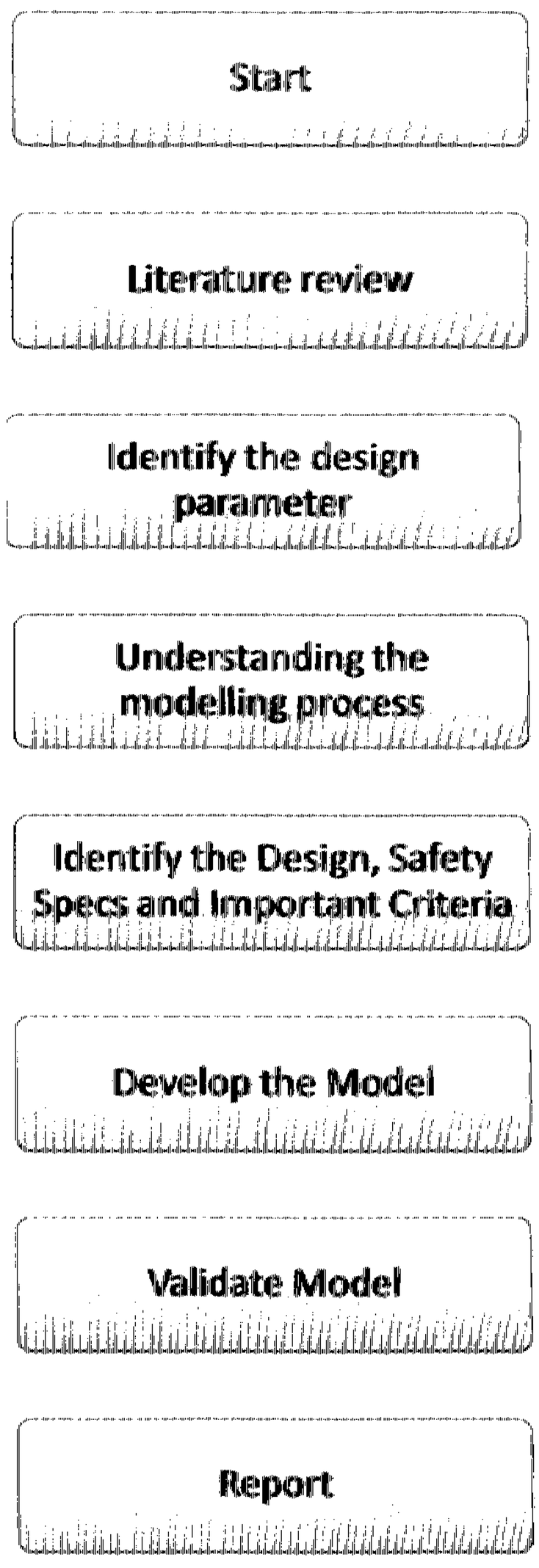

Figure 3.14: Flow chart of research processes

3.11 Project Planning

The project will be conducted in two semesters, effectively 14 weeks. Refer Gantt chart below:

Gantt chart for 1st Semester

No.	Detail/Week	1	2	3	4	5	6	7		8	9	10	11	12	13	14
1	Selection of Project Topic															
2	Preliminary Research Work															
3	Submission of Extended Proposal Defense						X									
4	Proposal Defense															
5	Project work continues															
6	Submission of Interim Draft Report														X	
7	Submission of Interim Report															X

Mid-sem Break

Table 3.1: Gantt chart for FYP 1

X Suggested milestone

Progress

Gantt chart for 2nd Semester

No.	Detail/Week	1	2	3	4	5	6	7		8	9	10	11	12	13	14
1	Project Work Continues															
2	Submission of Progress Report									X						
3	Project Work Continues															
4	Pre-EDX												X			
5	Submission of Draft Report													X		
6	Submission of Dissertation (soft bound)														X	
7	Submission of Technical Paper														X	
8	Oral Presentation															X
9	Submission of Project Dissertation (hard bound)															X

Mid-Sem Break

Table 3.2: Gantt chart for FYP 2

X Suggested milestone

Progress

CHAPTER 4

RESULTS AND DISCUSSION

4.1 Data Gathering and Analysis

4.1.1 Data Analysis (X-Tron I)

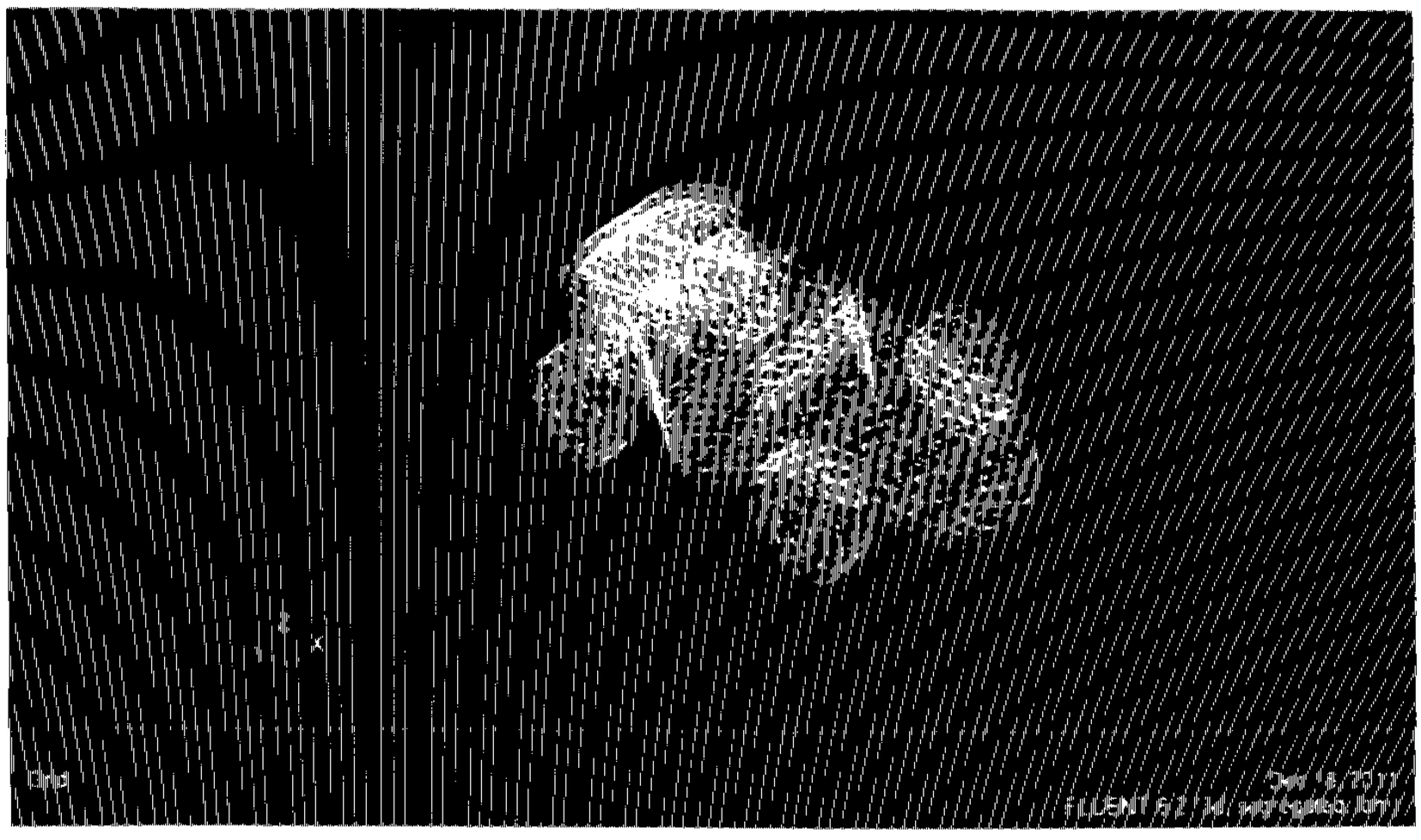

Figure 4.1: The grid shape of the Perodua Eco-Challenge 2011 Model after meshed in Gambit

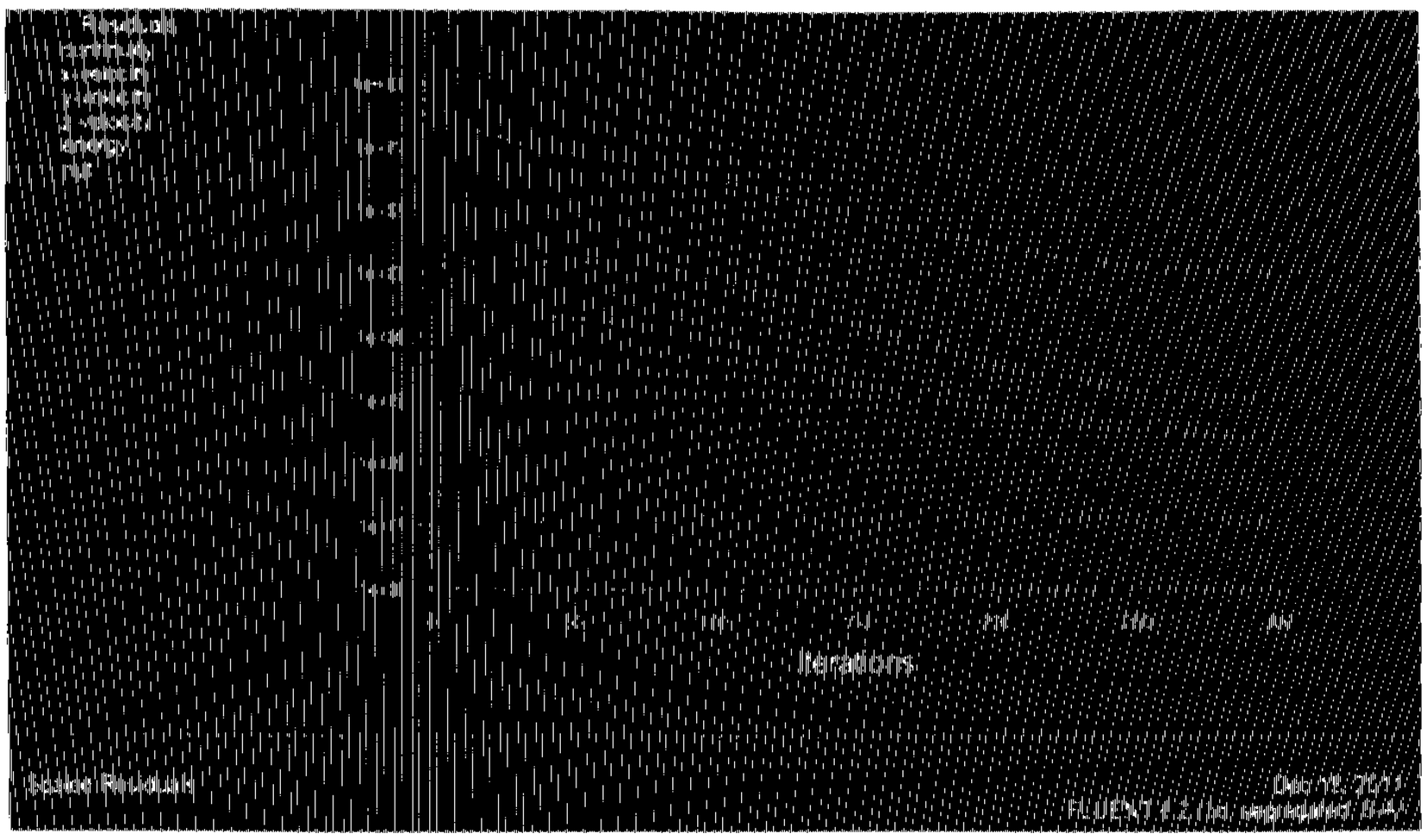

Graph 4.1: The residual shows the energy residual converges after 50 iterations while continuity residuals converge after 300 iterations.

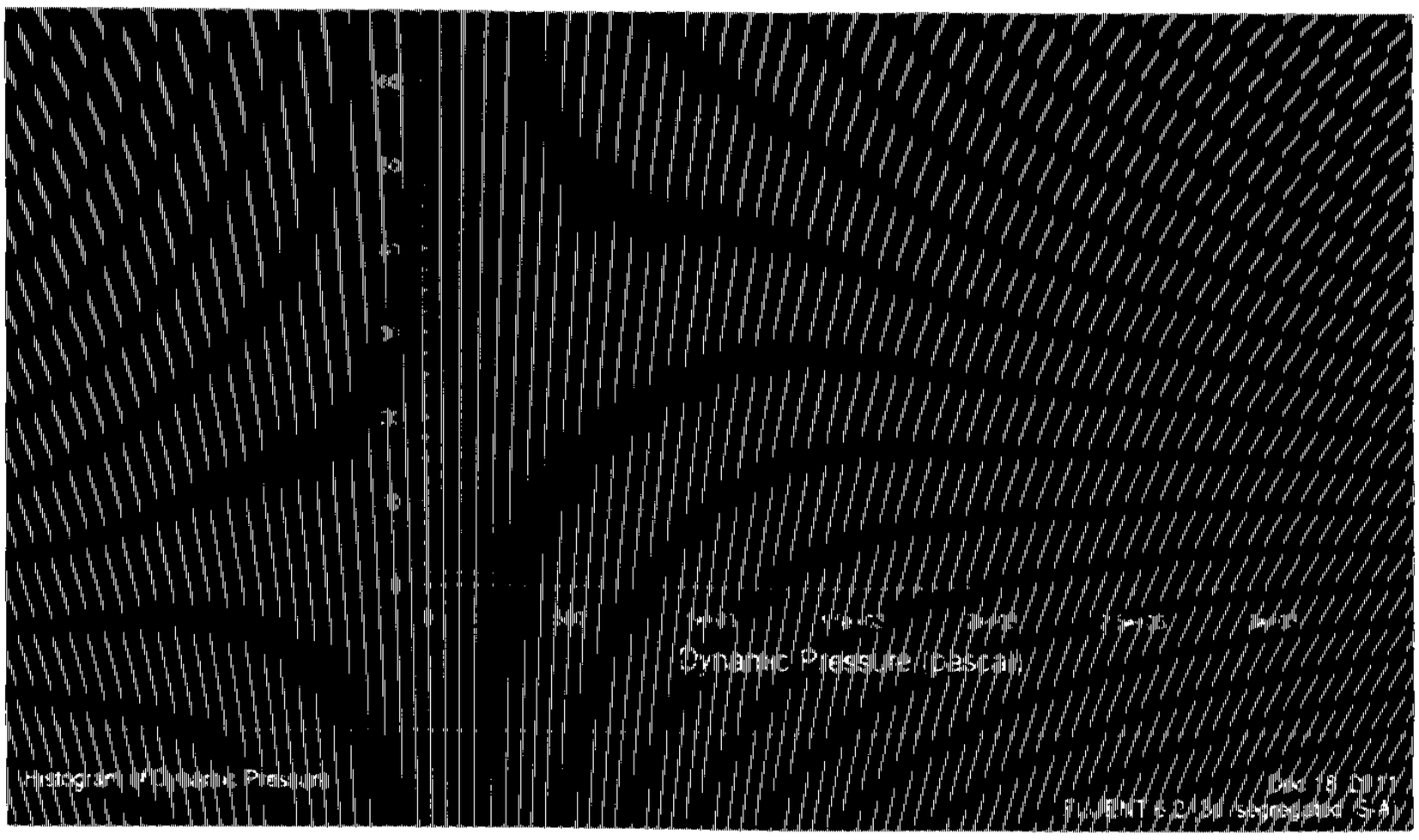

Chart 4.1: Histogram of dynamic pressure

The histogram of dynamics pressure shows the largest number of cell is 206418 cells or 55.66183 % are between 828.71375 Pascal to 1104.9517 Pascal. Then followed by 111893 cells or 30.172607 % are between 1104.9517 Pascal to 1381.1896 Pascal. This means the majority of dynamic pressure is between 828.71375 Pascal to 1381.1896 Pascal which is dominate mostly in the front and also top of the car body.

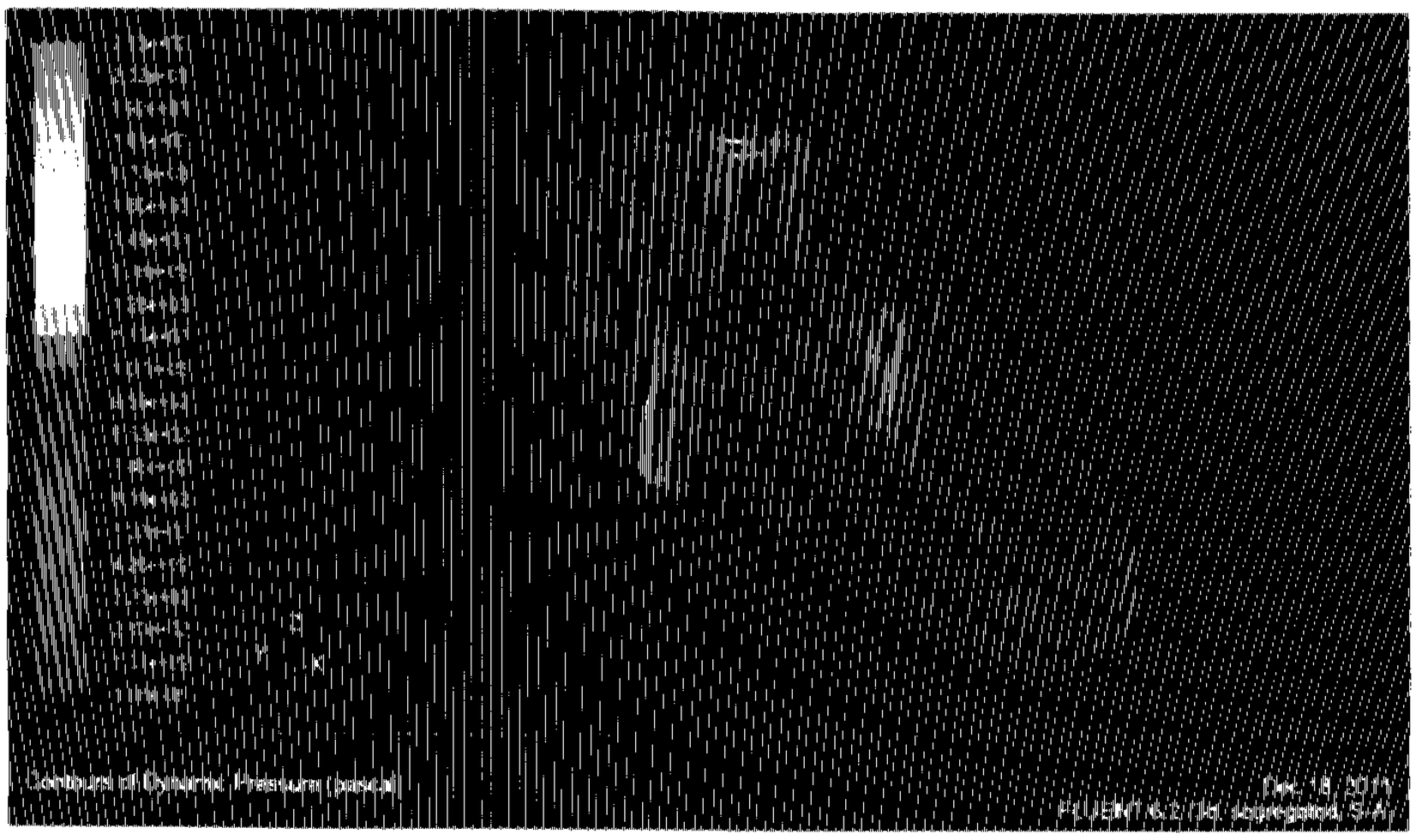

Figure 4.2: Contours of dynamic pressure

Dynamic pressure is closely related to the kinetic energy of a fluid particle, since both quantities are proportional to the particle's mass (through the density, in the case of dynamic pressure) and square of the velocity.

Where: $q = \frac{1}{2} \rho V^2$

q= dynamic pressure in pascals,

ρ= fluid density in kg/m3 (e.g. density of air),

V= fluid velocity in m/s.

Dynamic pressure is in fact one of the terms of Bernoulli's equation, which is essentially an equation of energy conservation for a fluid in motion. As dimensional analysis, it shows the aerodynamic stress experienced by car traveling at 40 m/s. The contours of dynamic pressure show the location of high and low dynamics pressure areas. The highest dynamic pressure areas concentrated at the most end both left and right side of the car body. The open shape design also caused high pressure at internal topside of the body. The lowest dynamics pressure area concentrated at the most front side of the body and also at driver compartment.

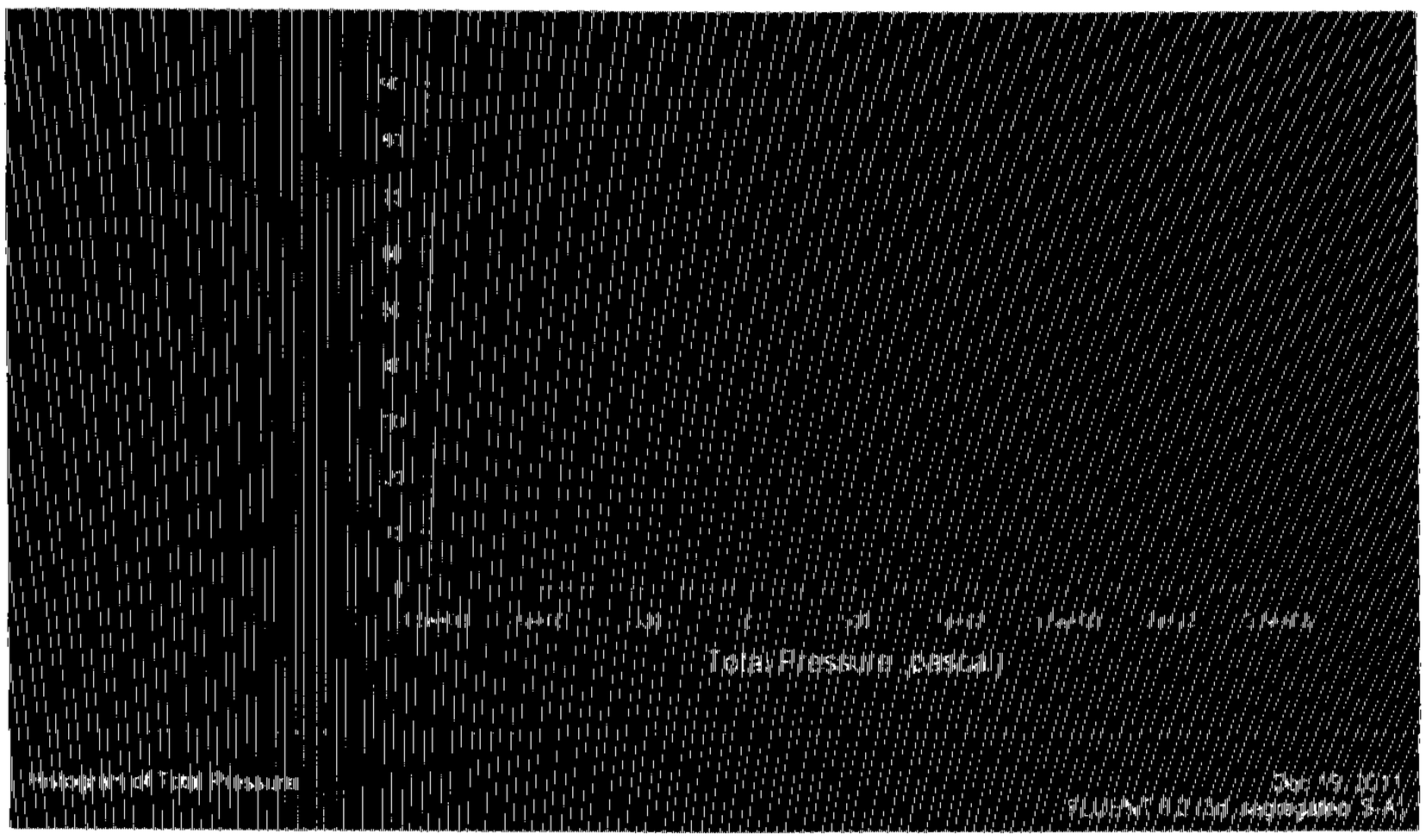

Chart 4.2: Histogram of total pressure

The histogram of total pressure shows the largest number of cell is 306434 cells or 82.631734 % are between 979.14469 Pascal to 1322.6732 Pascal. This means the majority of dynamic pressure is between 979.14469 Pascal to 1322.6732 Pascal which is located mostly in the front of the car body.

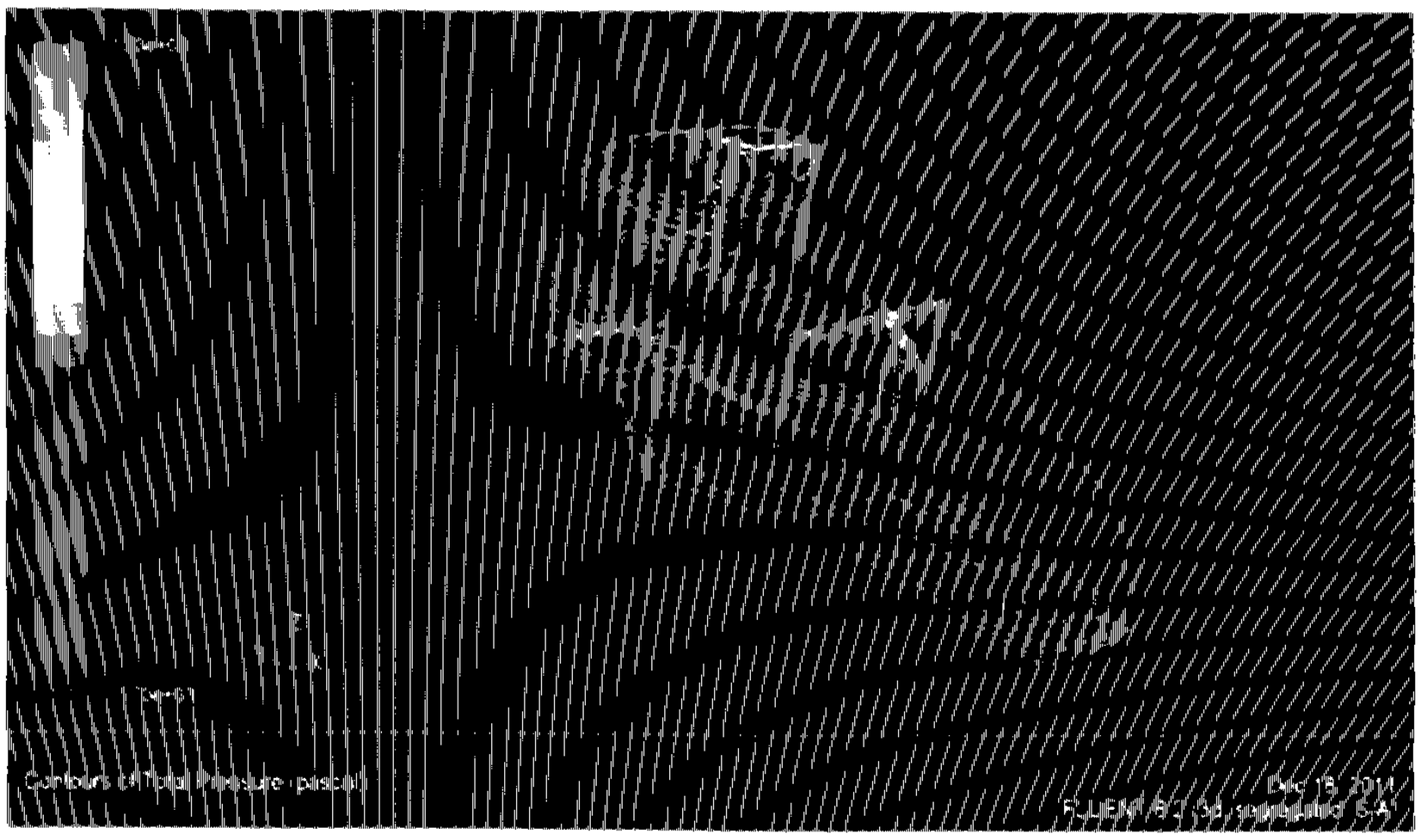

Figure 4.3: Contours of total pressure

Although road vehicle aerodynamics may not generally lend itself to simple mathematical analysis, there is one relationship that is absolutely fundamental to the study of air flows, and that is the Bernoulli equation. For low-speed flows, this equation gives the relationship between air speed and pressure. It can be written in several different ways, but aerodynamicists normally prefer it in the form given below:

Total Pressure = Static Pressure + Dynamic Pressure

(pressure)+ ½ (density) x (speed) ^{2} is constant

Or in mathematical symbols

$p + \frac{1}{2} \rho V^2 = \text{constant}$

where p is the pressure, ρ is the density, and V is the speed.

This diagram shows the contour profiles of total pressure distribution of stream model. The highest pressure is 1330 Pascal while the lowest is -1030 Pascal. The pressure drag is the different between highest and lowest pressure. Thus,

Pressure Drag = Maximum Pressure – Minimum Pressure

= 1330 Pascal - (- 1030 Pascal)

= 2360 Pascal

Zone Name	Pressure Force	Viscous Force	Total Force	Pressure Coefficient	Viscous Coefficient	Total Coefficient
PEC 2011	379.65286	011.510696	391.16355	6.198414	0.18792973	6.3863437

Area of surface projected onto plane y:

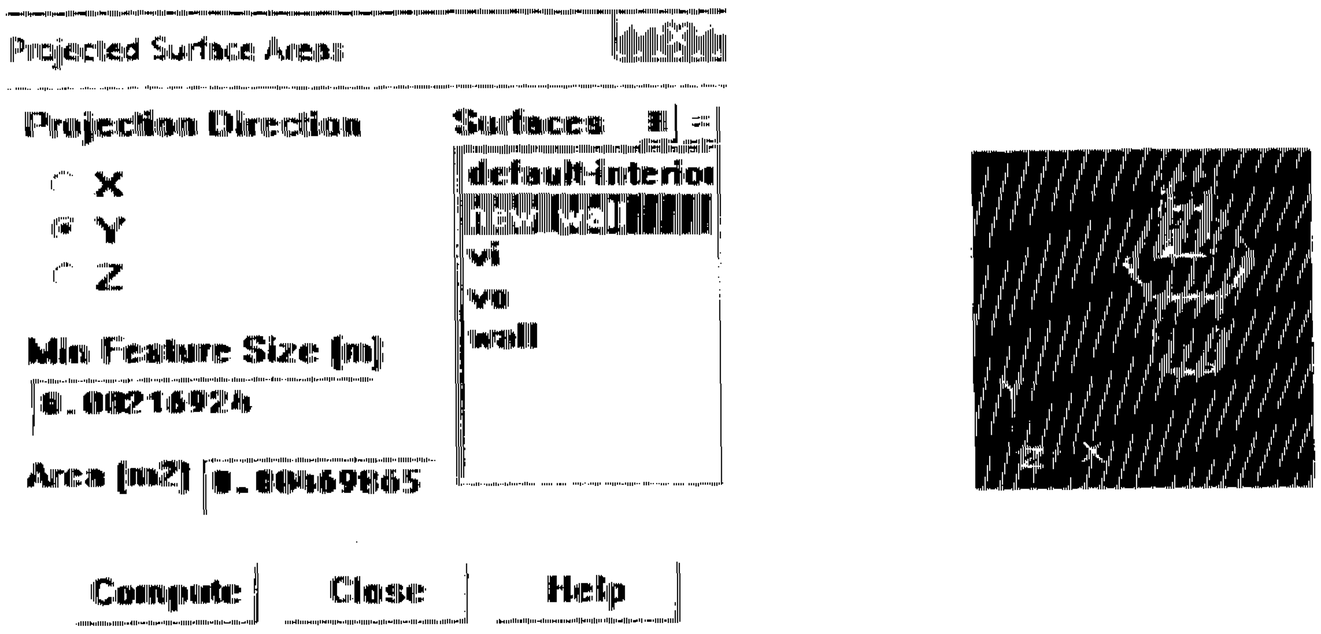

The Drag Force = 0.5ρ V^2 A C^d formula, where

A = frontal area

ρ = density of the air

V = speed of the vehicle relative to the air

0.5ρ V^2 = maximum dynamic pressure

Hence, the drag coefficient, C^d is

Drag Force = 0.5ρ V^2 A C^d,

3.9116355 N = 2030 Pa x 0.00469865m^2 x C^d,

C^d = 0.41

Figure 4.4: Path lines sequence flow color by velocity magnitude (m/s)

From the figure 4.4, the simulation path line color by the velocity magnitude whiles the car moving at 40 m/s. The flow begins from number 1 until number 9. The minimum velocity magnitude path line is 0 m/s while the maximum is 53.96749 m/s. At number 1, the flow starts to move around the surface body at low velocity. At number 2, the flow starts to leave the body surface while maintain the low velocity magnitude at the front of the body. At number 3, the velocity starts to leave the front of the body. At number 4 till number 6, the higher magnitude range larger than 20m/s start to leave the surface of the body with turbulent flow. At number 7 till 9, the flow starts to leave away from the surface body completely.

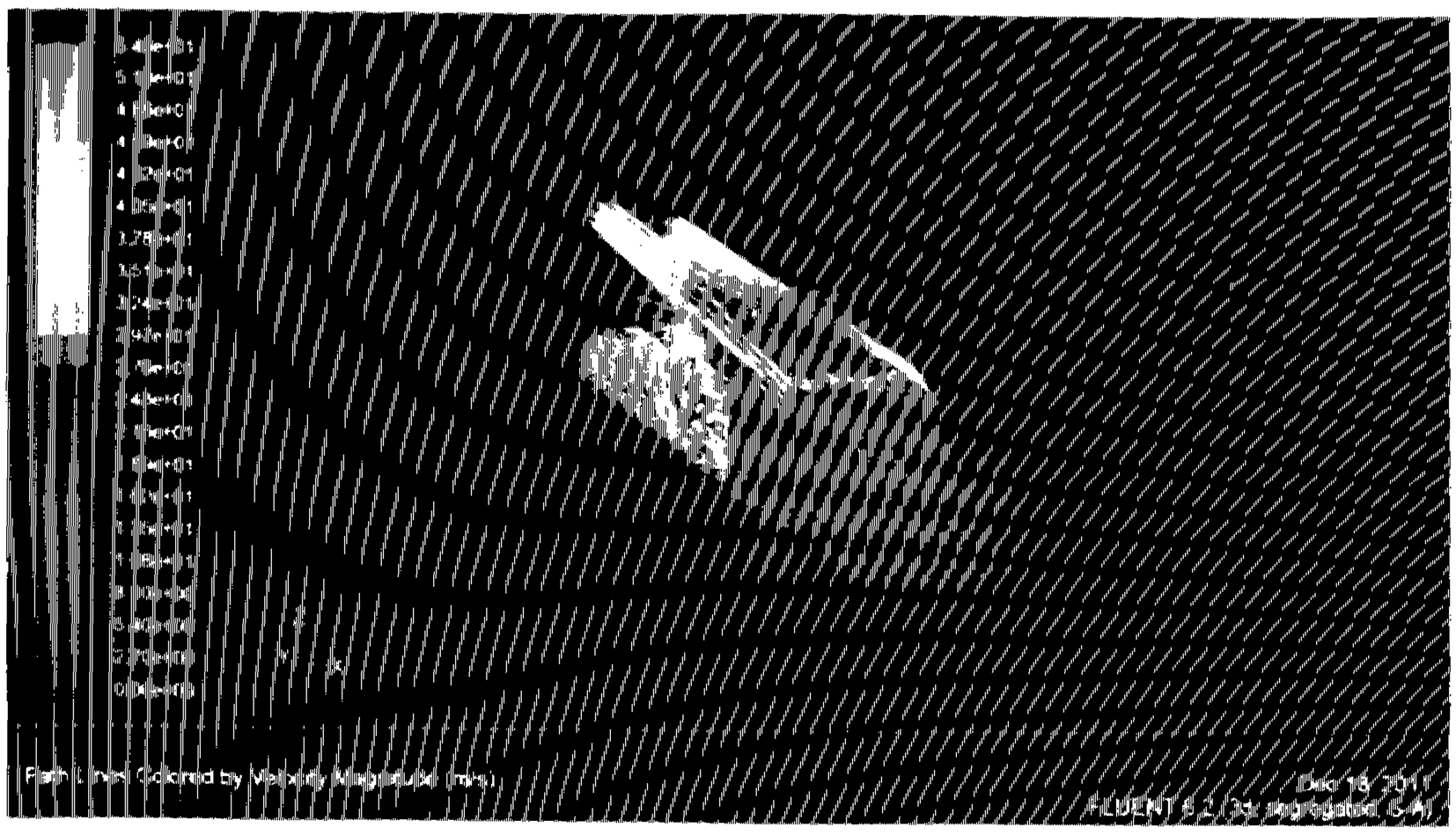

Figure 4.5: The path lines colored by velocity magnitude isometric view (m/s)

From the figure 4.5, it may be seen that the trailing vortices produce drag by modifying the pressure distribution around the vehicle. This contribution to drag is commonly called trailing vortex drag.

Figure 4.6: The path lines colored by velocity magnitude back view (m/s)

From the figure 4.6, the vortices draw air away from the rear of the vehicle, creating low pressure there, and thereby pulling the flow down. Because the air is swirling with a high speed, the pressure in the vortex is low, as predicted by the Bernoulli relationship, and therefore any surface exposed to the influence of a vortex will be subjected to a reduced pressure. A reduced pressure over the rear of the vehicle will obviously increase the drag. It is also possible to deduce from momentum considerations that if the air is being pulled towards the rear of the car, corresponding reaction will pull the vehicle backwards.

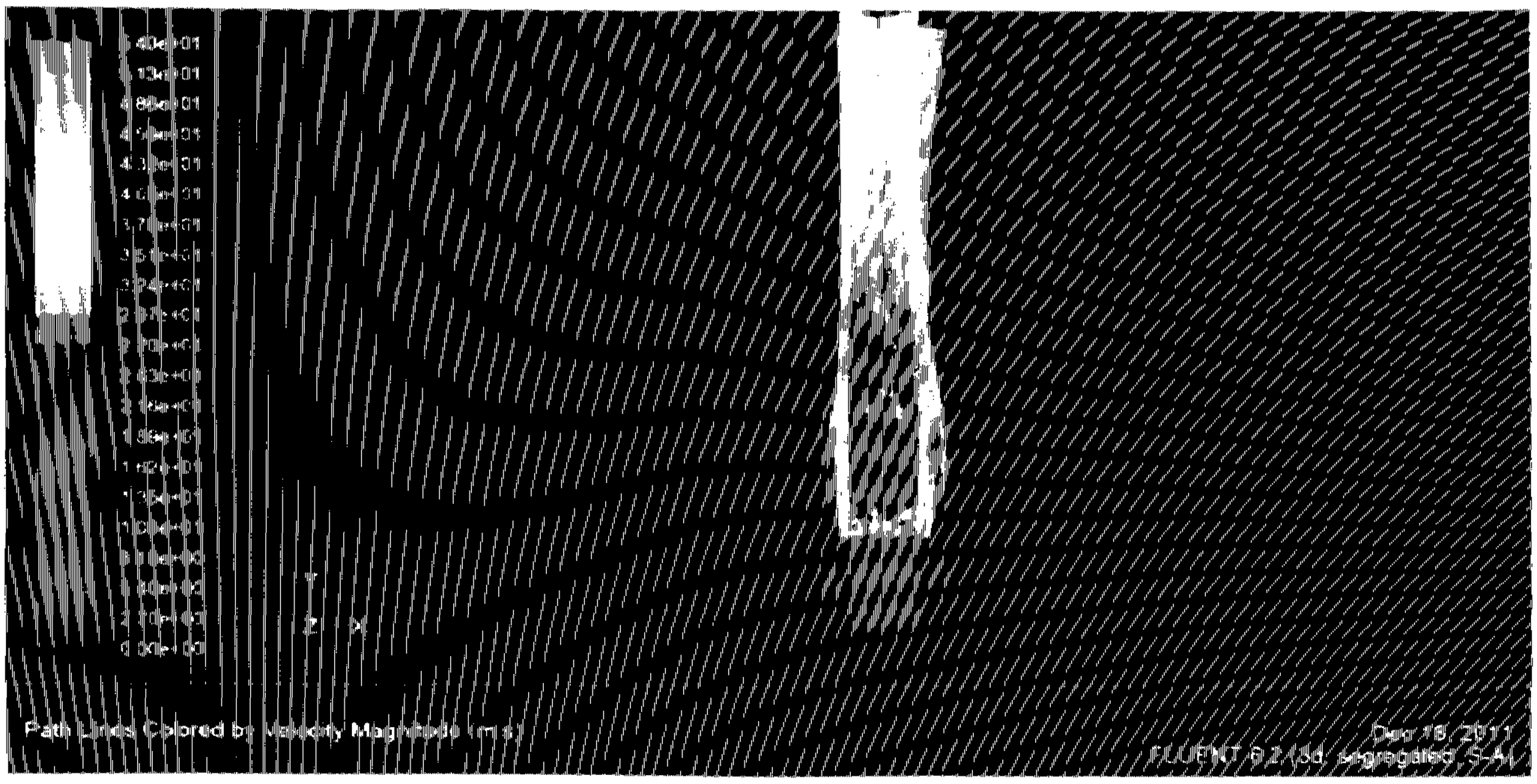

Figure 4.7: The path lines colored by velocity magnitude top view (m/s)

From the figure 4.7, it can be conclude that the velocity is much lower in the front side of the car while higher in the upper middle of the car in y-direction. The bottom at the underside of the car creates twin vortices with velocity more than 20 m/s, while the upper side of the car creates laminar flow around the car surface with the velocity quite similar to the wind velocity (40 m/s).

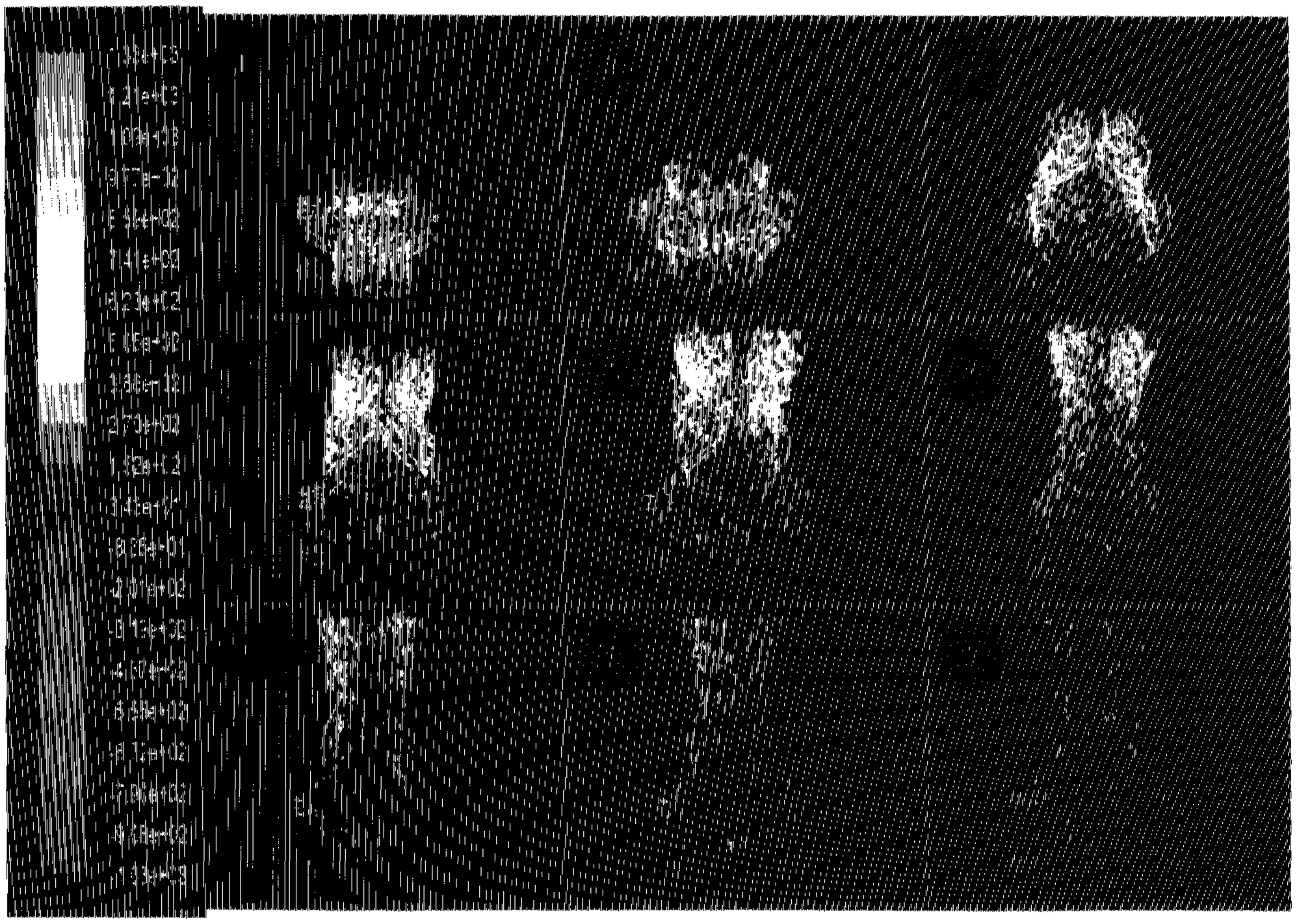

Figure 4.8: Path lines sequence flow color by total pressure magnitude (Pascal)

From the figure 4.8, the simulation path line color by the total pressure magnitude while the car moving at 40 m/s. The flow begins from number 1 until number 9. The minimum total pressure magnitude path line is -1025.836 Pascal while the maximum is 1329.958 Pascal. At number 1, the flow starts to move around the front of car body with high pressure with more than 800 Pascal. At number 2, the pressure inside the car body compartment is maximum at 1329.958 Pascal as the body 'catch' the air flow. At number 3, the high pressure starts to leave the front car body completely. The presence of the air movement inside the car body increases the internal pressure. At number 4 till number 6, the intermediate range pressure between 200 Pascal to 600 Pascal start to leave the surface body. At number 7 till number 9, the total pressure start to leave the car body completely while the high pressure still trapped inside the car body.

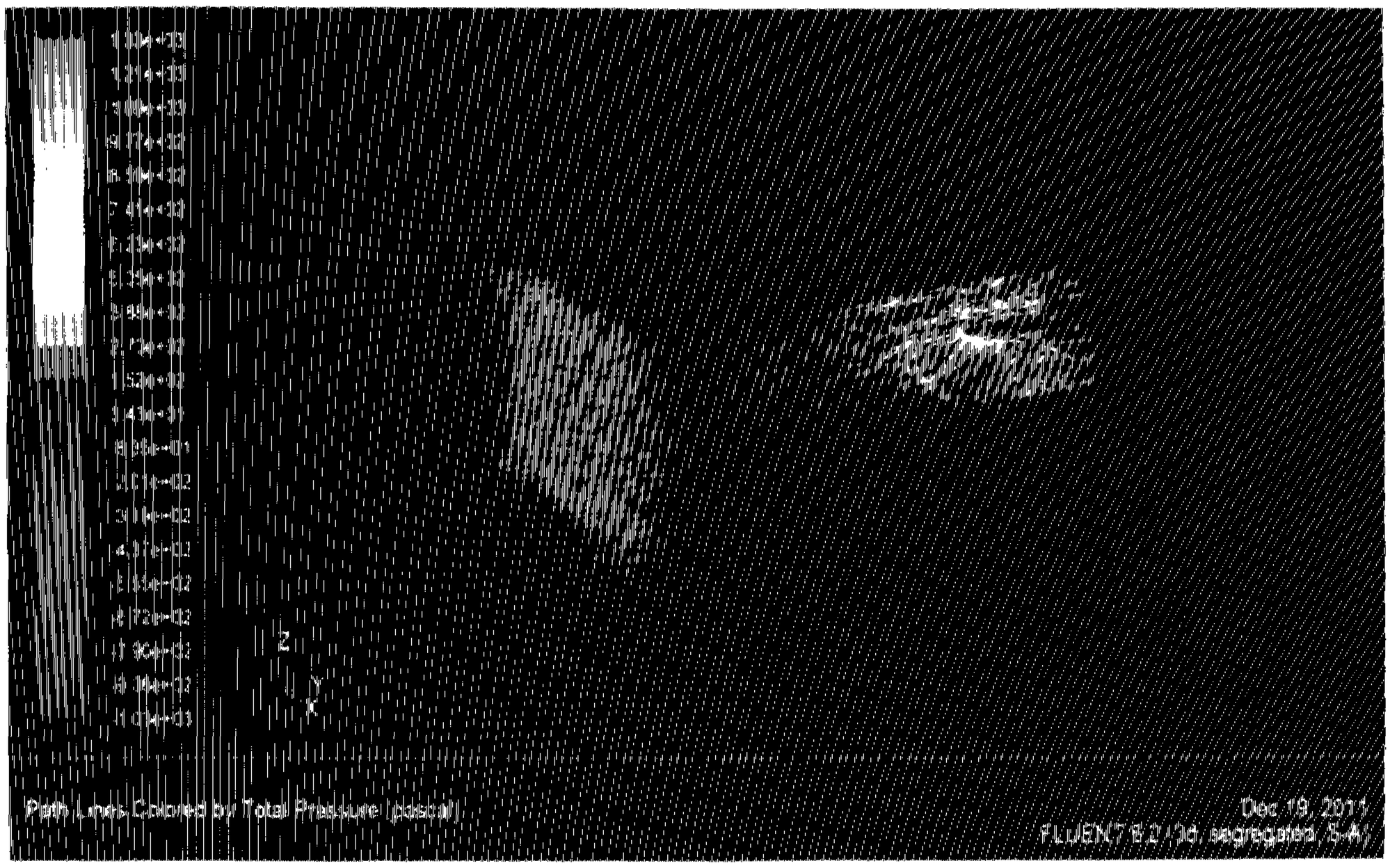

Figure 4.9: The path lines colored by total pressure magnitude (Pascal)

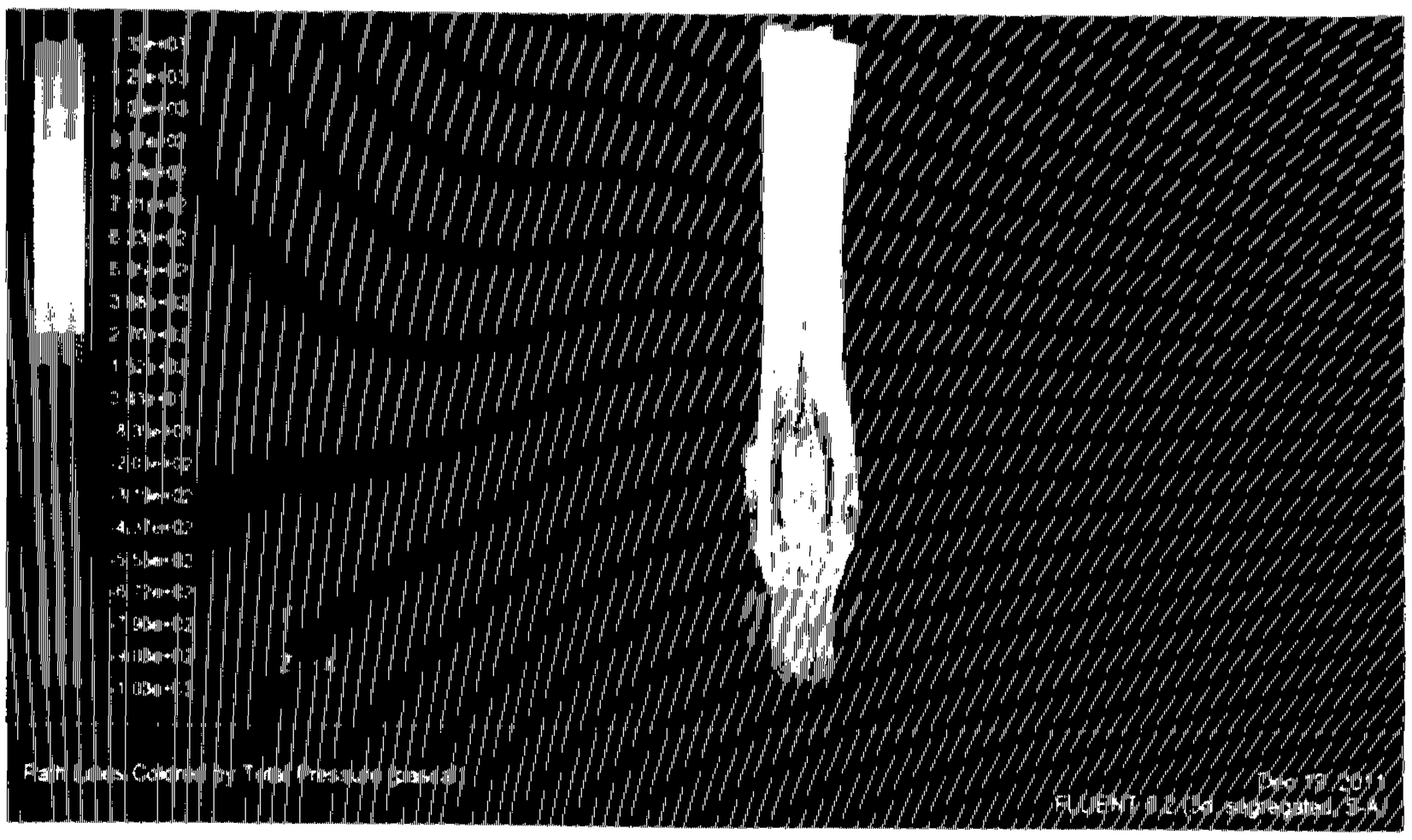

Figure 4.10: The path lines colored by total pressure magnitude (Pascal)

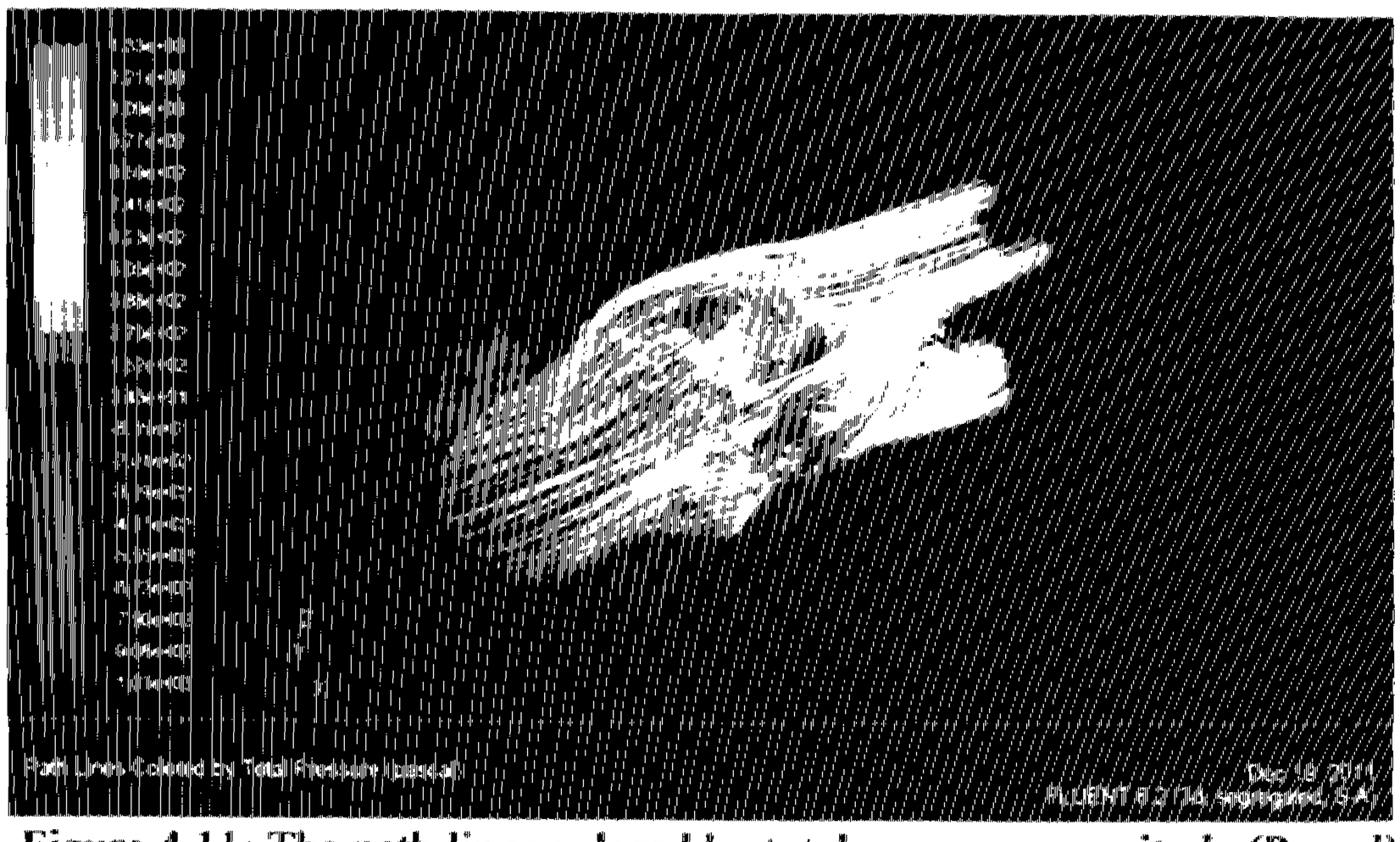

Figure 4.11: The path lines colored by total pressure magnitude (Pascal)

From the figure 4.11, it can be conclude that the total pressure is much higher in the front of the car body compare to the bottom side. It is good to reduce the lift coefficient. The tire total pressure in the front left side is a bit higher at 271 Pascal compare the front right side at -1030 Pascal. The different is due to different gap between tire and car body. The highest pressure at 1330 Pascal trapped in the car body due to the 'open' design thus cause higher drag coefficient.

4.2 Result and Disscussion

4.2.1 Software

If there are problem with the continuity residual, it could be related to improper boundary conditions, but usually it is related to the solver settings. Try to **reduce the momentum under relaxation factor to 0.4** and to **increase the pressure under relaxation factor to 0.5 or 0.6.** Reduce turbulent variables under relaxation factor to 0.4 but 'do not' under-relax turbulent viscosity (keep the under relaxation factor equal to 1).

If the 'floating point error: invalid number' error appear, the solver setting should be revise in several aspects. From numerical computation view point, the basic operations performed by computer are represented inside computer in what is called floating point numbers. The errors that are either because of invalid numeric computation initiated by user or limitation of machine that is used are floating point errors. There are eight possibilities of the error:-

1) Invalid Operations

Simplest example is if one uses Newton Raphson root finding method to solve f(x)=0 and for some Nth iteration if we get x = x(N) such that derivative of function f(x), f'(x(N))=0 then formula for calculating next iterate x(N+1) = x(N) - f(x(N))/f'(x(N)) requires division by f'(x(N)) which is zero. Here you get divide by zero type of floating point error.

2) Over or Underflow

Another type is having data with either too large or too small magnitude called 'overflow' or 'underflow' respectively. Such data cannot be physically represented on computer for direct processing by arithmetic processing part of processor.

3) Rounding off errors

While rounding off a decimal number, some significant digits are lost which cannot be recovered. For instance, if we round off 0.1 to integer (not greater than it called 'floor' of the given number) then it is zero. If this value if further used for computation then it may lead to several errors.

4) Solver and iteration

The shorter time step and adjusting under relaxation factor can make the process better. Set the 1/3 under relaxation factor as default and also lower the values of under relaxation factor. Use the coupled implicit solver. Try to change under-relaxation factors and if it is unsteady problem maybe time step is too large. Improving the ratio in the solve/control/limits, might help. Reduce the Courant number. The Courant number reflects the portion of a cell that a solute will traverse by advection in one time step:

$$C_r = \frac{\bar{v}\Delta t}{\Delta l}$$

Where:

C_r = Courant number

delta l = dimension of the grid cell at each location

v =average linear velocity at that location

delta t = maximum time step size

If you still get the error, initialize the domain with nothing to 'Compute from...' Then click 'init'. Again select the surface from which you want to compute the initial values & iterate. Another reason could be a to high Courant number - that means, that the steps between two iterations are too large and the change in the results is too large as well (high residuals).

5) Grid problems

This error caused by different grid scale. In Gambit, the dimension to be set in millimeter, while in Fluent the scale also must be set in millimeter. Standardize the unit should be work. Use lower and coarser mesh first compare to higher grid mesh. High grid mesh is so heavy thus may cause computers resources/memory insufficient.

6) Boundary conditions

Set the wall boundary condition instead of an axis boundary condition will cause Fluent fail to run the mesh file. The error sign 'floating point error' will appeared due to the boundary conditions do not represent real physic. Wrong boundary condition definition might cause the floating point error. For example, set an internal boundary as interior.

7) Multiprocessor issues

If the error occurred while the process running in a multiprocessor, try run the process in a single processor.

8) Wrong initiation

Initiating the case with wrong conditions may lead to floating point error when the iterations start.

This is the steps that have been concluded to analysis the car model:-

1. Read the grid file

2. Select segregated and implicit solve

3. Define model viscous with Spalart-Allmaras

4. Define Materials constant air density (default setting)

5. Operating condition with default setting

6. Boundary condition: Velocity inlet with 40m/s outflow plane (default)

7. Solve solution: Pressure = PERSTO

   Momentum = second Order Upwind

   Pressure-velocity coupling = SIMPLE

   Modified Turbulent viscosity = First Order Upwind

8. Turn on residual Plotting

9. Initialize the solution: Compute from velocity inlet

10. Iterate with 2000

4.2.2 Design

From the result of the datum simulation, the design should be closed for all the body to reduce the effect of pressure drag. The design also should be closer to the streamline shape while also take account the packaging of the car. The design should be rounded in the corner without sharp edges. Sleek design will encourages smooth flow. Smoothly continuous surface with no sudden changes in direction, and no gaps, excrescences, or surface detail. The underside of the vehicle is just as important as the visible upper surfaces. To minimize pressure drag it is necessary to keep the flow attached as far back as possible; this also implies continuous surface contours without sharp corners or facets. In addition, it is important that the pressure should be allowed to rise as much as possible towards the rear of the vehicles, and this means that the cross-sectional area should preferably reduce gradually towards the rear, as the teardrop shape. The gradual reduction is necessary in order to prevent separation due to strongly adverse pressure gradients.

4.3 Result

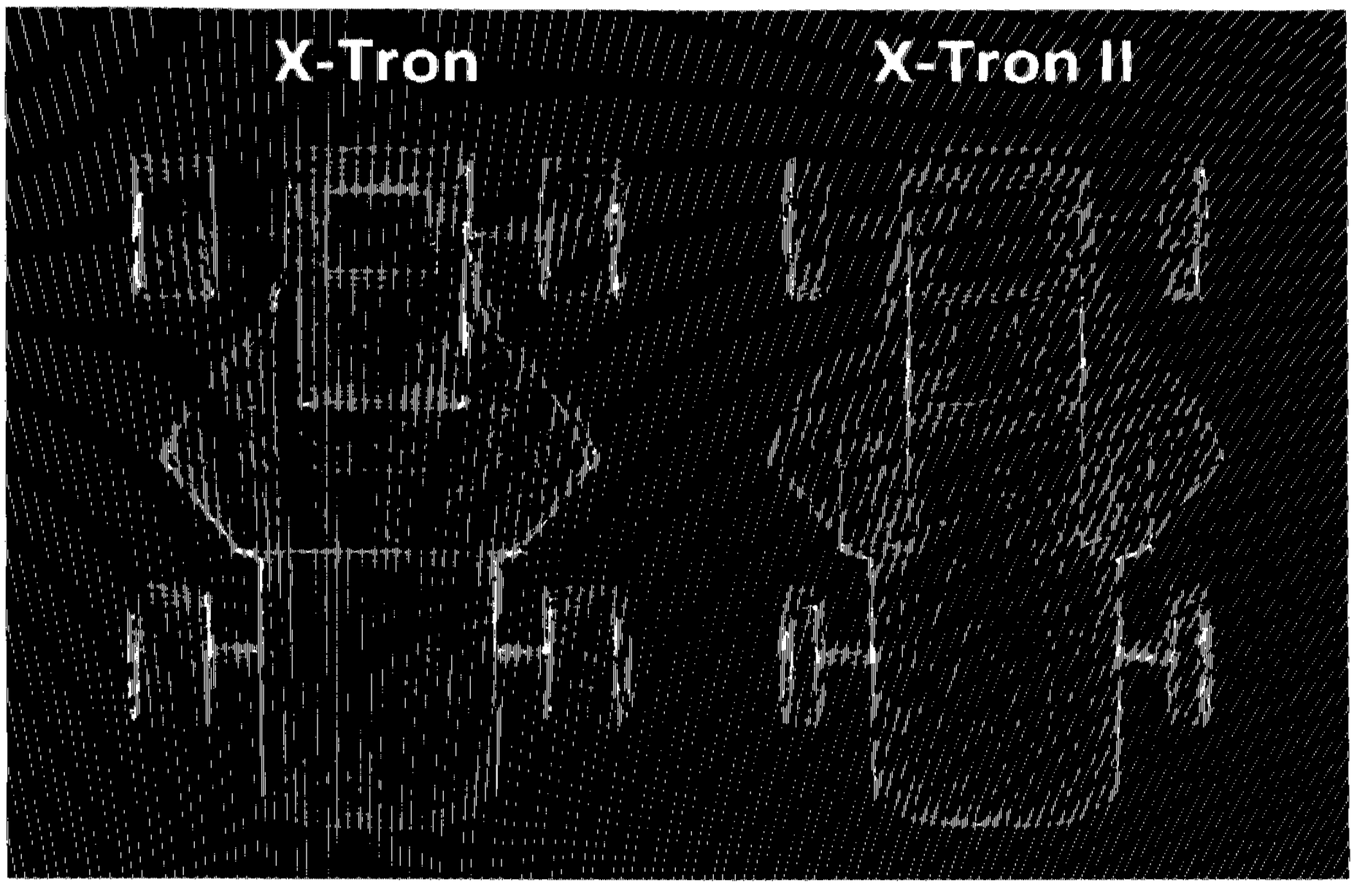

Figure 4.12: Optimized total pressure distribution contour for X-Tron I (left) to optimal X-Tron II (right)

From the result of the datum simulation, the model should be closed in the cockpit to reduce the effect of pressure drag. The design also should be closer to the streamline shape while also take account the packaging of the car. Smoothly continuous surface with no sudden changes in direction, and no gaps, excrescences, or surface detail. The underside of the vehicle is just as important as the visible upper surfaces.

The models are classified into four platforms which are X-Tron (I and II), Stream (I and II), Code (Alpha, Beta and Omega) and Probe (I, II, and III). The design result can be seen in Table 4.1:

Criterion / Model	Frontal Area (m²)	Dynamic Pressure (Pascal)	Total Force (Newton)	Drag Coefficient C_d	Maximum Total Pressure (Pascal)	Minimum Total Pressure (Pascal)	Pressure Drag (Pascal)
X-Tron I	0.469865	2030	391.16355	0.4100	1330	-1030	2360
X-Tron II	0.467334	2140	330.0000	0.3300	1460	-1824	3284
Stream I	0.4933213	1740	259.96781	0.3029	982	-948	1930
Stream II	0.7489129	2480	322.6400	0.1737	1330	-1480	2810
Alpha	0.3704476	1880	211.30717	0.3034	1140	-548	1688
Beta	1.177772	2310	500.17608	0.1838	1050	-993	2043
Omega	0.8554627	2300	209.41505	0.1064	875	-1060	1935
Probe I	0.8501946	2470	661.49391	0.3150	1020	-767	1787
Probe II	0.7791405	1610	213.12732	0.1699	727	-253	980
Probe III	0.7310987	1440	157.41193	0.1495	729	-588	1317

Table 4.1: Drag coefficients for all models at 40m/s

4.4 Model Prototype and Wind Tunnel Experiment.

The scale model will be designed in CATIA and fabricate with 3D printer. The model will be test in the wind tunnel based on the pilot test done before. The validation is to verify the result between wind tunnel experiment results with simulation results. The test will be conducted within similar parameters. The size of the model and the wind speed will be set similar in both analysis. With this method, the variance between the wind tunnel experimental results with the simulation result can be calculated. The parameters are the wind speed at 30 m/s and cross section area at 2125.43mm^2.

From the wind tunnel experiment:

Run	Run 1	Run 2	Run 3	
Speed (m/s)	Drag force (N)			Average
5	0.1	0.05	0.02	0.057
10	0.14	0.07	0.1	0.107
15	0.17	0.09	0.14	0.133
20	0.13	0.16	0.21	0.167
25	0.23	0.26	0.28	0.251
30	0.35	0.37	0.38	0.367
35	0.48	0.42	0.6	0.5

Table 4.2: The drag force data from wind tunnel experiment (refer appendix)

$$C_d = \frac{F_d}{\frac{1}{2} \cdot A \cdot \rho_L \cdot v^2}$$

Where:

A = cross sectional area exposed to flow

ρ_L = fluid density (density of air 1.2 kg/m^3)

C^d = 0.367/ (0.5 x 0.00212543m^2 x 1.2 x 30^2)

= **0.3198**

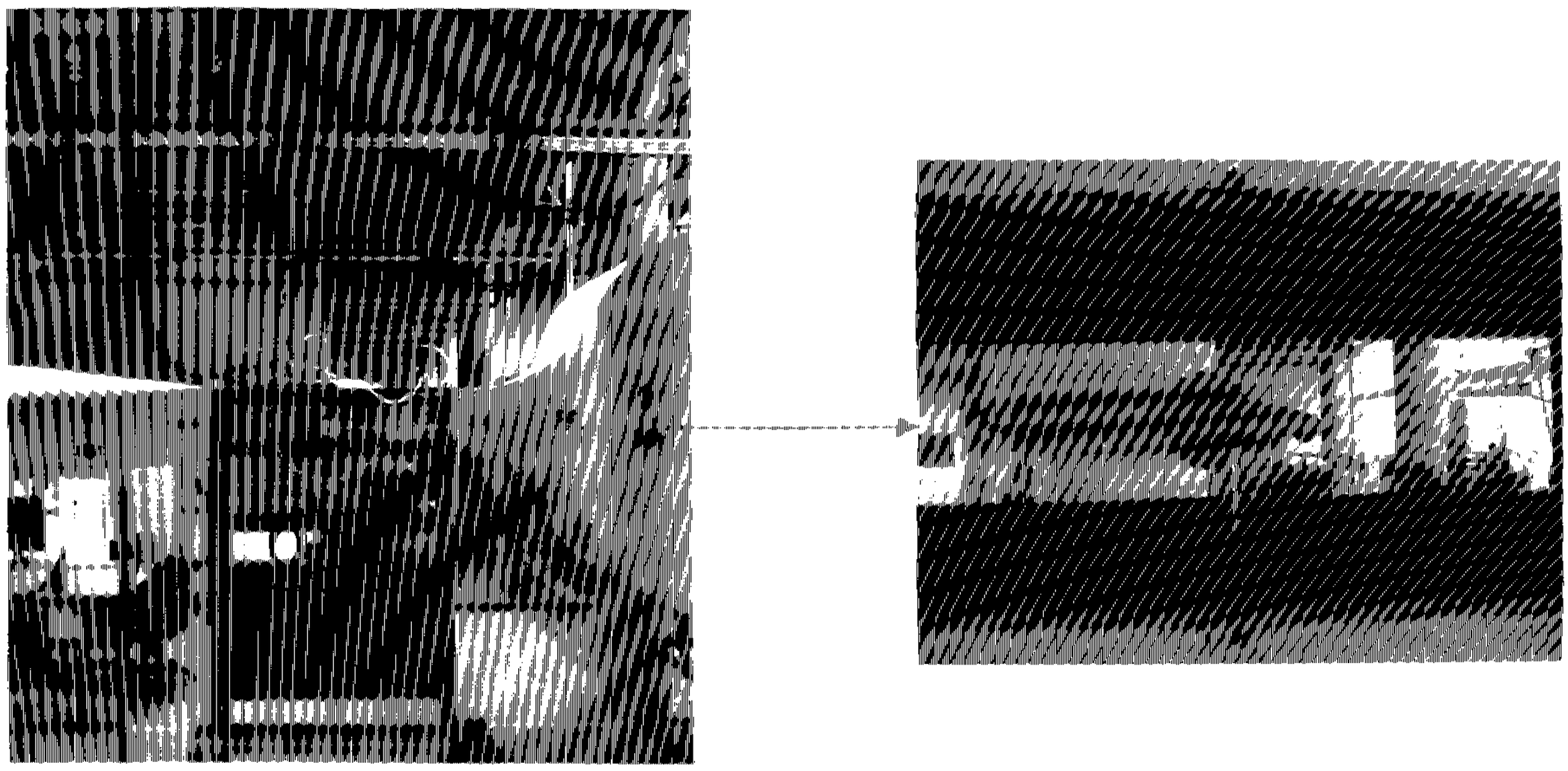

Figure 4.13: The Probe I model being place in wind tunnel

From the simulation:

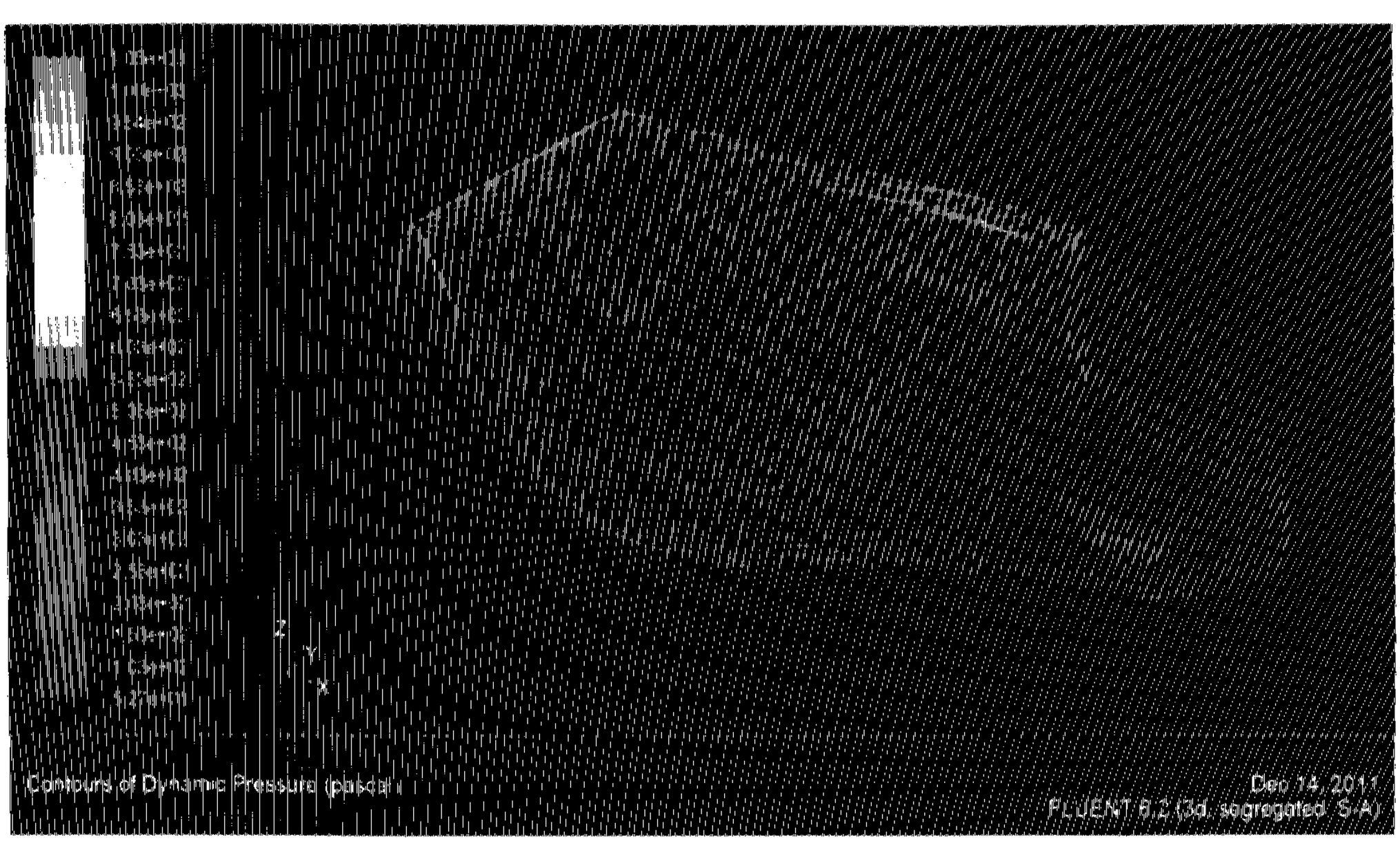

Figure 4.14: The Probe I model in simulation

Zone Name	Pressure Force	Viscous Force	Total Force	Pressure Coefficient	Viscous Coefficient	Total Coefficient
Probe 1	-0.61489147	-0.088417031	-0.7033085	-1.0039044	-0.14435434	-1.1482588

The Drag Force = $0.5\rho V^2 AC^d$

Where:

A = frontal area

ρ = density of the air

V = speed of the vehicle relative to the air

$0.5\rho V^2$ = maximum dynamic pressure

Hence, the drag coefficient, C^d is

Drag Force = $0.5\rho V^2 A C^d$,

$0.7033085\ N = 1050\ Pa \times 0.00212543 m^2 \times C^d$,

$C^d = \mathbf{0.3151}$

From the result, the variance for the result is,

$$\frac{0.3198-0.3151}{0.3151} \times 100\% = \mathbf{1.49\%}$$

The variance is very small which is **1.49%**. Hence, the simulation result can be regard as similar to the experimental result.

CHAPTER 5

CONCLUSIONS AND RECOMMENDATIONS

There are basically few types of parameters that act as sources of error in computational fluid dynamics results. First there are modeling errors that arise from the turbulence models used and the physical boundary conditions applied. The other errors stem from the numerical approximations. Here the grid design, the truncation error of the discretization scheme and the error from incomplete iterative convergence influence the solution. The floating point error caused by invalid numeric computation initiated by user or limitation of machine that being used. The possible rising issues such as invalid operations, over or underflow, rounding off errors , solver and iteration, grid problems, boundary conditions, multiprocessor issues and wrong initiation must be cater to discard this error.

The wind tunnel model should be build to validate the data from the simulation. When evaluating or testing a wind turbine, particularly for performance determination, one of the most critical measurements is that of wind speed. Uncertainty in wind speed measurements, error during a site assessment, a site calibration or a wind turbine performance test, all contribute to the overall uncertainty in predicted annual energy yield. In economic terms, this translates into financial risk and in turn into higher cost of energy. By adopting best practice in the design, selection, calibration, deployment and use of anemometry, uncertainty can be minimized. For low-accuracy quick results, computational fluid dynamics method modeling is relatively cheap, but if large quantities of more reliable data are required, then the wind-tunnel is currently better source.

REFERENCES

[1] http://en.wikipedia.org/wiki/Automotive_aerodynamics

[2] Buckley F. T., Marks C.H. and Walston W.N., A study of aerodynamics methods for improving fuel economy,US National Science Foundation, final report SIA 74 14843, University of Maryland, Dept. of Mech. Engineering, 1978

[3] Joseph Katz, January 1995, Race Car Aerodynamics – Designing for Speed, 1st Edition

[4] (Dr. V Sumantran and Dr. Gino Sovran, 1996, Wolf-Heinrich Hucho, 1998)

[5] R.H. Barnard, January 1996, Road Vehicle Aerodynamic Design – An Introduction, 1st Edition

[6] Gerhardt H. J. Kramer C. and Ammerschlager T., Aerodynamics optimization of a group 5 racing car, 4th Colloquium on Industrial Aerodynamics, Aachen 1980

[7] GAO Guang-Jun and WANG Xiao-Ya, Optimization Research on Aerodynamic Figure of the Box Car under Cross Wind Key Laboratory of Traffic Safety on the Track, Ministry of Education, Central South University Changsha, China

[8] Smith C., Tune to Win, Aero Publishers, Fallbrook Calif., USA, 1978

[9] Graysmith J.J.,Baxendale A.J.,Howell J.P. and Haines T., Comparison between CFD and experimental results, Proc. Vehicle Aerodynamics Conference, Loughborough,RAeS,18-19 July 1994,pp. 30.1-11

[10] Buchheim R., Maretzke J. and Piatek R., The control of aerodynamic parameters influencing vehicle aerodynamics, SAE paper No. 850279, 1985

[11] Carr G. W., Potential for aerodynamics drag reduction in car design, in: Impact of Aerodynamics on Vehicle Design, Proc. International Assosiation for Vehicle Design: Technological Advances in Vehicle Design, SP3, ed. Dorgham M.A., 1983, pp 44-56

[12] Cogotti A., Aerodynamic characteristics of car wheels, Impact of Aerodynamics on Vehicle Design, Proc. International Association for Vehicle Design: Technological Advances in Vehicle Design, SP3, ed. Dorgham M. A., 1983, pp 96-173

[13] Hoerner S. F., Aerodynamic Drag, Hoerner, PO Box 342, Brick Town N.J. 08723, USA

[14] Barnard R.H., The aerodynamic tuning of a group C sports car, Journal of Wind Engineering and Industrial Aerodynamics, Vol. 22,Elsevier Science Publications,1986,pp. 279-89

APPENDIXES

CATIA v5

Mechanical Design Solutions that provides products for intuitive specification driven modeling for solid, hybrid, assembly design and integrated drafting. From concept to detailed design and onto drawing production, the CATIA Version 5 Mechanical Design products accelerate core activities of product development. Mechanical Design Products allows the user to create parts in a highly productive and intuitive environment, to enrich existing mechanical part design with wireframe and basic surface features and then easily establish mechanical assembly constraints, automatically positions parts and checks assembly consistency. Advanced Drafting capabilities are also provided through the associative drawing generation from 3D part and assembly designs. Mechanical Design products can address 2D design and drawing production requirements with a stand-alone state-of-the-art 2D tool interactive drafting. The model was design in part design of mechanical assembly in one piece block in order to ease the analysis work. Hence the block will regard as one complete and simple shape volume afterwards. In CATIA v5 the modeling work is quite simple as the software owns user friendly attribute.

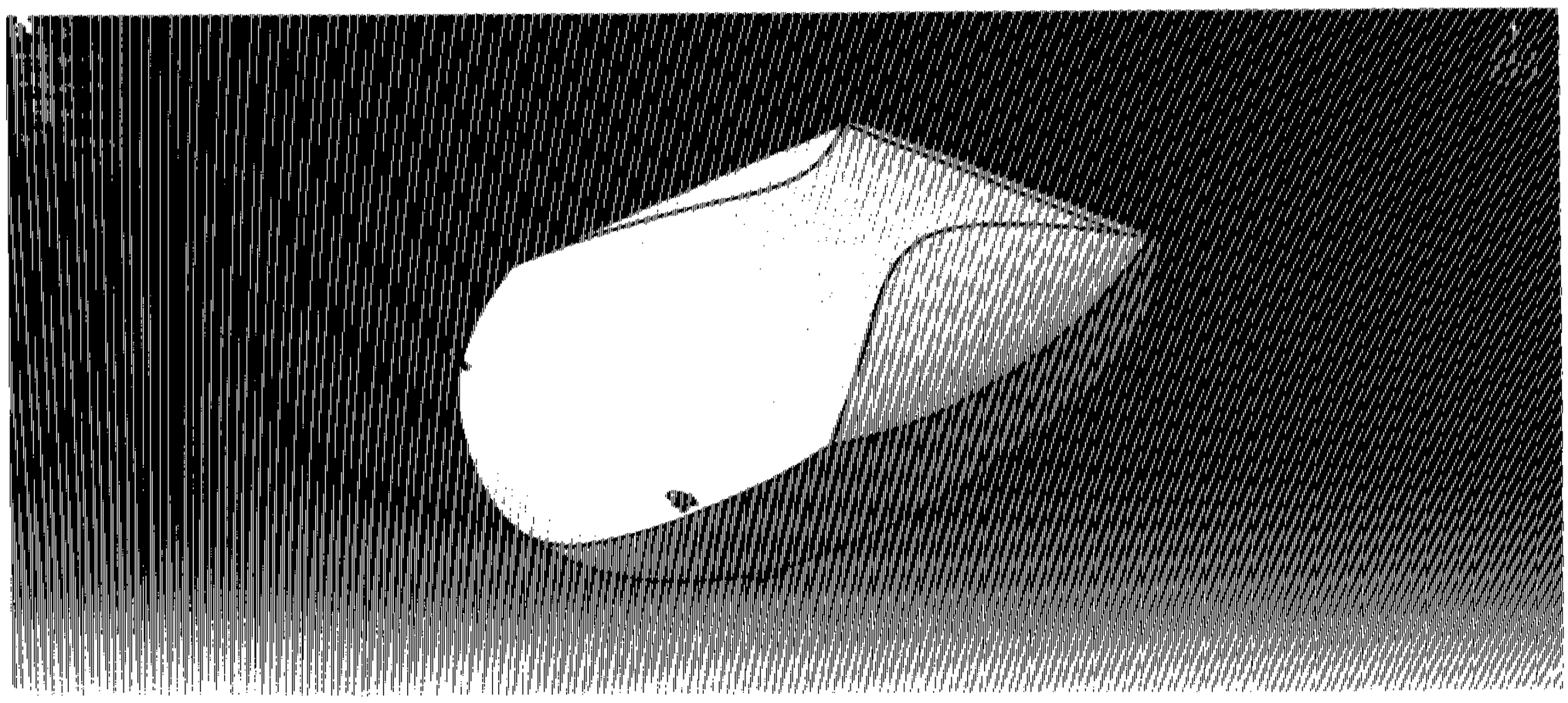

Stream model isometric view

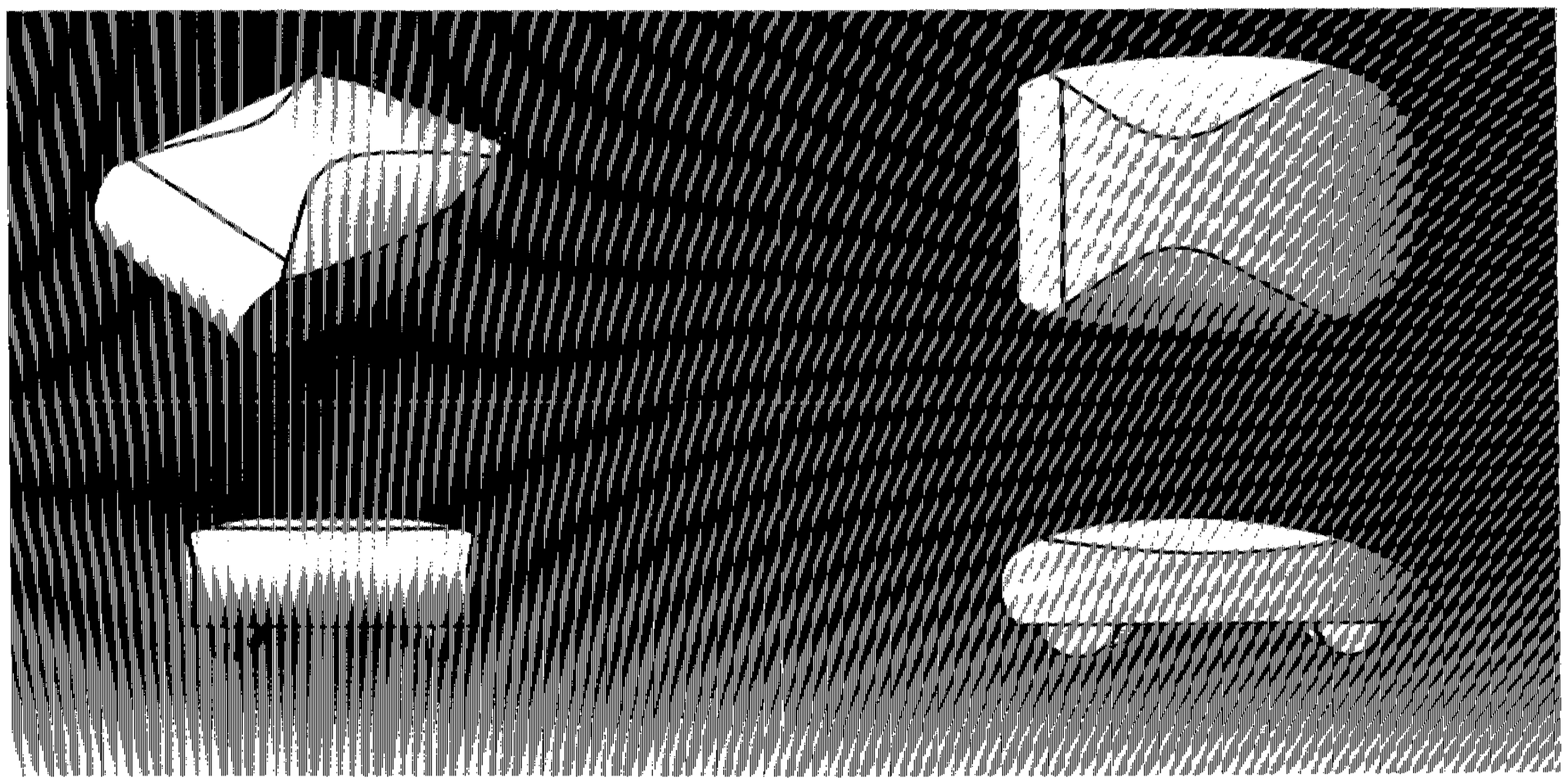

Stream model isometric multi-view

The model will be inserted in a rectangular box. The remove Boolean operation is used to remove the model thus will create a hollow in the rectangular box. Hence the box now can be regard as a rectangular with a car model mold inside it.

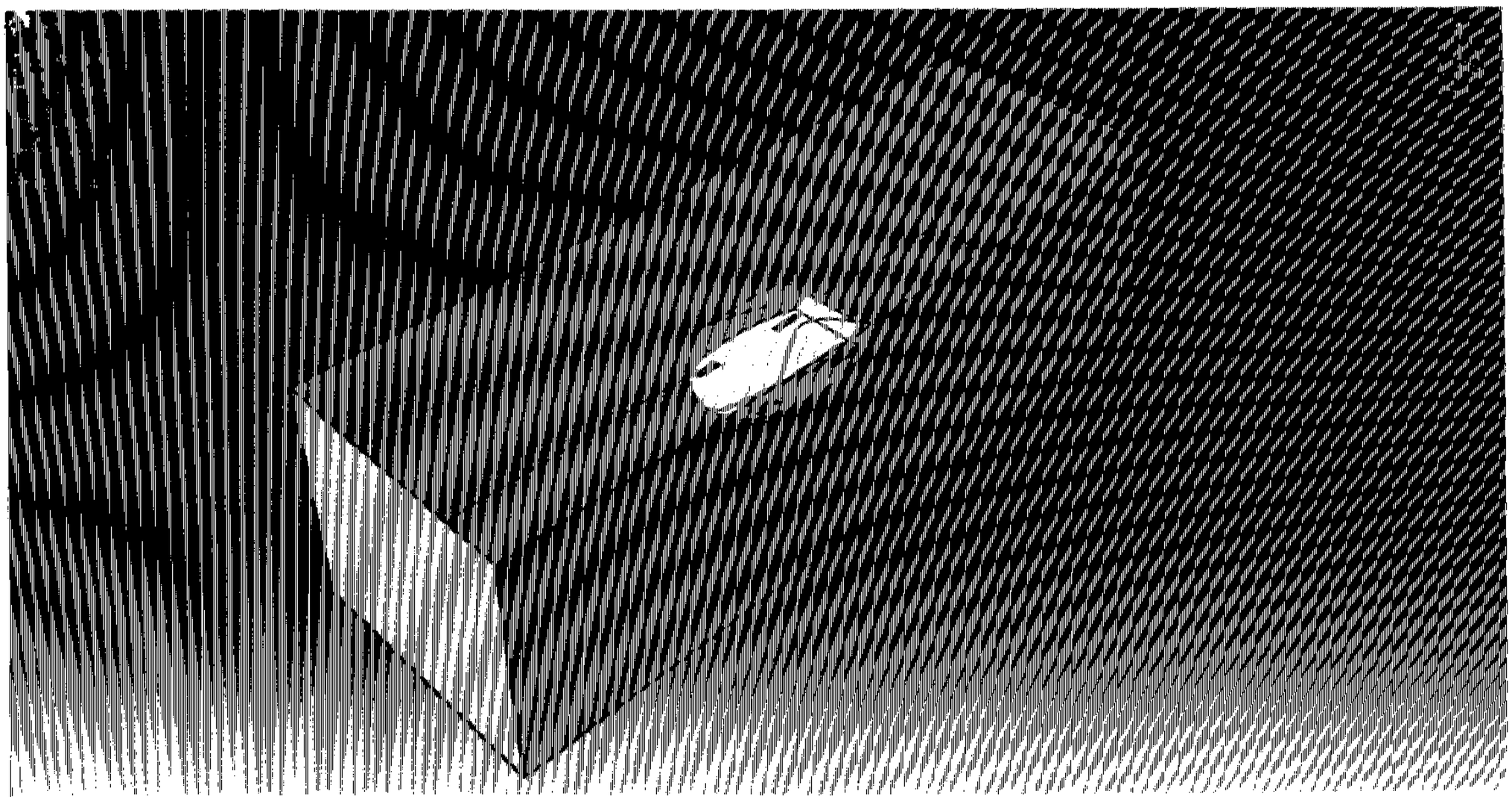

Stream model in rectangular box

The reason of this work is to analyze the model in one complete rectangular volume. The rectangular will be regards as air where air come in from the front side of the car and air leave at the backside of the car. This work will continue in GAMBIT v2.2.30.The file must be saved as igs file to allow GAMBIT to read it.

GAMBIT v2.2.30

The simulation was done by using two softwares which are GAMBIT v2.2.30and FLUENT v6.3.26. GAMBIT is Fluent's geometry and mesh generation software. GAMBIT's single interface for geometry creation and meshing brings together most of Fluent's preprocessing technologies in one environment. Advanced tools for journaling let you edit and conveniently replay model building sessions for parametric studies. GAMBIT's combination of CAD interoperability, geometry cleanup, decomposition and meshing tools results in one of the easiest, fastest, and most straightforward preprocessing paths from CAD to quality CFD meshes.

As a state-of-the-art preprocessor for engineering analysis, GAMBIT has several geometry and meshing tools in a powerful, flexible, tightly-integrated, and easy-to use interface. GAMBIT can dramatically reduce preprocessing times for many applications. Most models can be built directly within GAMBIT's solid geometry modeler, or imported from any major CAD/CAE system. Using a virtual geometry overlay and advanced cleanup tools, imported geometries are quickly converted into suitable flow domains. A comprehensive set of highly automated and size function driven meshing tools ensures that the best mesh can be generated, whether structured, multiblock, unstructured, or hybrid. GAMBIT's range of CAD readers, in this case CATIA, allows you to bring in any geometry, error free, into its meshing environment. GAMBIT also has an excellent boundary layer mesher for growing optimum grid cells off wall surfaces in your geometries for fluid flow simulation purposes.

The partial differential equations that govern fluid flow and heat transfer are not usually amenable to analytical solutions, except for very simple cases. Therefore, in order to analyze fluid flows, flow domains are split into smaller subdomains (made up of geometric primitives like hexahedra and tetrahedra in 3D and quadrilaterals and triangles in 2D). The governing equations are then discretized and solved inside each of these subdomains. Typically, one of three methods is used to solve the approximate version of the system of equations: finite volumes, finite elements, or finite differences. Care must be taken to ensure proper continuity of solution across the common interfaces between two subdomain. The subdomains are often called elements or cells, and the collection of all elements or cells is called a mesh or grid.

The presence of Gambit provides better algorithms and more computational power has become available to CFD analysts, resulting in diverse solver techniques. One of the direct results of this development has been the expansion of available mesh elements and mesh connectivity (how cells are connected to one another). The easiest classifications of meshes are based upon the connectivity of a mesh or on the type of elements present.

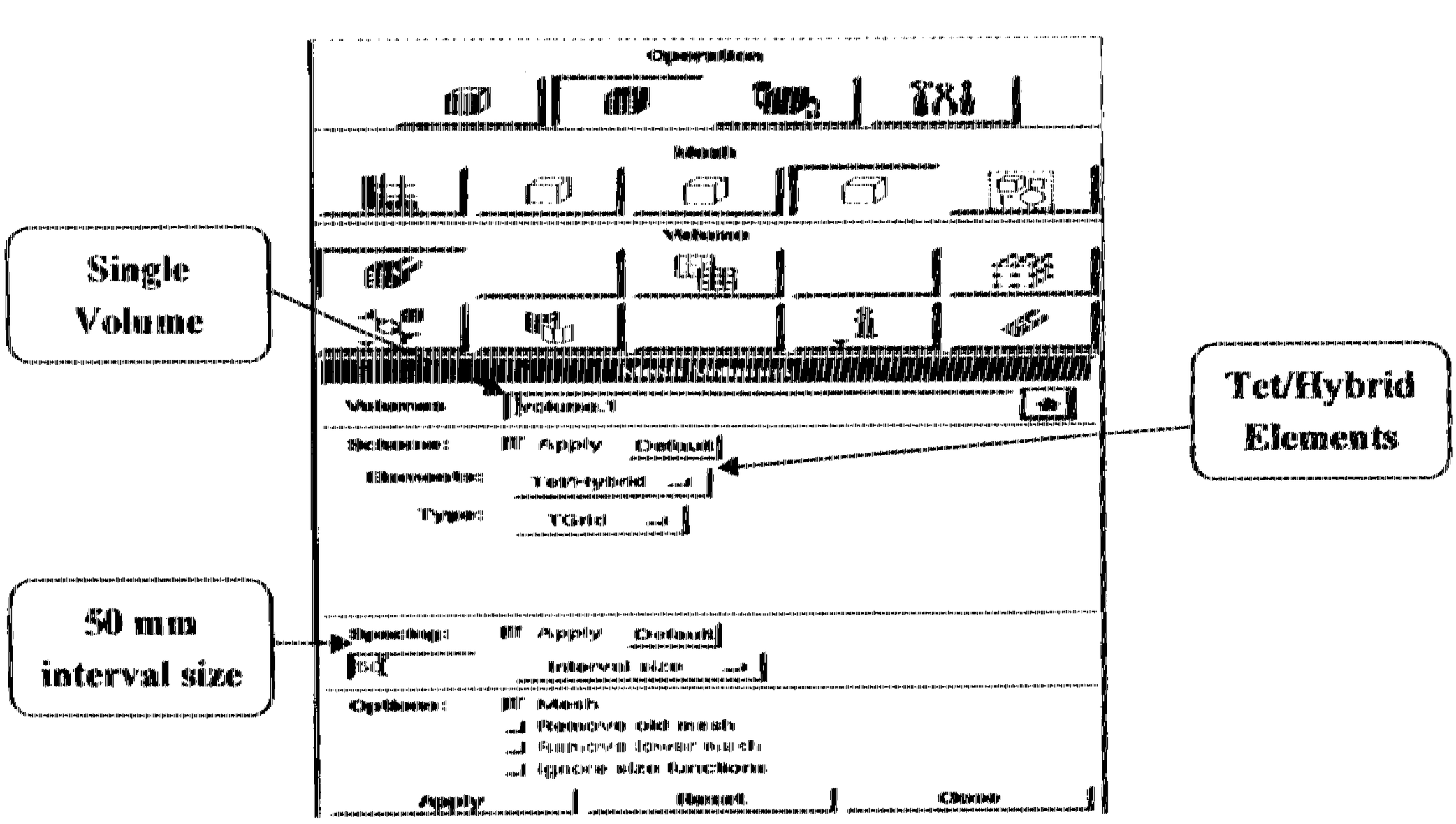

Volume Mesh Operation

Before meshing, ensure the wireframe is in green color and not yellow color. Green wireframe color the model is good while yellow color will cause error. Thus, the steps in the modeling CATIA software need to be revise again to clear the error. For example, conflict in the extrude command, hidden figures and others.

This analysis is only involved in single volume mesh operation only. Thus edge and face mashes should be ignore. In volume mesh operation there are Tet/Hybrid elements and TGrid type. Tet is the short form for tetrahedral mesh. A hybrid or non-conformal mesh it means it is a mix of structured hexahedral cells and unstructured tetrahedral cells. In the meshing of the 3D model used for this project, the element chosen is Tet/Hybrid and the type is TGrid. The Tet/Hybrid element is chosen because GAMBIT will automatically mesh the entire volume with unstructured three-dimensional grid according to the geometry of the model. The description for each option can be seen in Table 1 below:

Mesh	Description
Tet/Hybrid	Specifies that the mesh is composed primarily of tetrahedral elements but may include hexahedral, pyramidal, and wedge elements where appropriate.
TGrid	Specifies that the mesh is composed primarily of tetrahedral mesh elements but may include hexahedral, pyramidal, and wedge elements where appropriate.

Mesh element and type description.

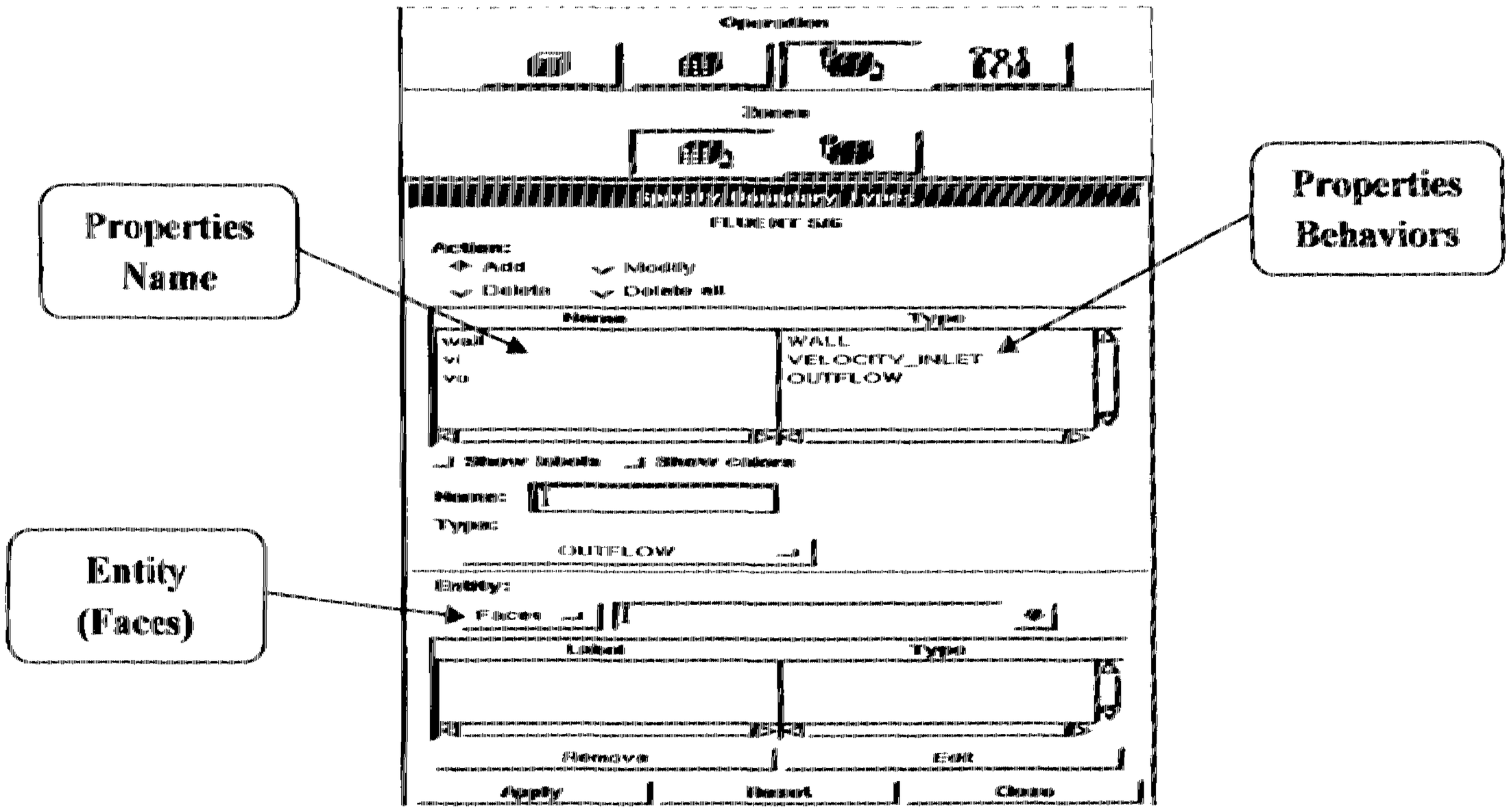

Specify Boundary Types

The boundary names of the rectangular consist of wall, vi/inlet velocity and vo/outlet velocity. The boundary entity is face entity. Referring to figure 5.14, the figure shows the location of boundary on the specific face. If the user not specifies the boundary as anything, then it will automatically be classified as a default interior by fluent.

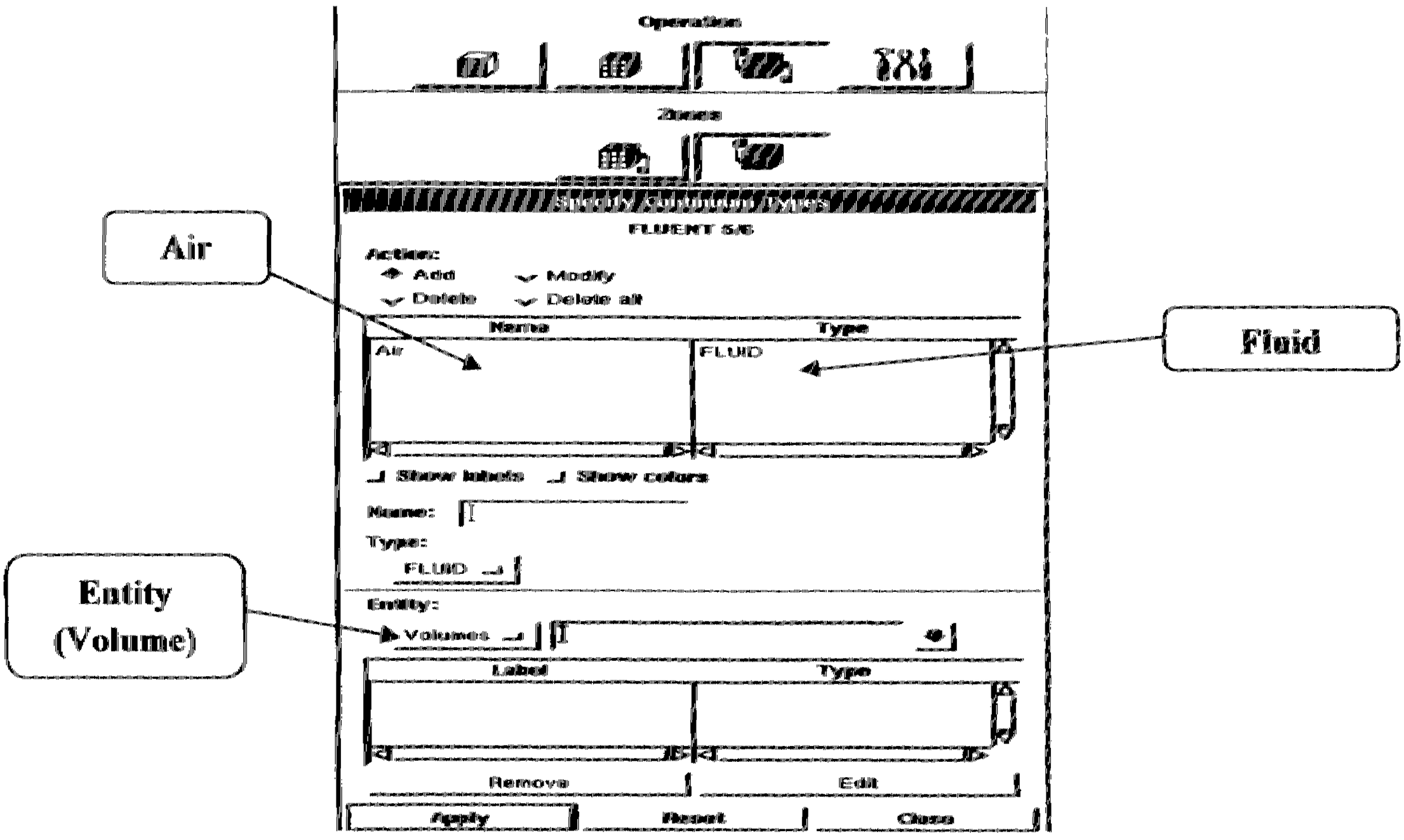

Specify Continuum Types

To specify the continuum type, just type the name as air and choose as fluid. The volume should be single volume and clicks apply. After done all the process, save the file as mesh file / msh.

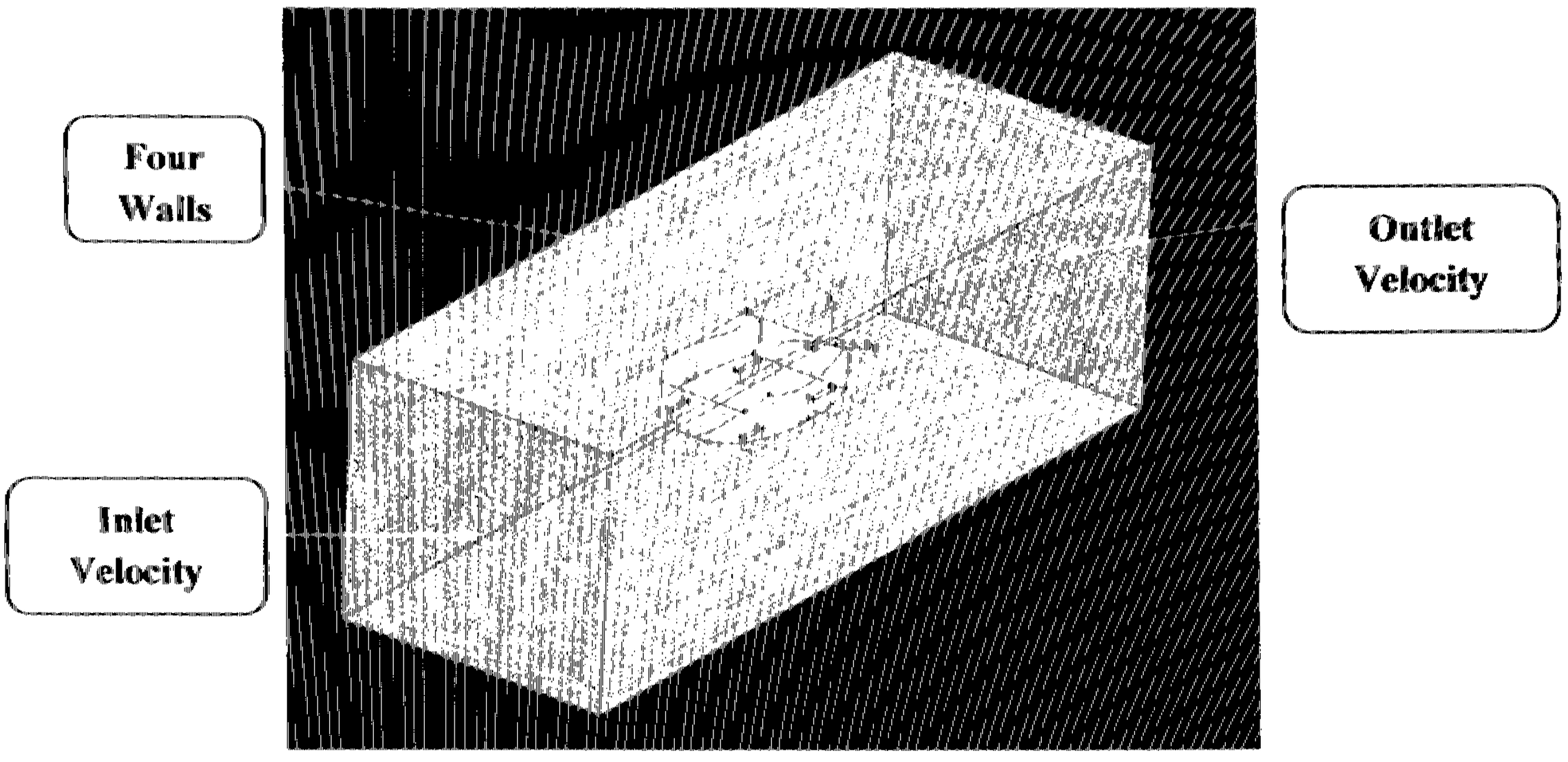

Isometric Meshed Rectangular Air Shape

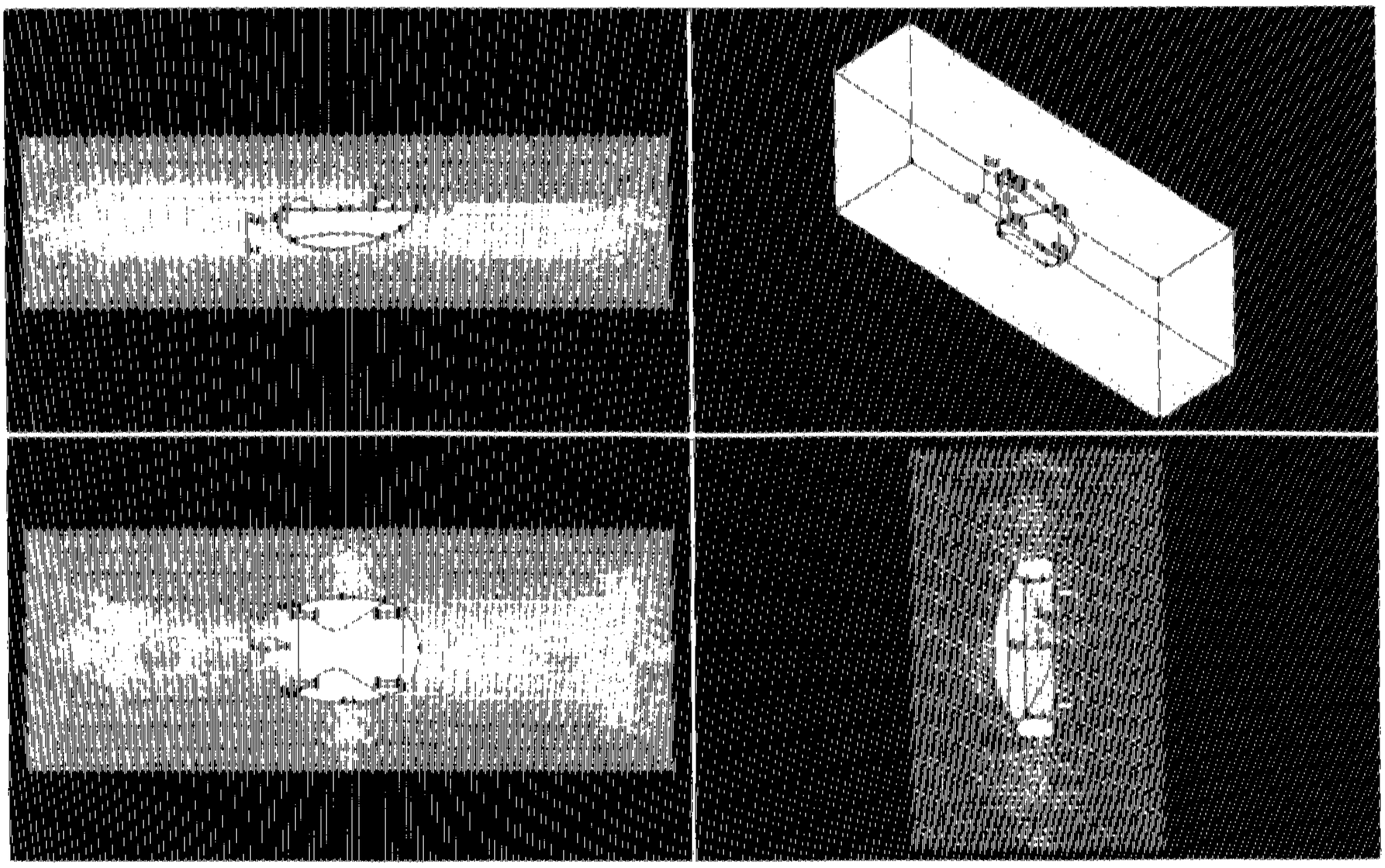

Multi View Meshed Rectangular Air Shape

FLUENT v6.3.26

FLUENT software contains the broad physical modeling capabilities needed to model flow, turbulence, heat transfer, and reactions for industrial applications ranging from air flow over an aircraft wing to combustion in a furnace, from bubble columns to oil platforms, from blood flow to semiconductor manufacturing, and from clean room design to wastewater treatment plants. Special models that give the software the ability to model in-cylinder combustion, aero acoustics, turbo machinery, and multiphase systems have served to broaden its reach.

Today, thousands of companies throughout the world benefit from the use of ANSYS FLUENT software as an integral part of their design and optimization phases of product development. Advanced solver technology provides fast, accurate CFD results, flexible moving and deforming meshes, and superior parallel scalability. User-defined functions allow the implementation of new user models and the extensive customization of existing ones.

The interactive solver setup, solution and post-processing capabilities of FLUENT make it easy to hold a calculation, examine results with integrated post-processing, change any setting, and then continue the calculation within a single application. Case and data files can be read into CFD-Post for further analysis with advanced post-processing tools and side-by-side comparison of different cases. The platform also allows data and results to be shared between applications using an easy drag-and-drop transfer, for example, to use a fluid flow solution in the definition of a boundary load of a subsequent structural mechanics simulation.

To start Fluent v6.3.26 from the command line, you can specify the dimensionality of the problem (2D or 3D), as well as the precision of calculation (single or double).

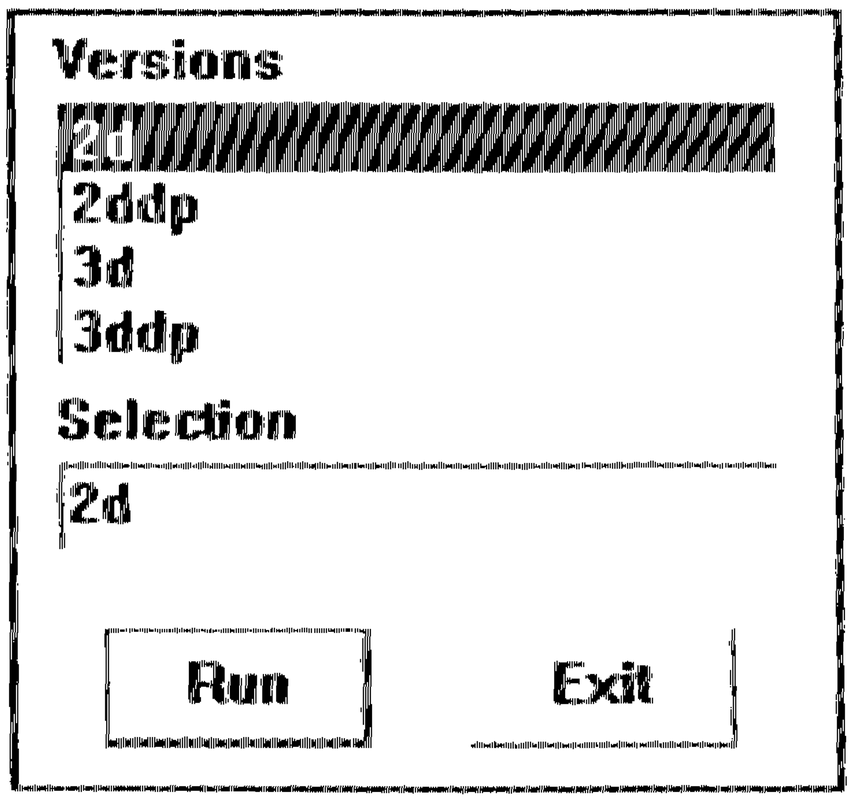

- **fluent6 2d** runs the two-dimensional, single-precision solver
- **fluent6 3d** runs the three-dimensional, single-precision solver
- **fluent6 2ddp** runs the two-dimensional, double-precision solver
- **fluent6 3ddp** runs the three-dimensional, double-precision solver

In this case, the fluent6 3d will be chosen to run the simulation.

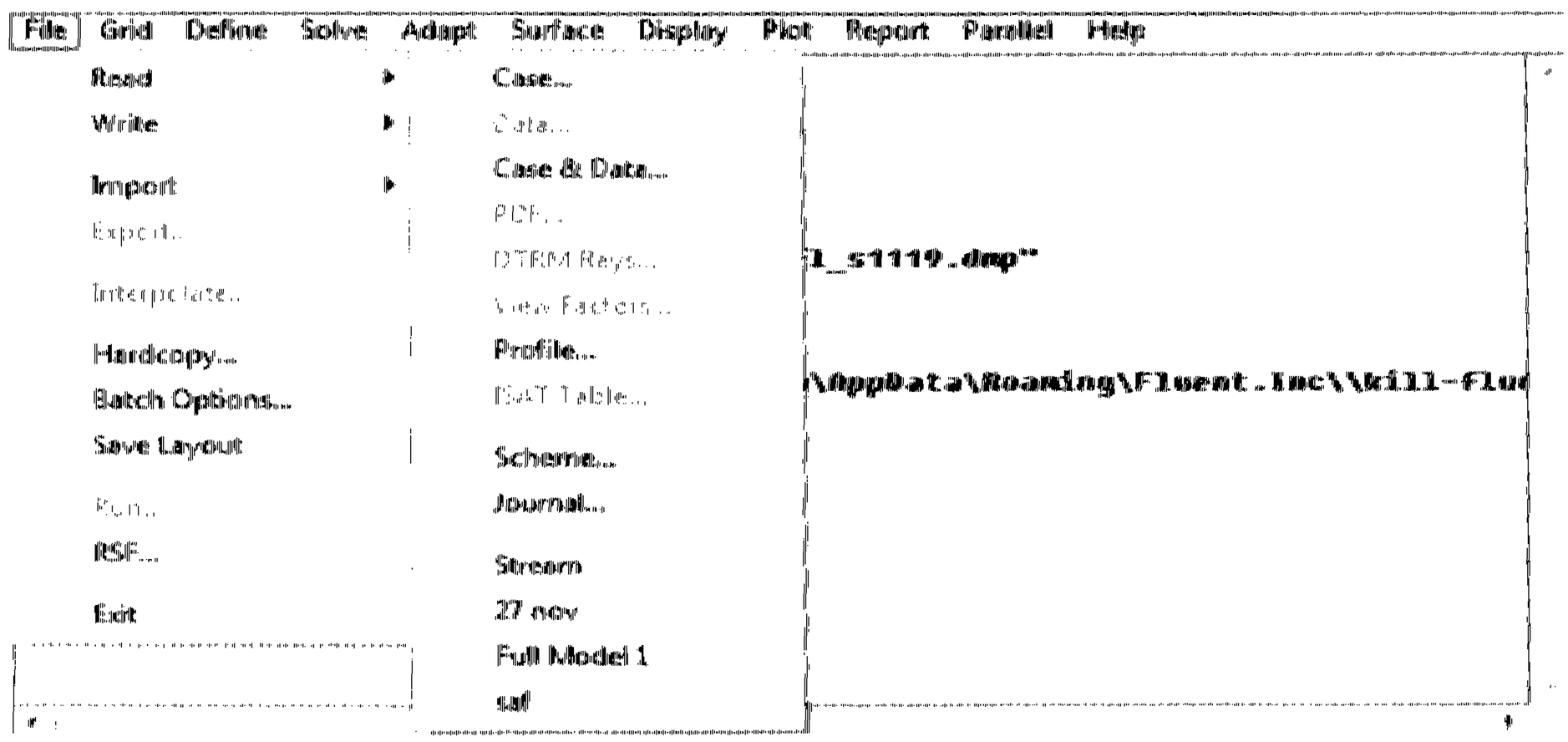

Select File/Read/Case to read the mesh file from GAMBIT.

Check the grid of the mesh file. Then check the scale of the model in millimeter.

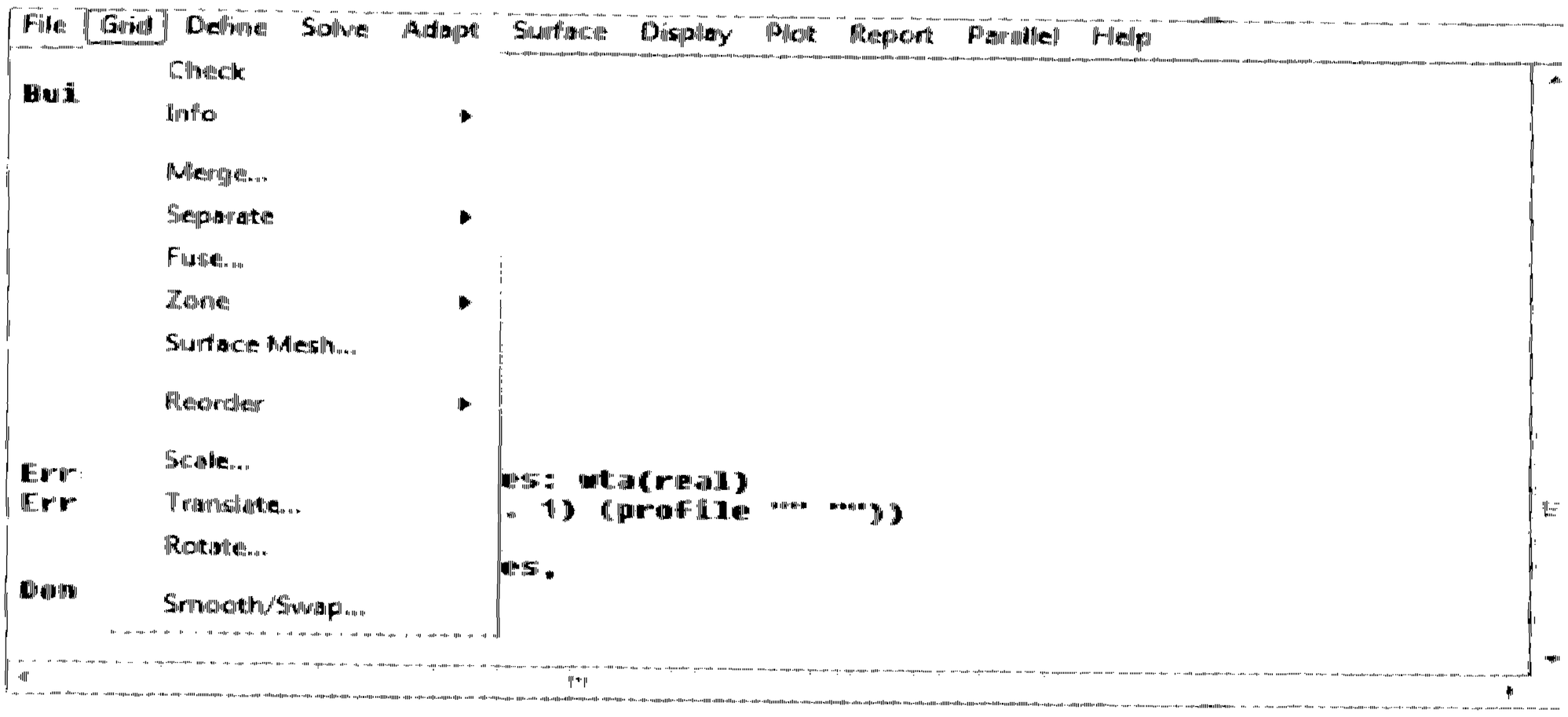

The type of flow modeled in fluent to analyze the flow around the car model is the three-dimensional flow along the axis of symmetry. For air flows, use the density-based implicit solver since it is the solver of choice for compressible, transonic flows without significant regions of low-speed flow.

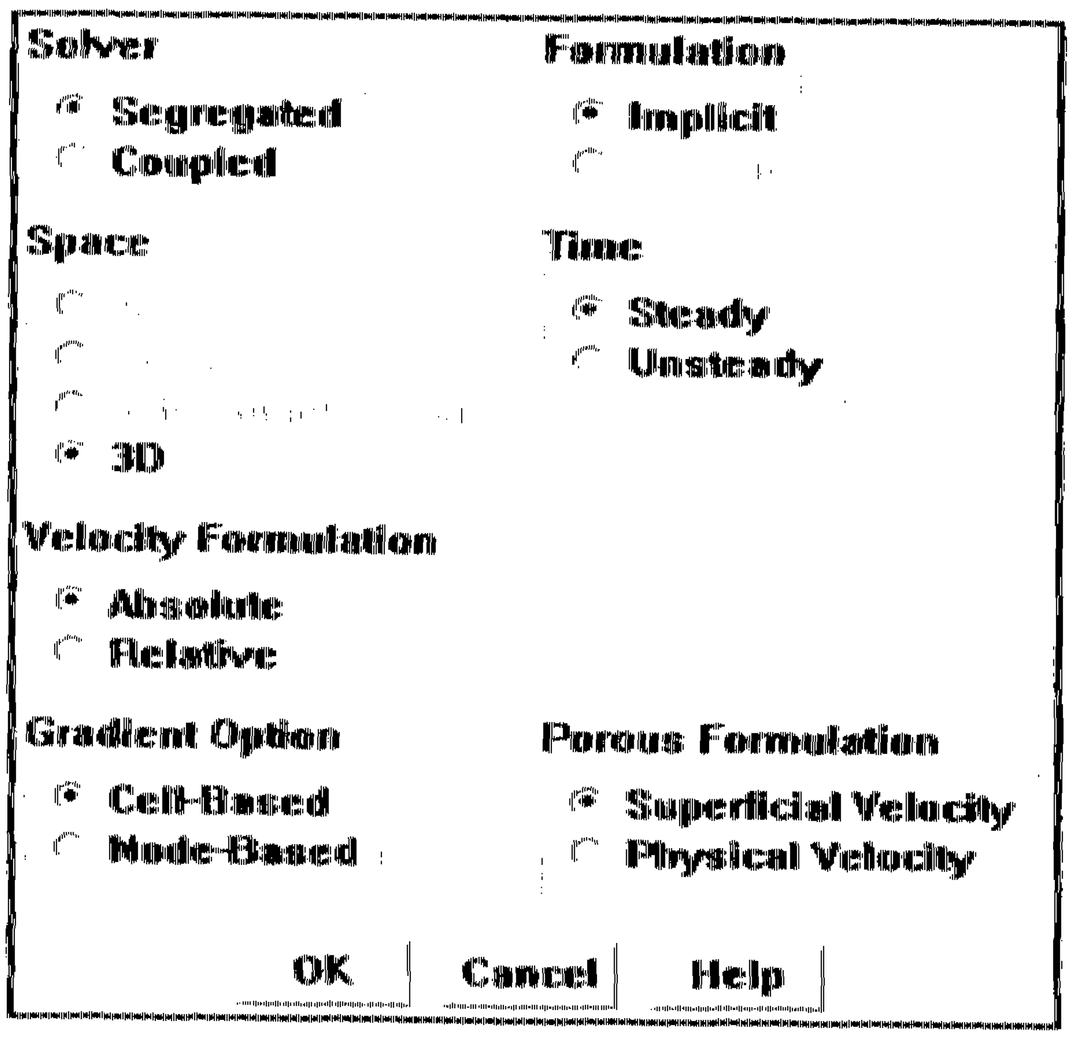

Define the model solver as segregated and choose the explicit formulation. In the explicit scheme a multi-stage, time-stepping algorithm Numerical Solution of the Euler Equations by Finite Volume Methods Using Runge-Kutta Time-Stepping Schemes is used to discretize the time derivative.

By default, fluent uses a 3-stage Runge-Kutta scheme based on the work by J. F. Lynn (*Multigrid Solution of the Euler Equations with Local Preconditioning, PhD thesis, University of Michigan, 1995*) for steady-state flows that use the density-based explicit solver.

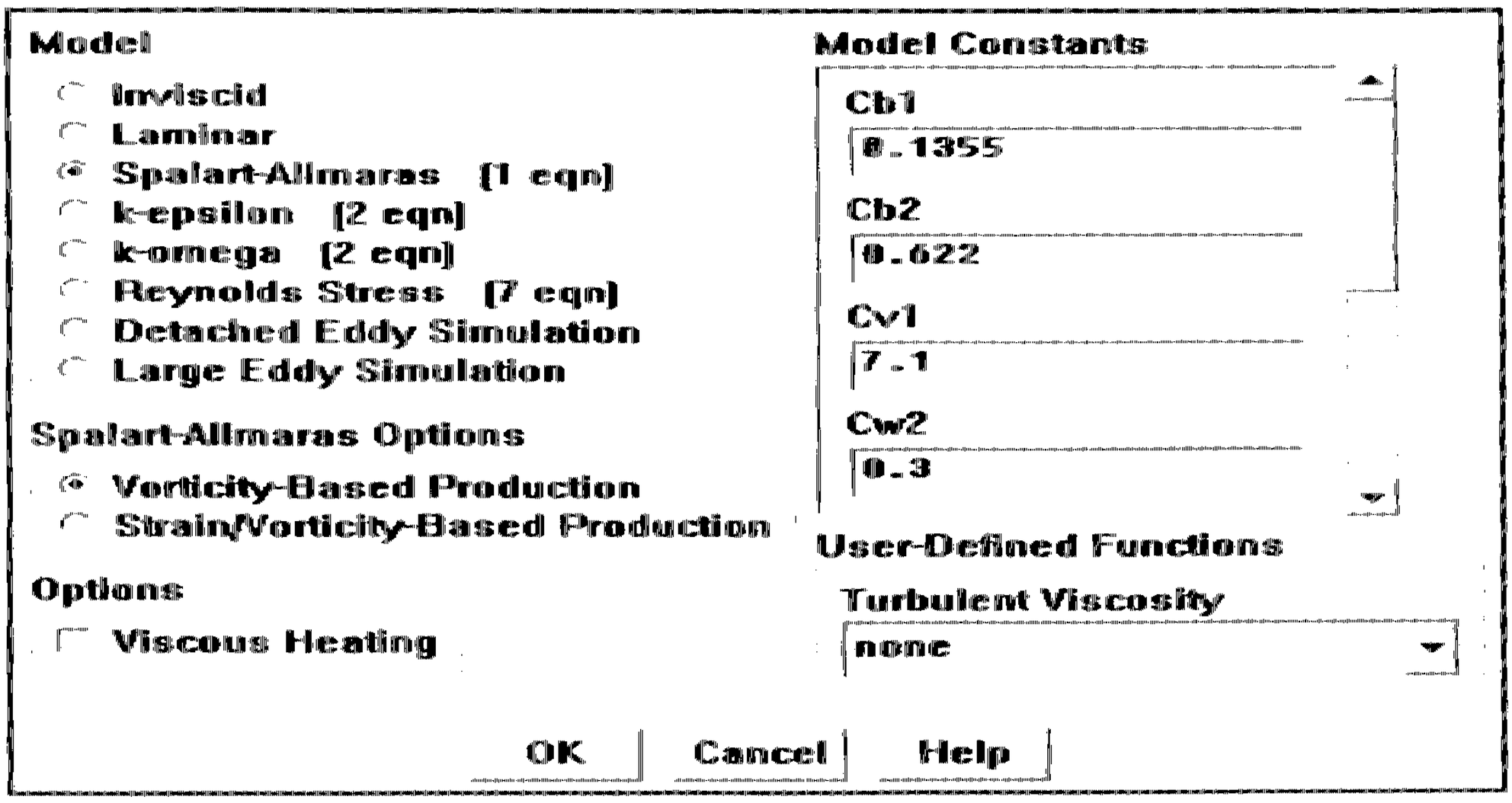

For viscous model, select Spalart-Allmaras model. It is a one equation model which solves a transport equation for a viscosity-like variable $\tilde{\nu}$. This may be referred to as the Spalart-Allmaras variable. Boundary conditions are set by defining values $\tilde{\nu}$ of Freestream boundary conditions are discussed in turbulence free-stream boundary conditions. Walls: $\tilde{\nu} = 0$

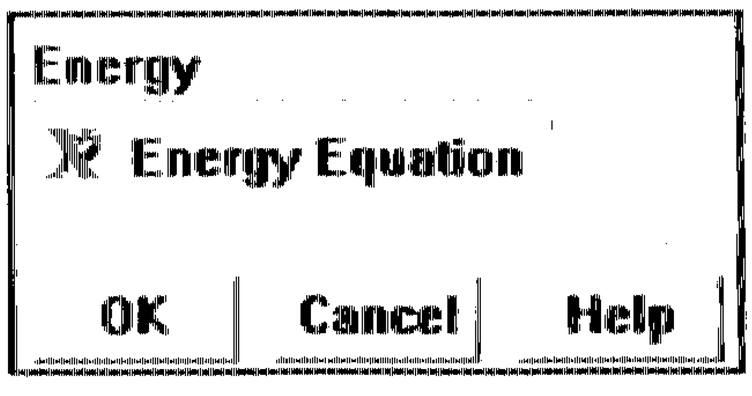

For the road vehicles, the effect of compressibility (air density changes) is negligible, the energy equation is not required, and a simplified 'incompressible' version of the Navier-Stokes equations can be used, thus save processor memory. Pressure work and kinetic energy are **always** accounted for when you are modeling compressible flow or using the density-based solver.

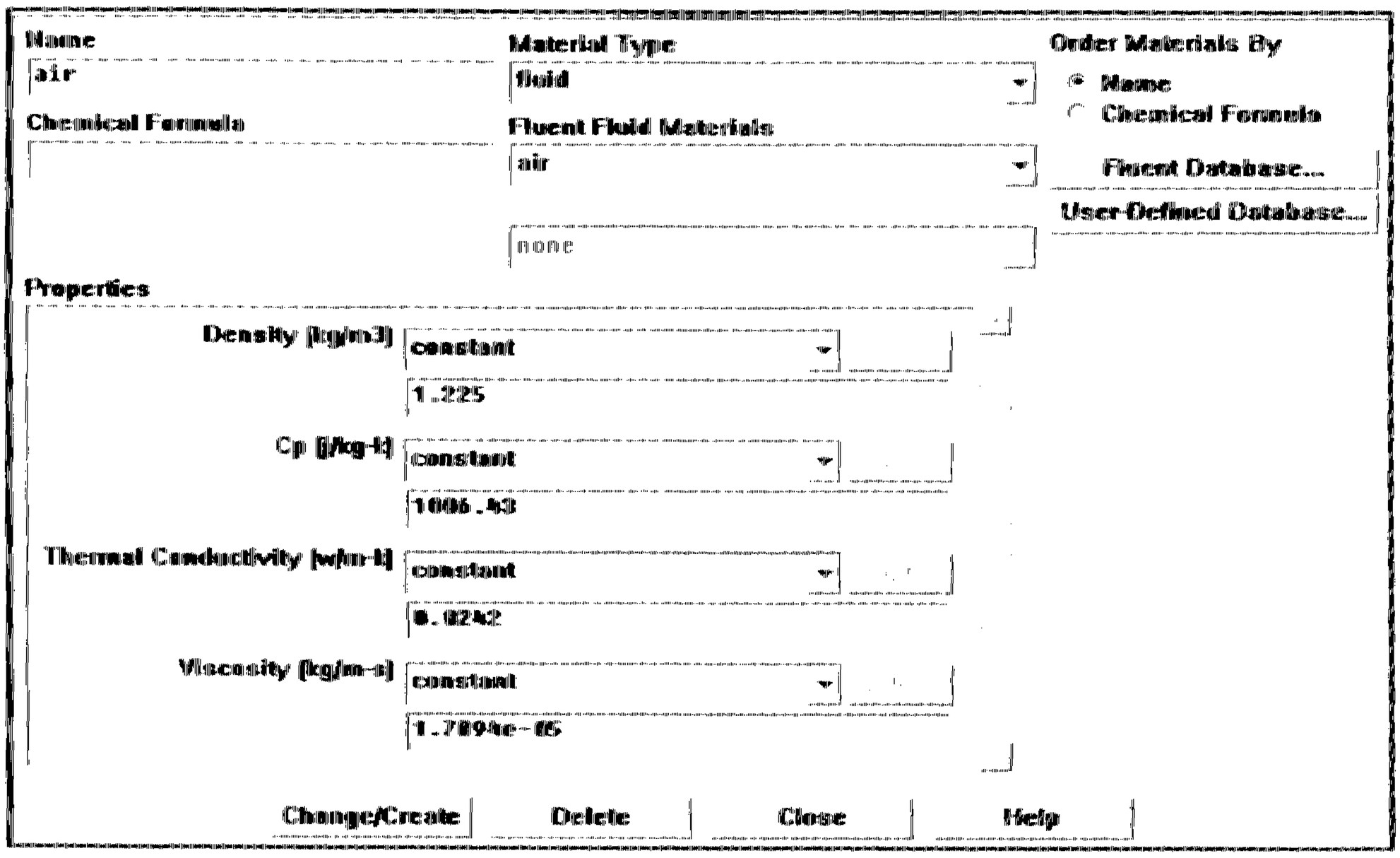

The material of the rectangular as set in the GAMBIT is air. Check the air properties such as density, specific heat capacity at constant pressure, thermal conductivity and viscosity. In default setting, fluent stores the data of air properties in the fluent database.

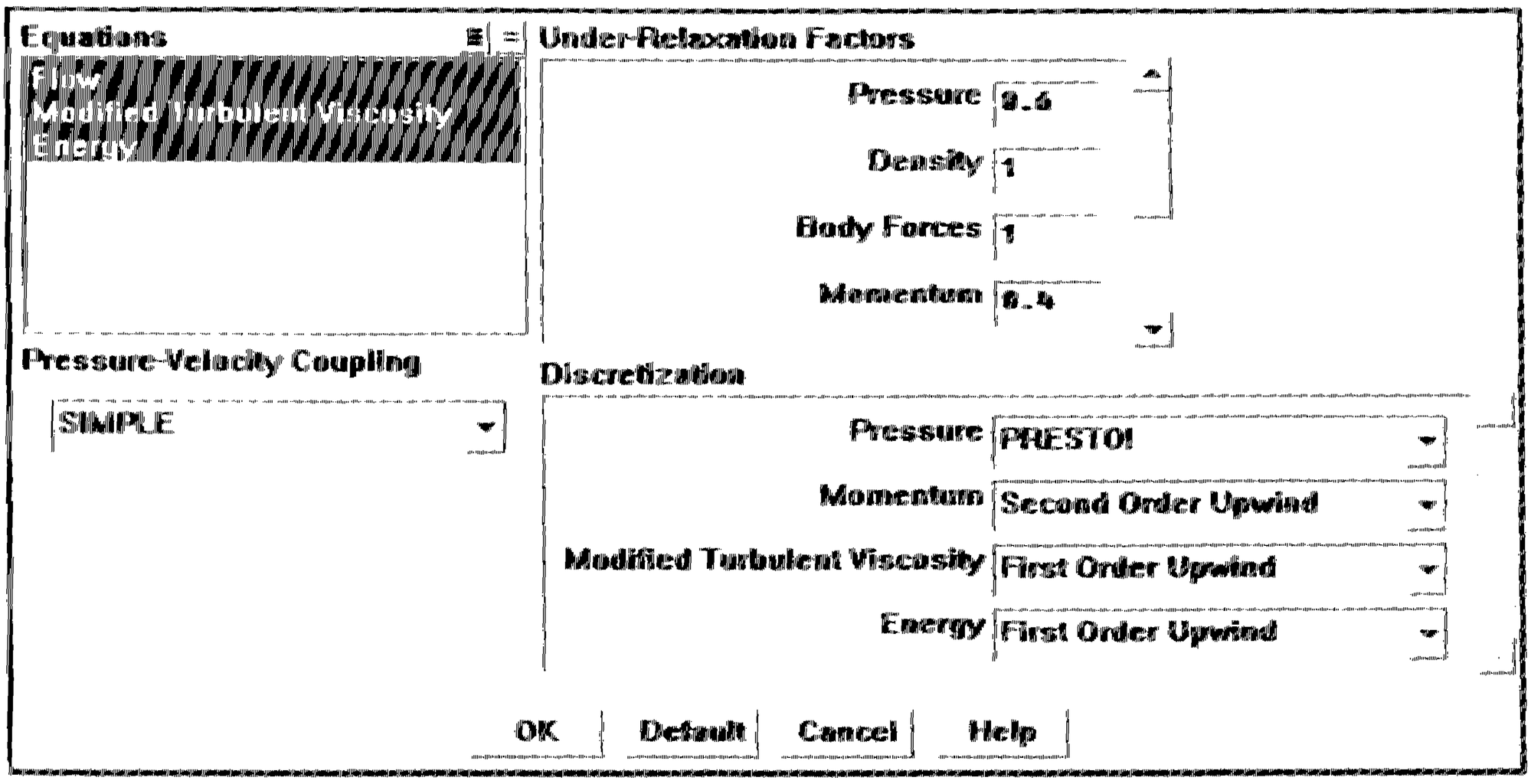

From figure above, there are three equations are those being used namely flow, modified turbulent viscosity and energy equations. Set the pressure-velocity coupling as SIMPLE [Semi-Implicit Method for Pressure-Linked Equations]. If a steady-state problem is being solved iteratively, it is not necessary to fully resolve the linear pressure-velocity coupling, as the changes between consecutive solutions are no longer small. The SIMPLE algorithm:

- An approximation of the velocity field is obtained by solving the momentum equation. The pressure gradient term is calculated using the pressure distribution from the previous iteration or an initial guess.
- The pressure equation is formulated and solved in order to obtain the new pressure distribution.
- Velocities are corrected and a new set of conservative fluxes is calculated.

For this case use pressure discretization as PRESTO! To discretize momentum equation, one needs pressure values on the control volume faces.

Standard pressure discretization interpolates the pressure on the faces using the cell center values. On the other hand PRESTO! discretization for pressure actually calculates pressure on the face. This is possible using staggered grids where velocity and pressure variables are not "co-located".

PRESTO! discretization gives more accurate results since interpolation errors and pressure gradient assumptions on boundaries are avoided. This scheme works better for problems with strong body forces (swirl) and high Rayleigh number flows (natural ventilation). PRESTO! however, is more computationally costly, since you need more memory for "alternate" grids.

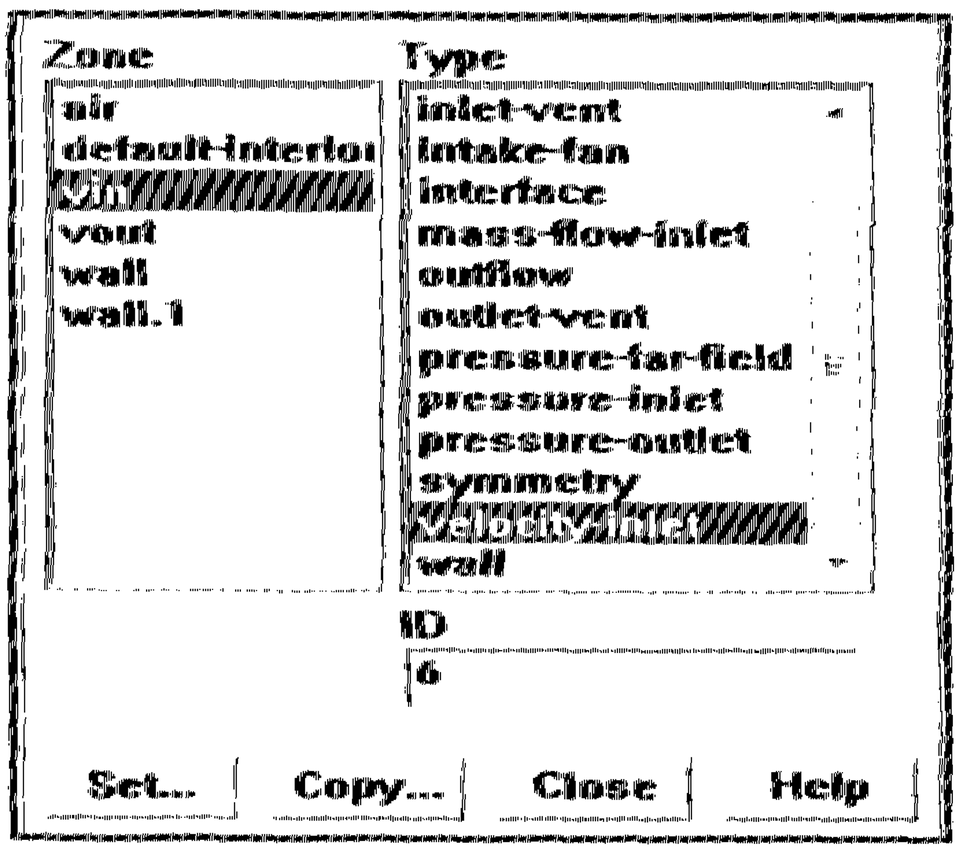

The boundary condition can be set as figure above. In zone column the input velocity/vin may be chosen and in type column, select velocity-inlet and click set.

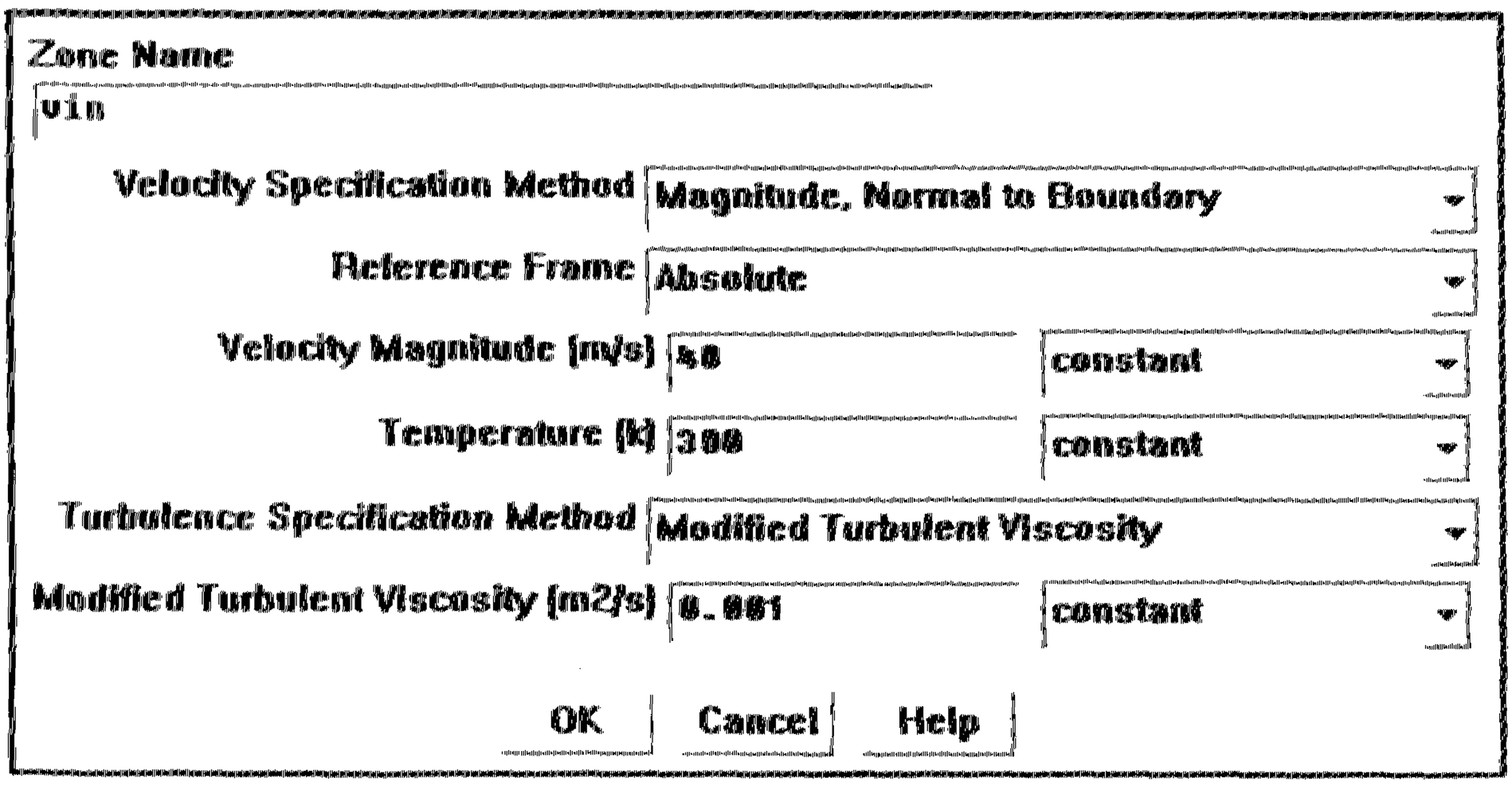

Set the velocity magnitude as 40 m/s which is about 144 km/h. Use default data for other settings.For all the repetition experiment, the velocity magnitude will be 40 m/s.

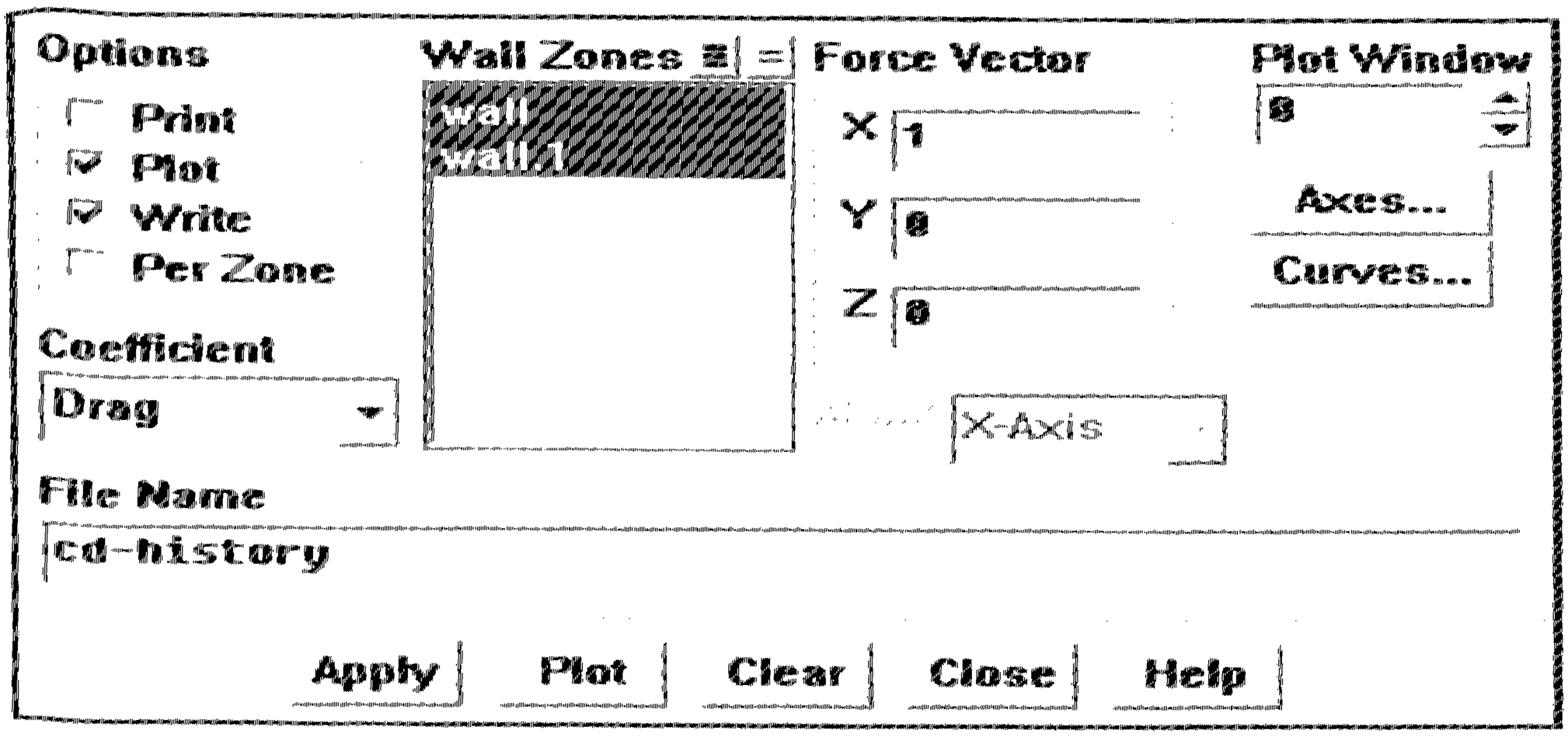

The forces can be monitor on tab solve/monitors/forces. This is an important data in order to calculate the drag coefficient. In option, tick plot and write. Select wall zones as wall.1 which is the wall of the car model inside the rectangular. The force vector is needed in x-direction only.

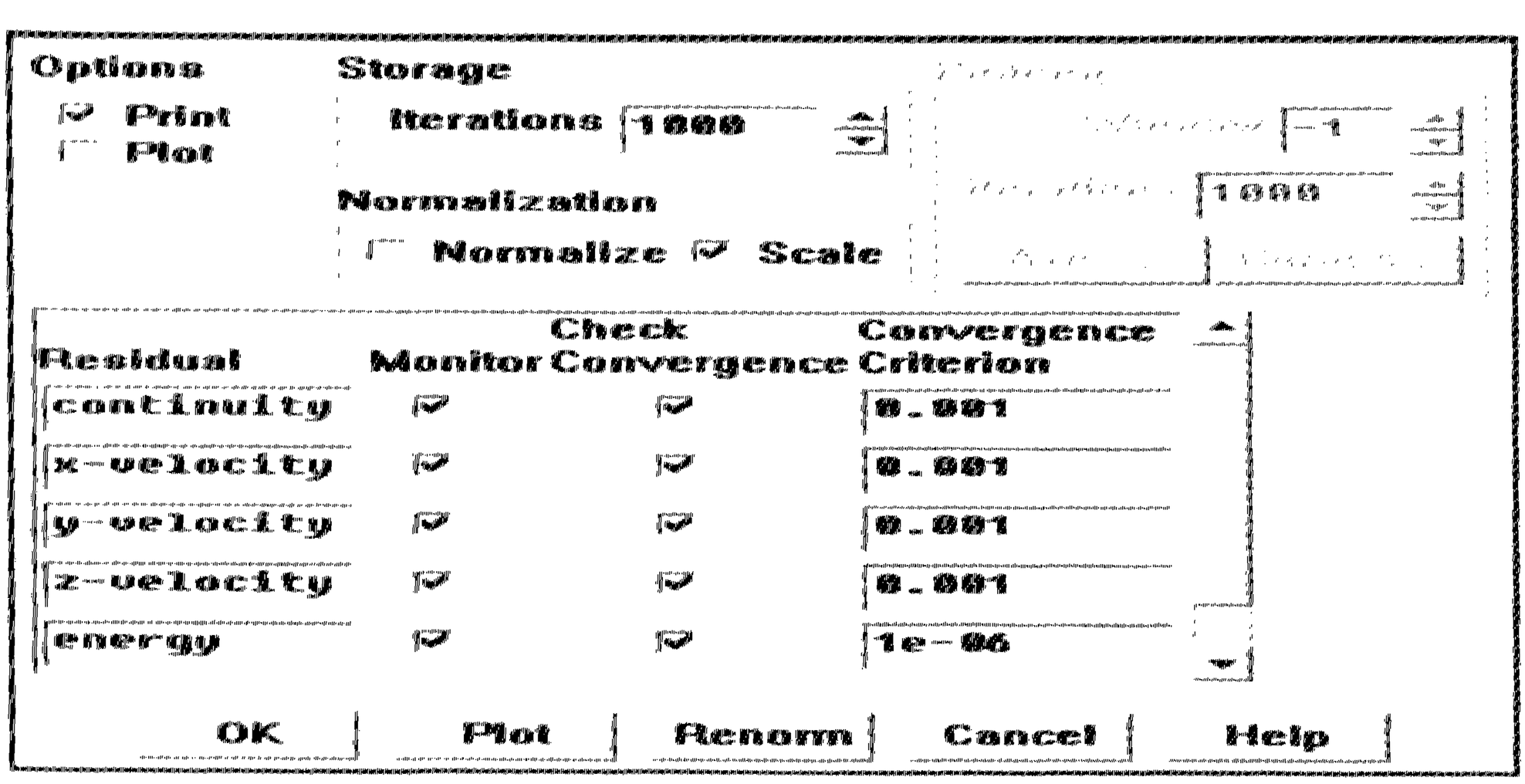

The residual graph can be monitor on tab solve/monitors/residual. The residual consist of continuity, x-velocity, y-velocity, z-velocity and energy. Tick to check for both monitor and convergence. The convergence criterion for all residual is 0.001 except for energy which is 10e-06. The storage for iterations is set to be 1000. Tick print and plot the residual.

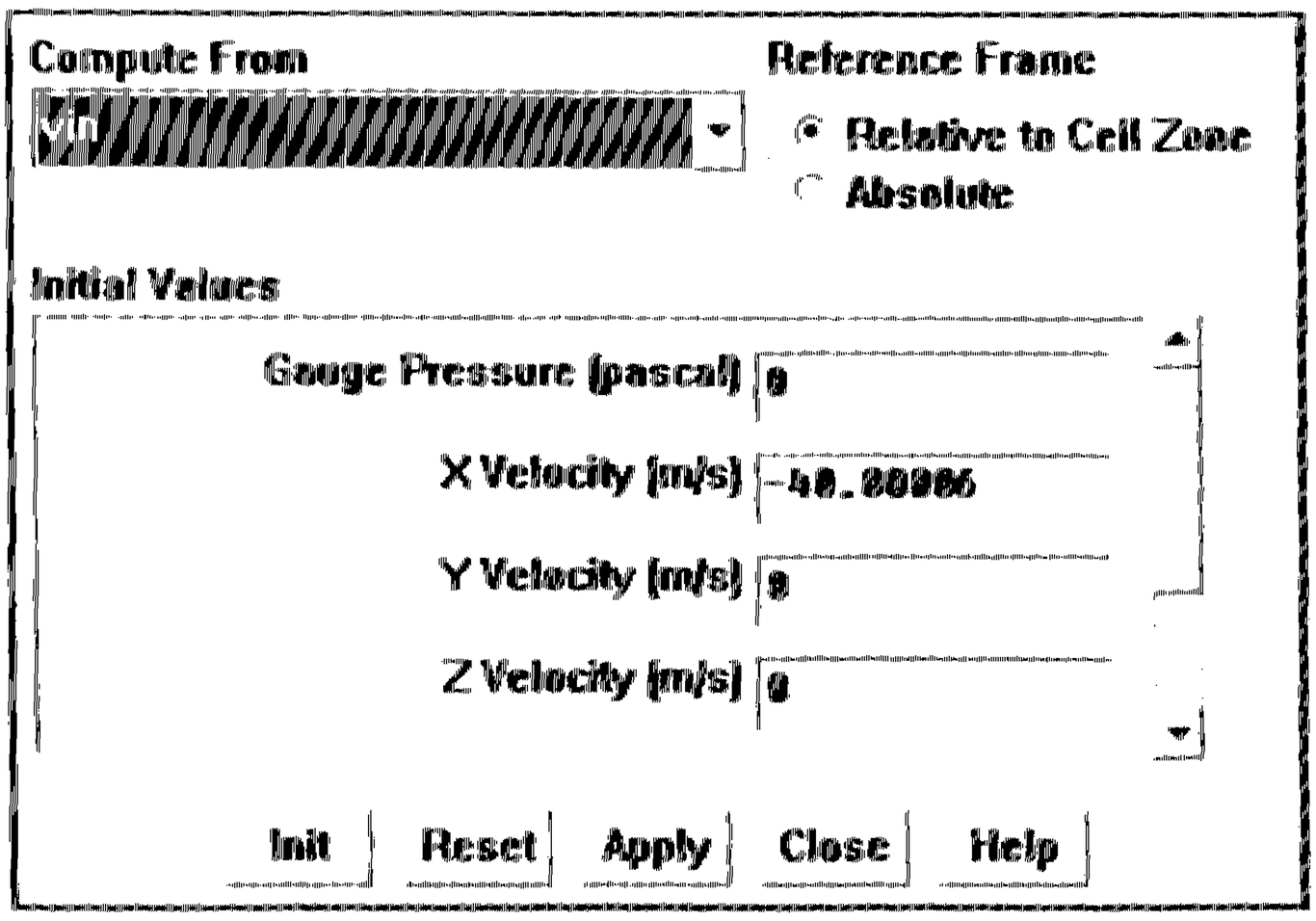

The simulation should be initialized in tab solver/initialize. Compute the data from inlet velocity and the magnitude will be appeared. The default setting will set only in x-direction as velocity inlet in the rectangular parallel to the x-axis.

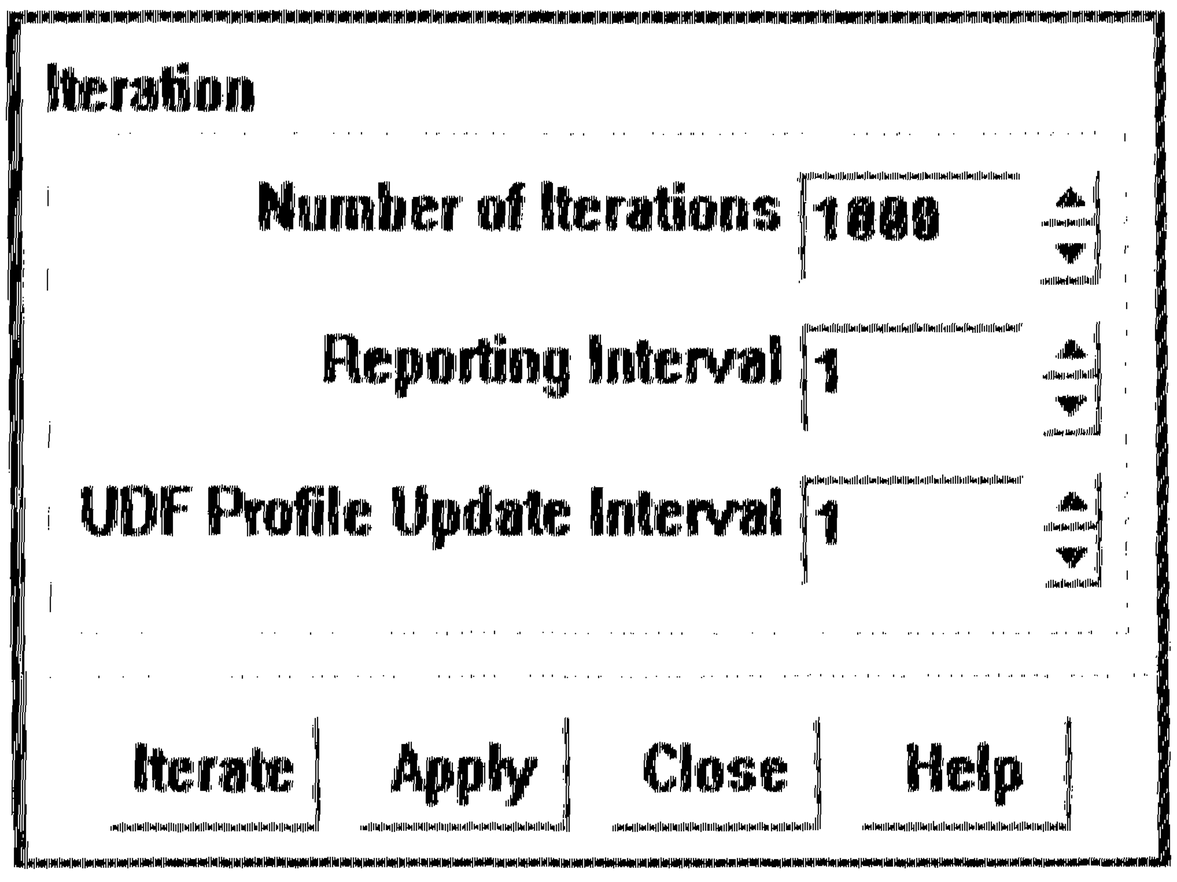

Lastly, click iterate on solve/iterate tab. Set the number of iteration as 1000. All the residual will target the convergence criterion those been set previously. For the continuity, x-velocity, y-velocity and z-velocity, the convergence criterion residual is 0.001 except for energy which is 10e-06.

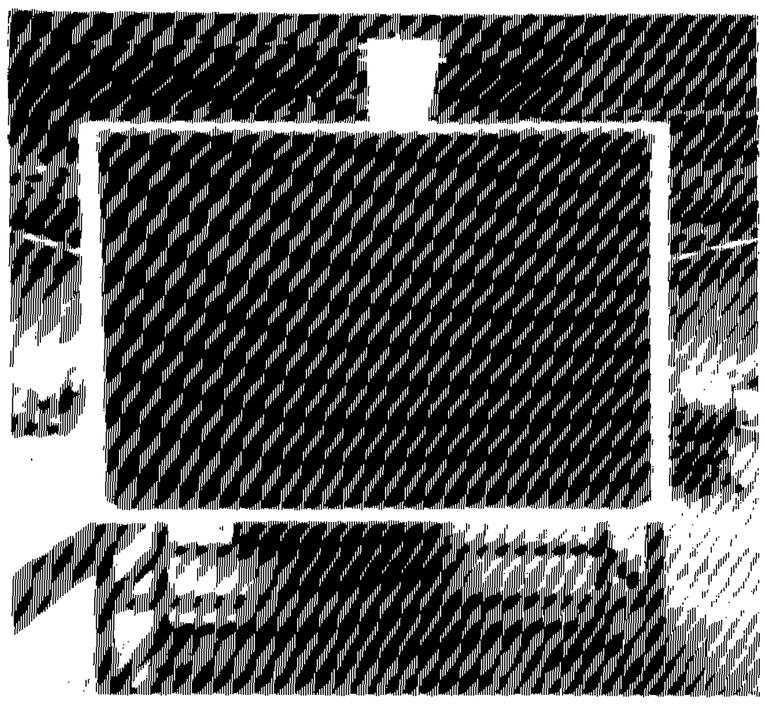

Settling Chamber

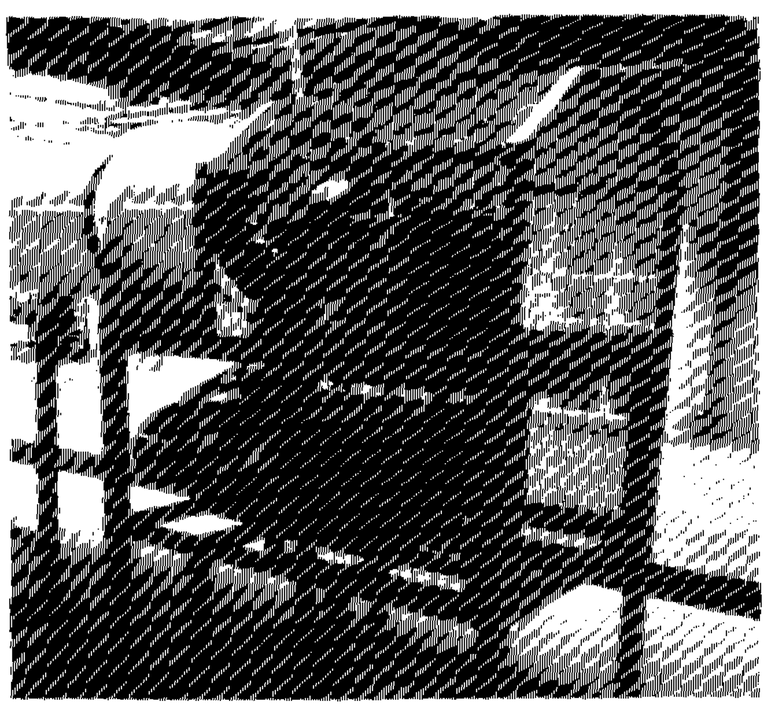

Motor

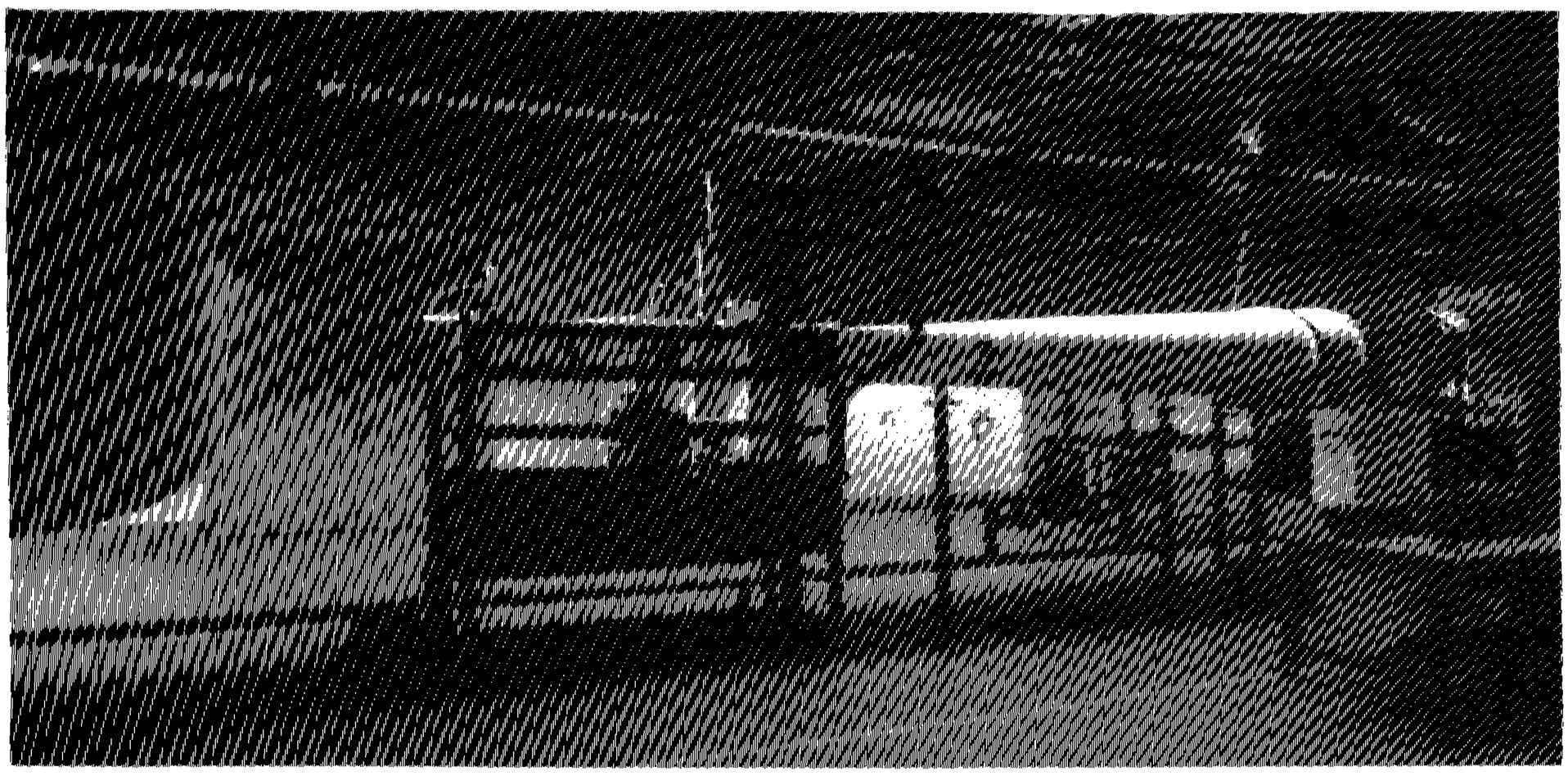

Universiti Teknologi PETRONAS Open loop wind tunnel

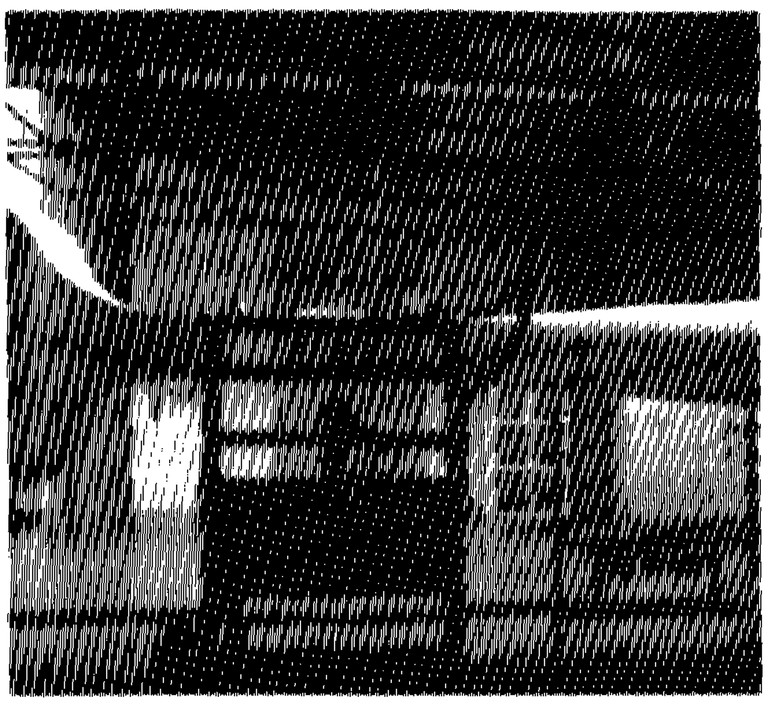

Contraction (left) and Diffuser (right) section

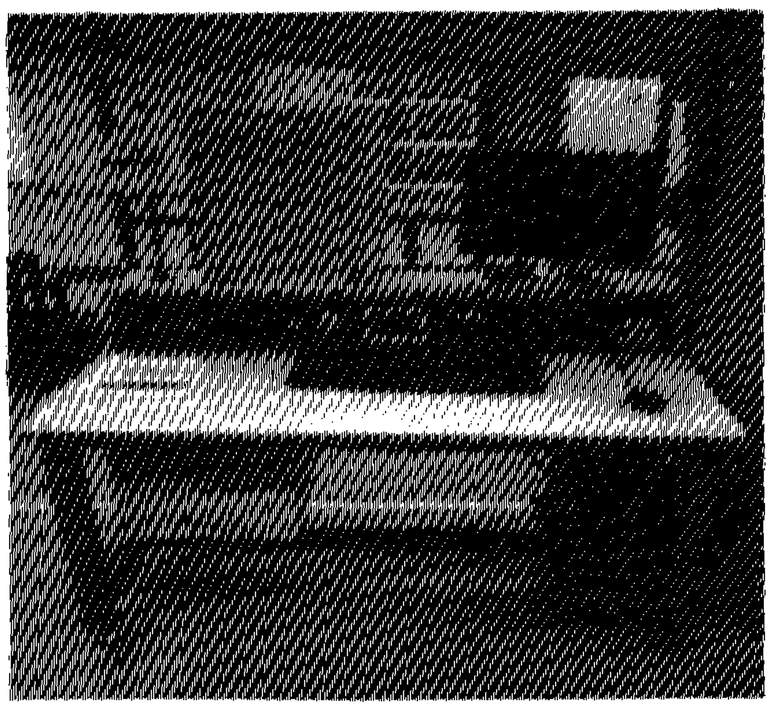

Control Panel

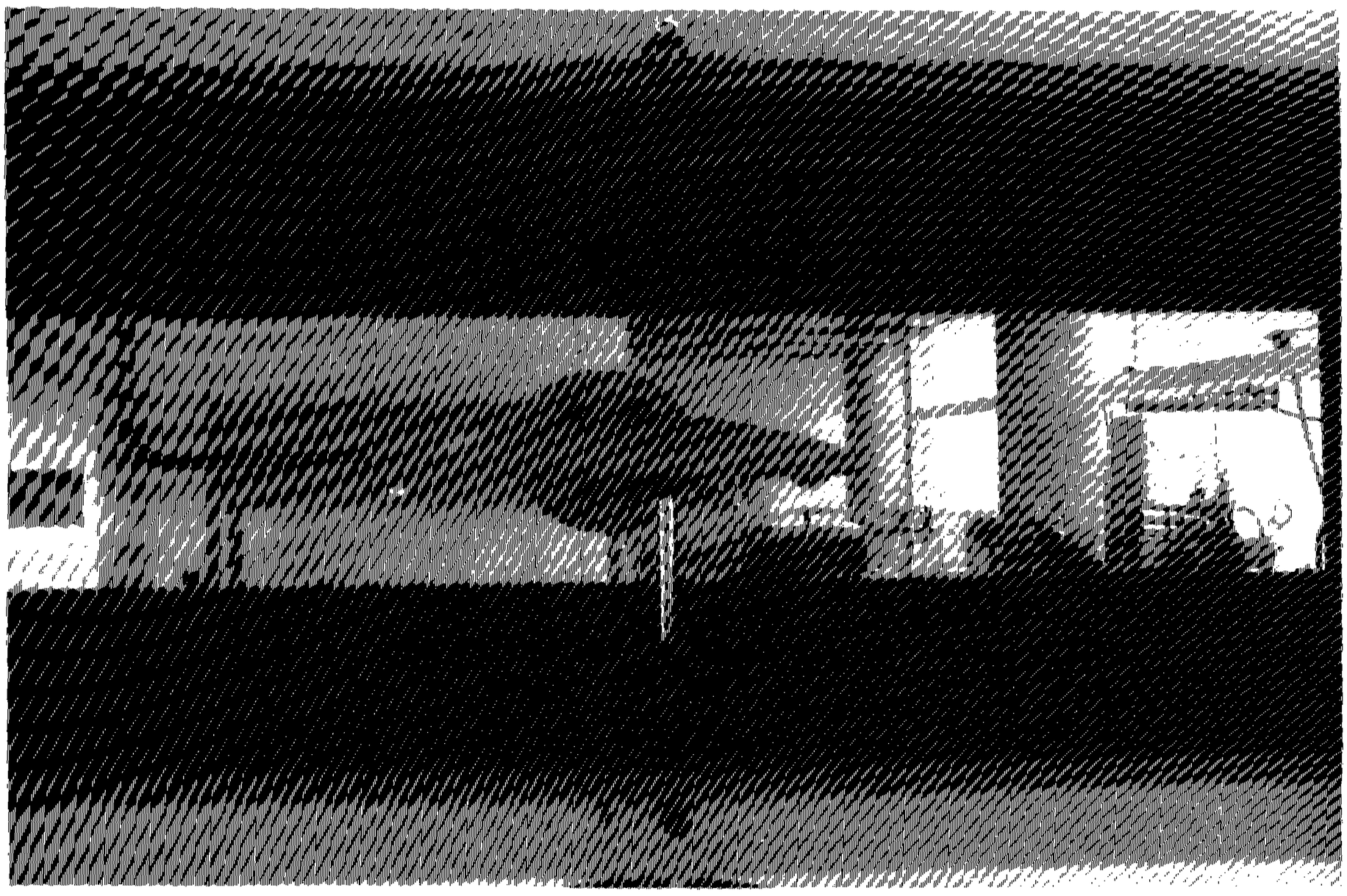

Probe I model mount in the wind tunnel

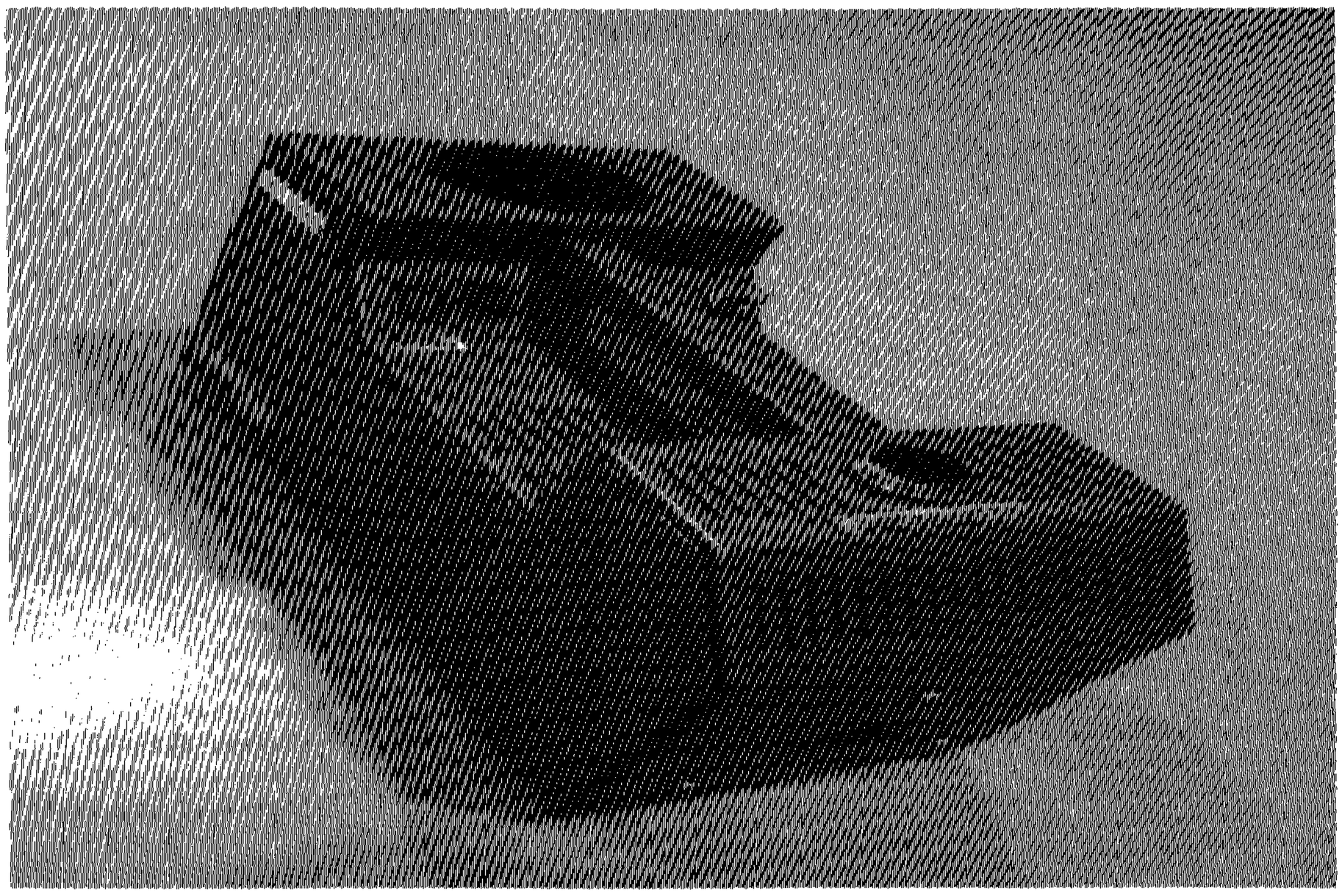

Smoke generator

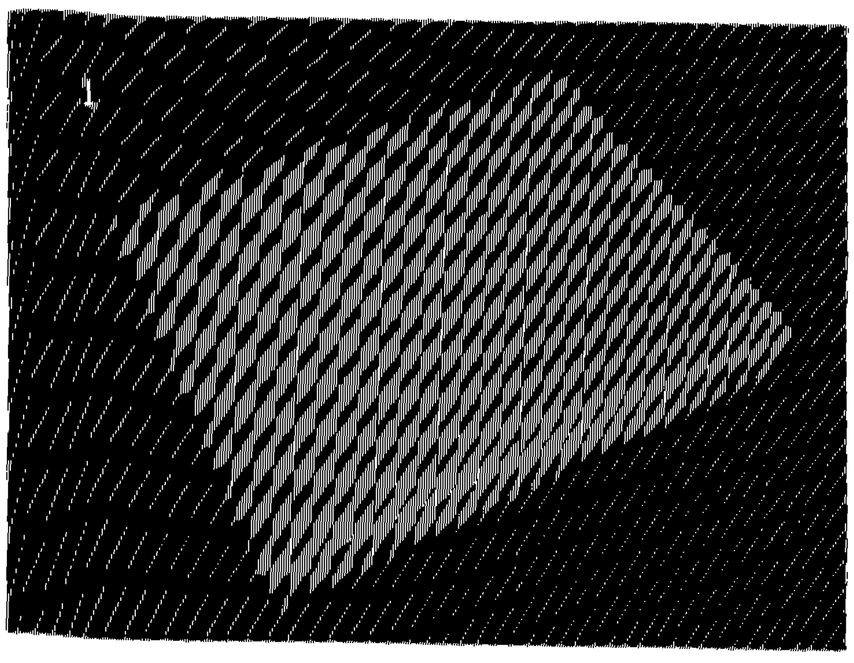

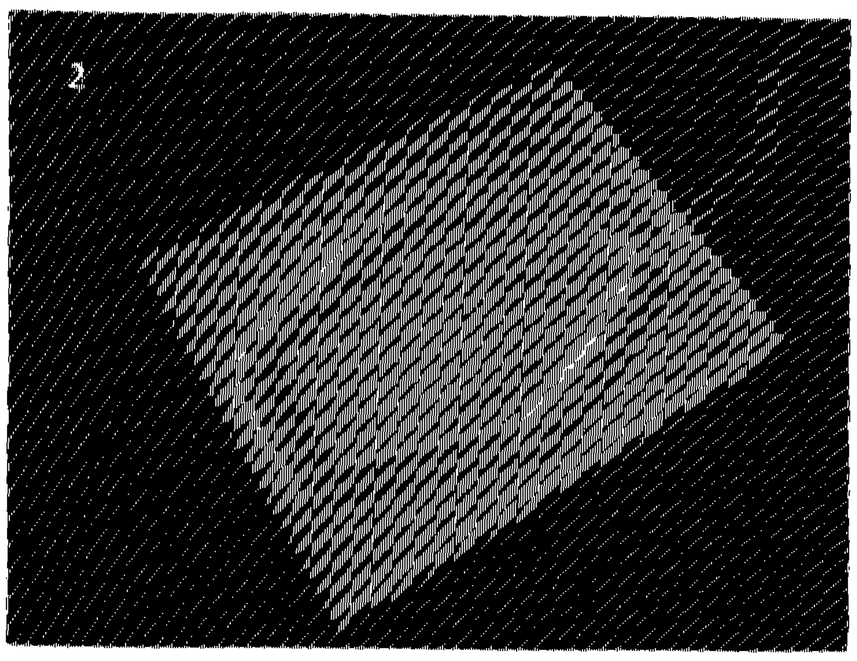

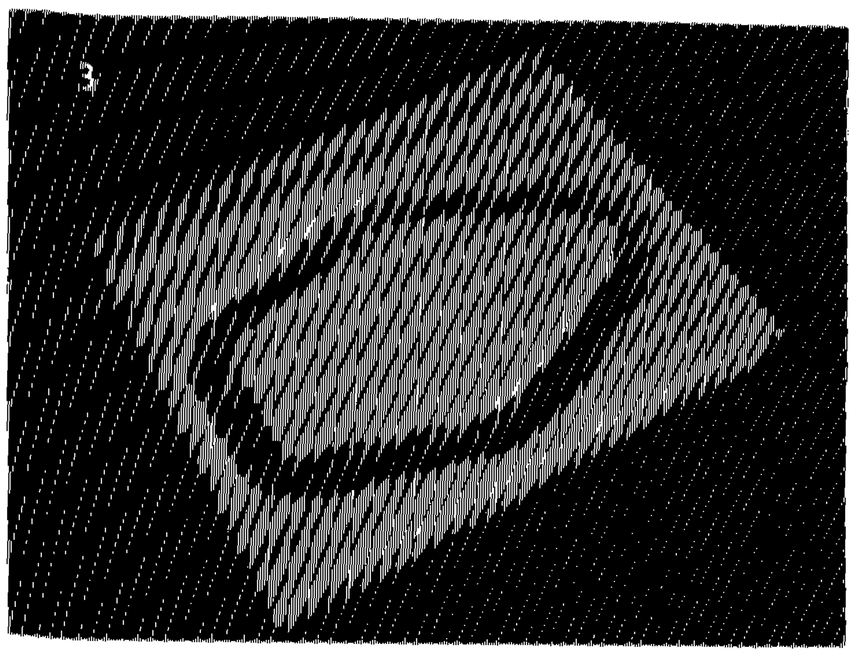

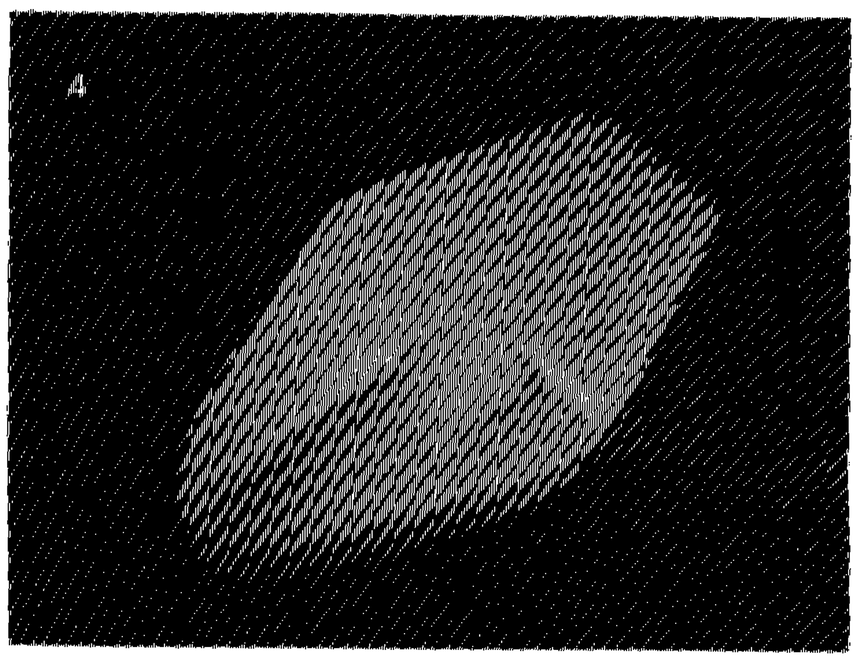

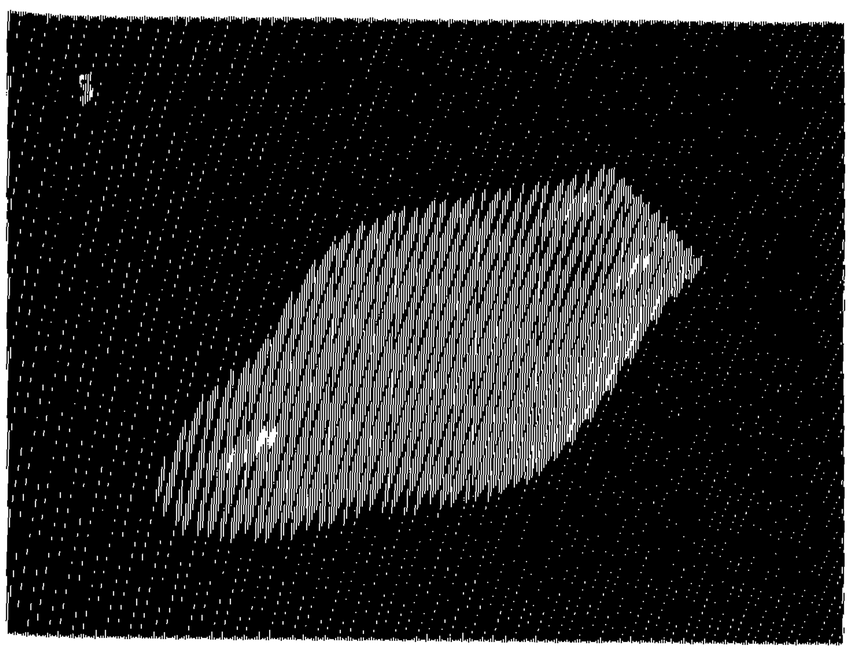

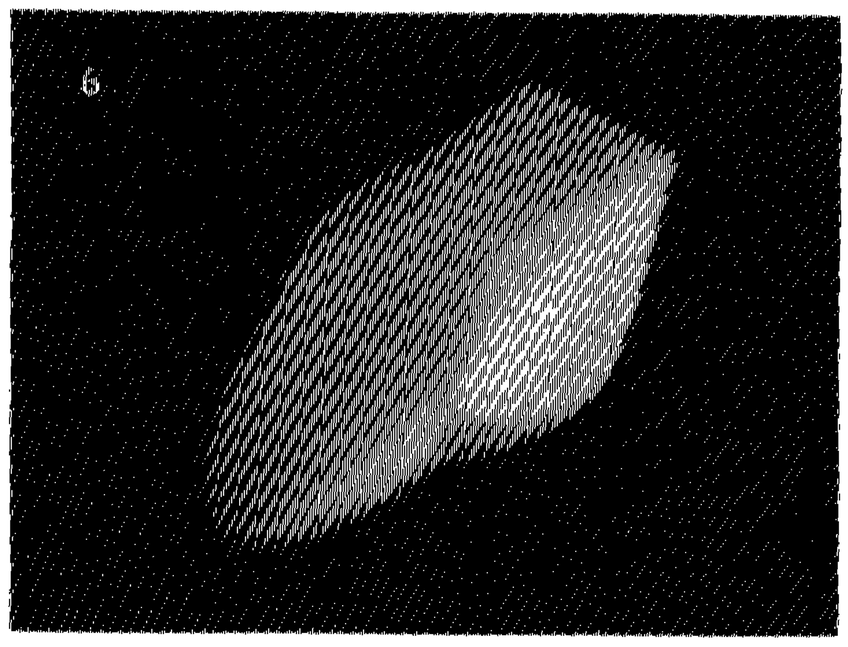

Peeling off process from after finish printing in 3D printer

Run 1

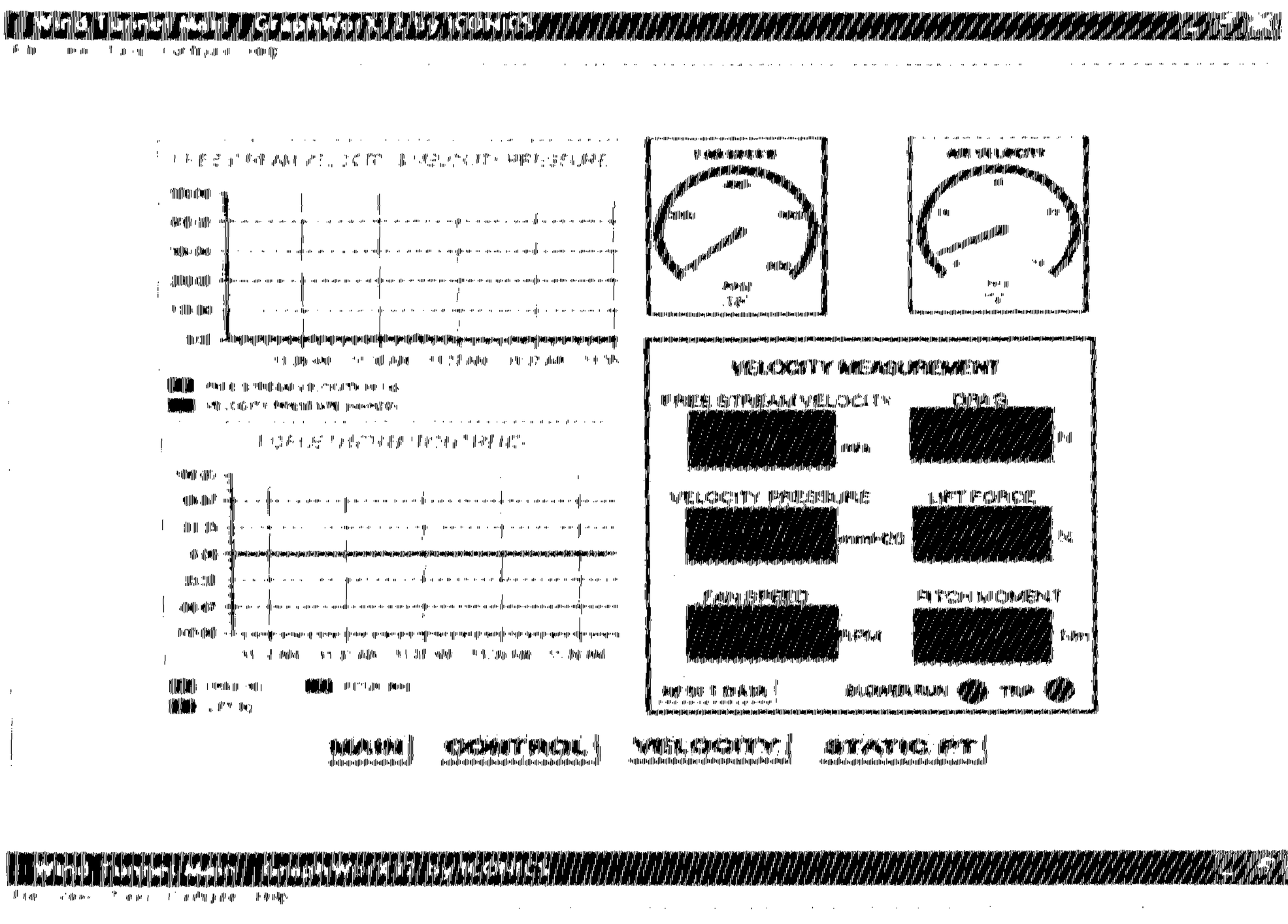
VELOCITY MEASUREMENT
FREE STREAM VELOCITY
DRAG
VELOCITY PULSATIVE
LIFT FORCE
CALIBRATED
PITCH MOMENT
MAIN
CONTROL
VELOCITY
STATIC PT

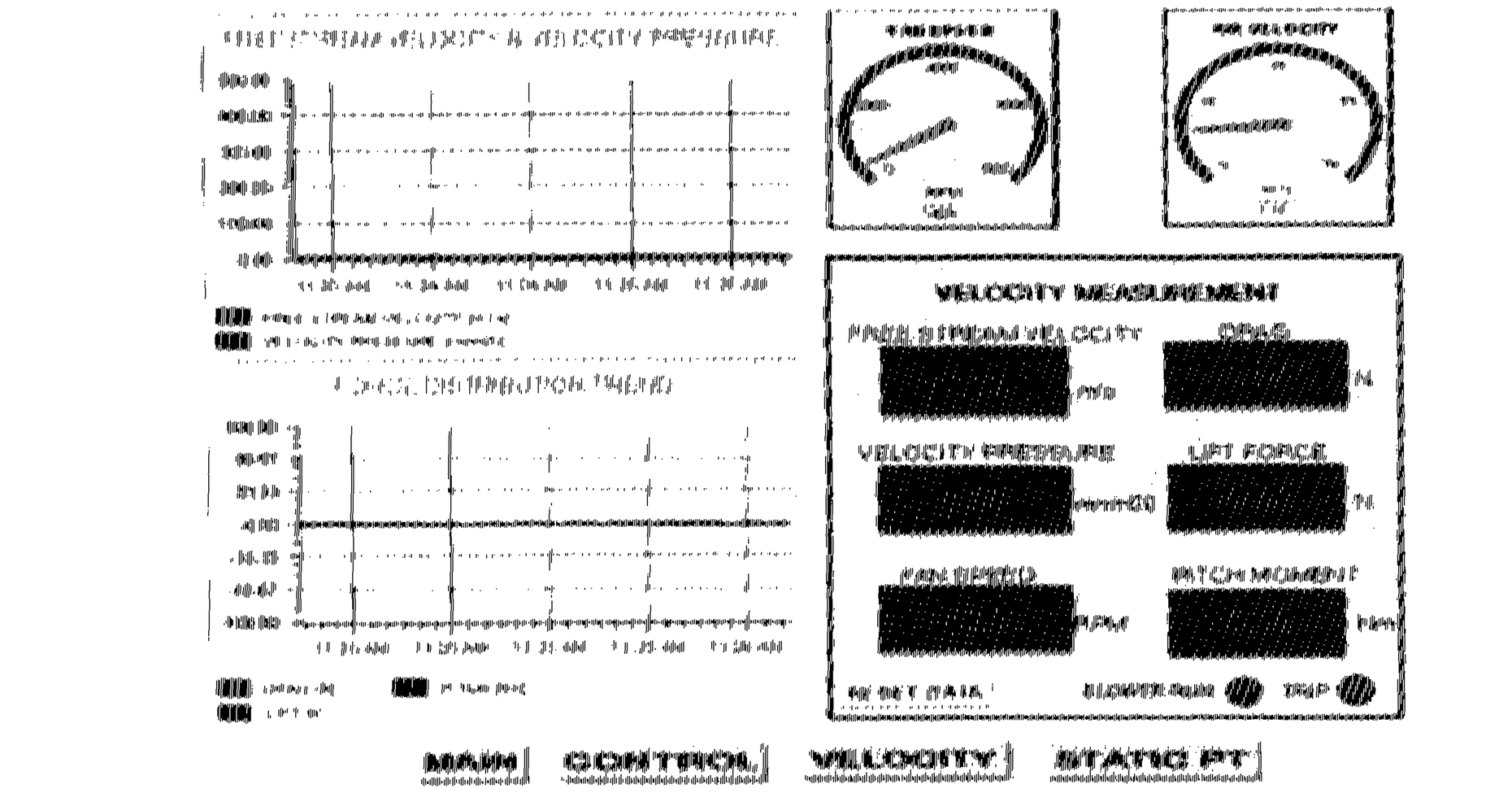
VELOCITY MEASUREMENT
MAIN
CONTROL
VELOCITY
STATIC PT

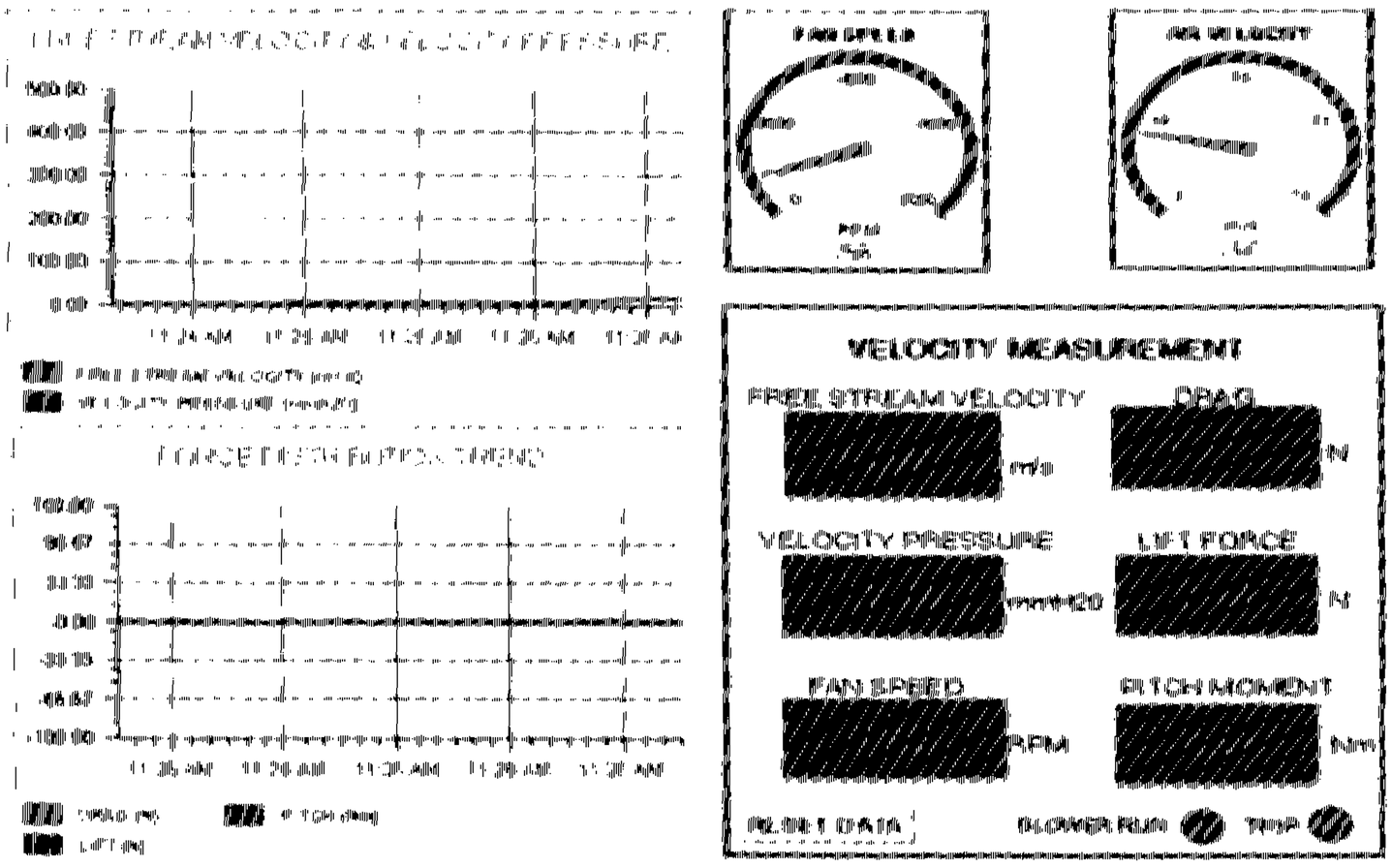
FAN SPEED
AIR VELOCITY
VELOCITY MEASUREMENT
FREE STREAM VELOCITY
DRAG
mph
N
VELOCITY PRESSURE
LIFT FORCE
mm-H2O
N
FAN SPEED
PITCH MOMENT
RPM
N-m
BLOCKAGE RUN
TARE
MAIN
CONTROL
VELOCITY
STATIC PT

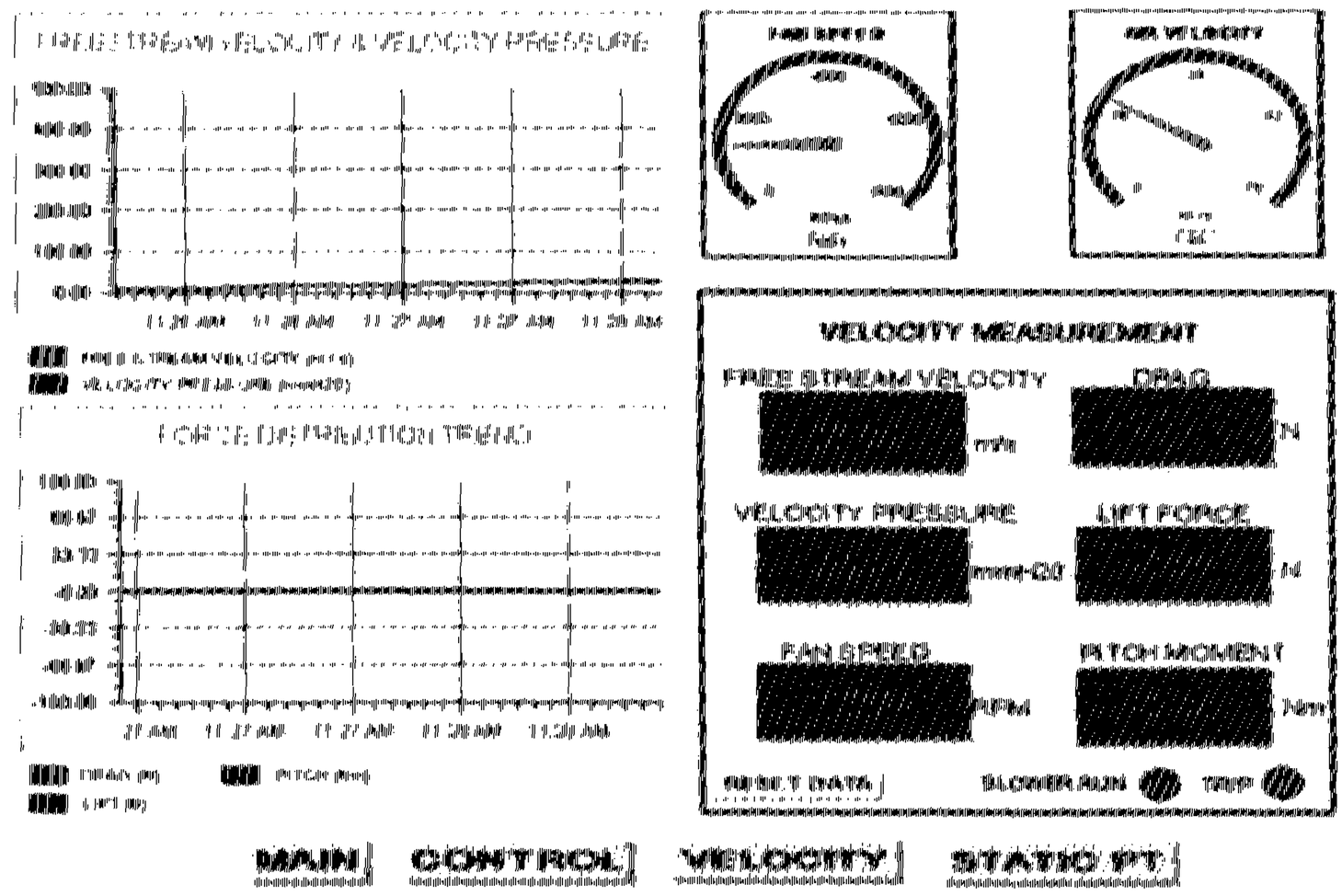
FAN SPEED
AIR VELOCITY
VELOCITY MEASUREMENT
FREE STREAM VELOCITY
DRAG
mph
N
VELOCITY PRESSURE
LIFT FORCE
mm-H2O
N
FAN SPEED
PITCH MOMENT
RPM
N-m
BLOCKAGE RUN
TARE
MAIN
CONTROL
VELOCITY
STATIC PT

File View Tools Configure Help

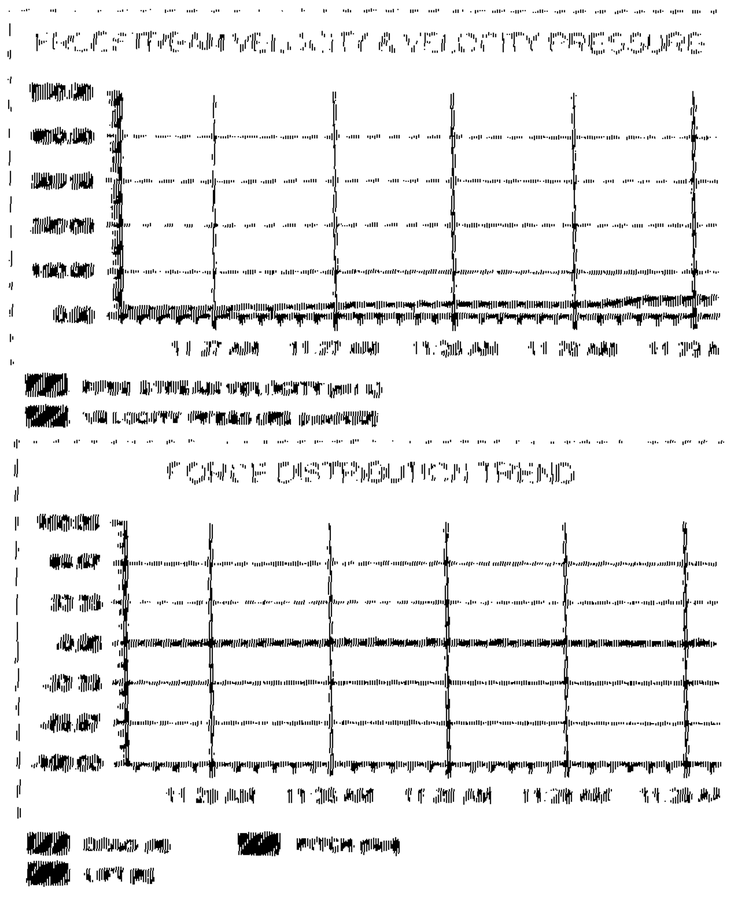

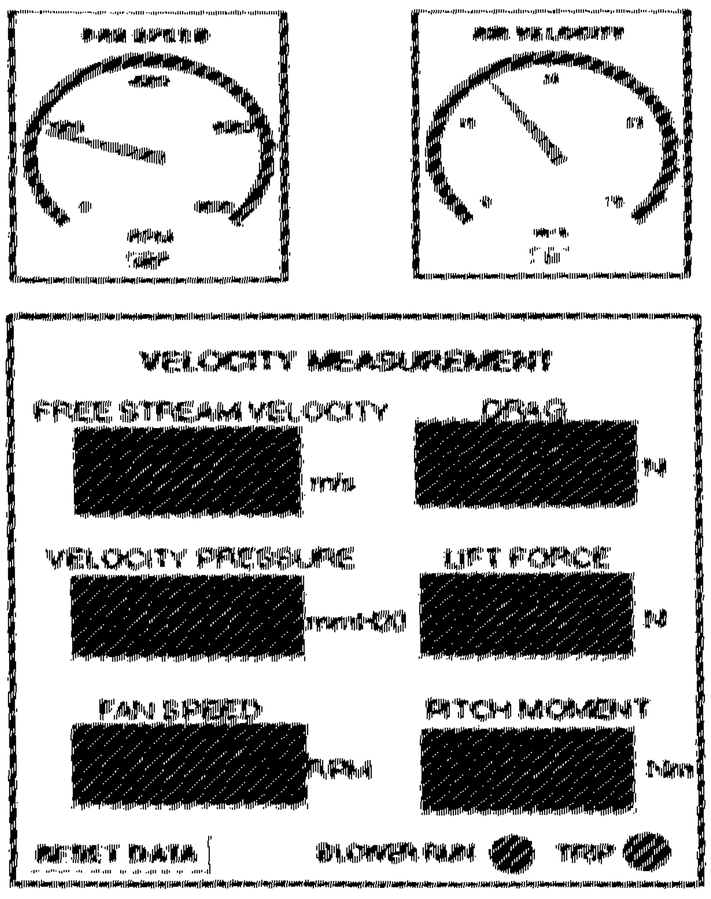

MAIN | CONTROL | VELOCITY | STATIC PT

Wind Tunnel Main - GraphWorX32 by ICONICS

File View Tools Configure Help

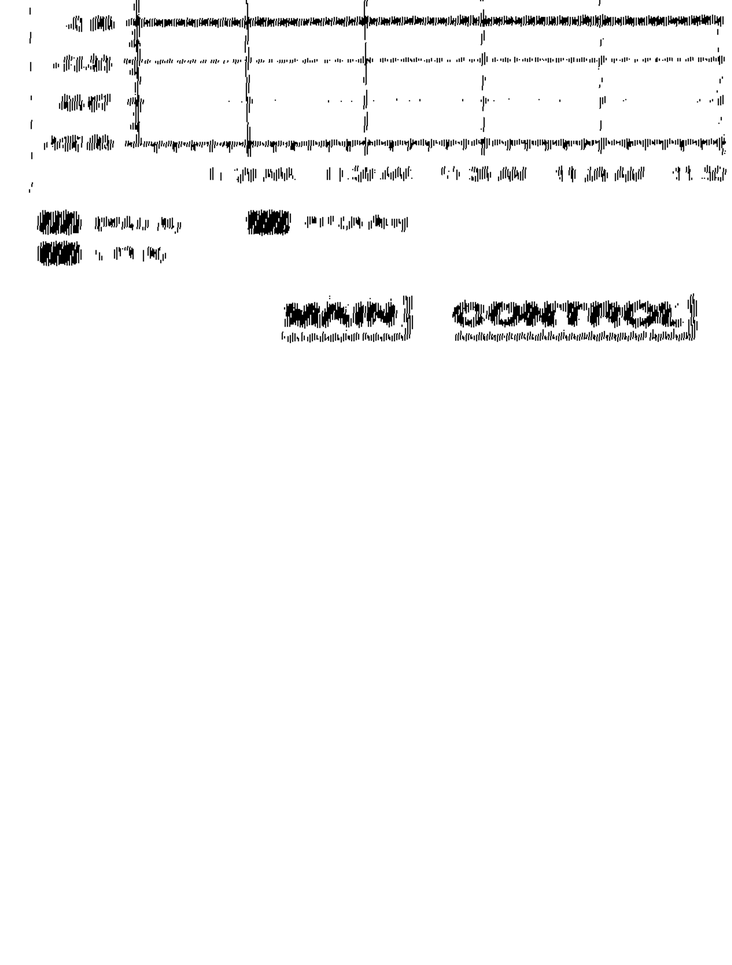

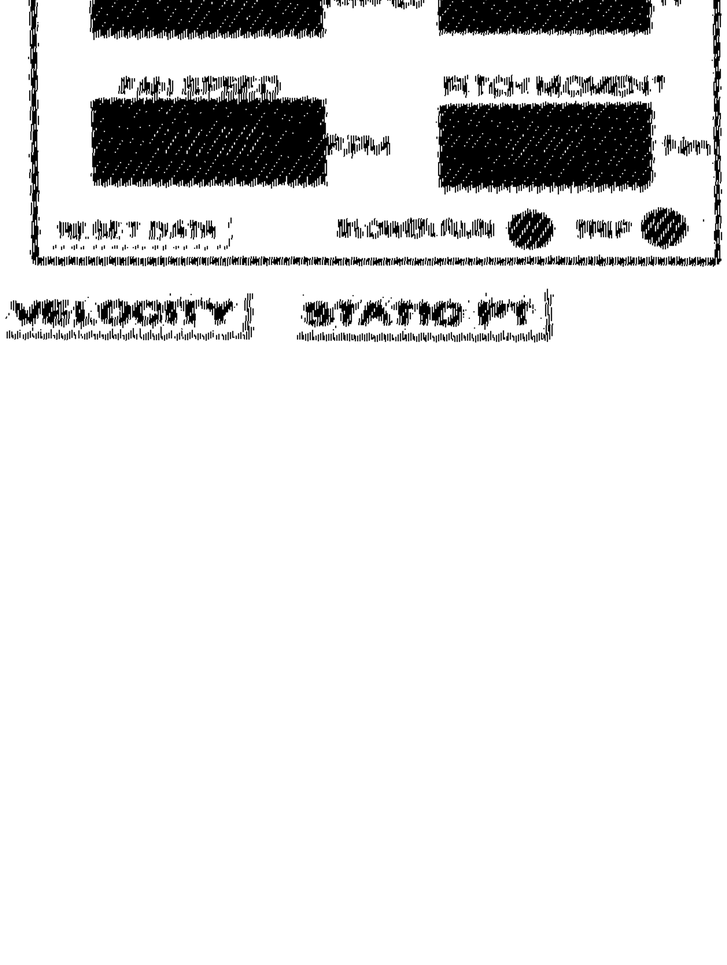

MAIN | CONTROL | VELOCITY | STATIC PT

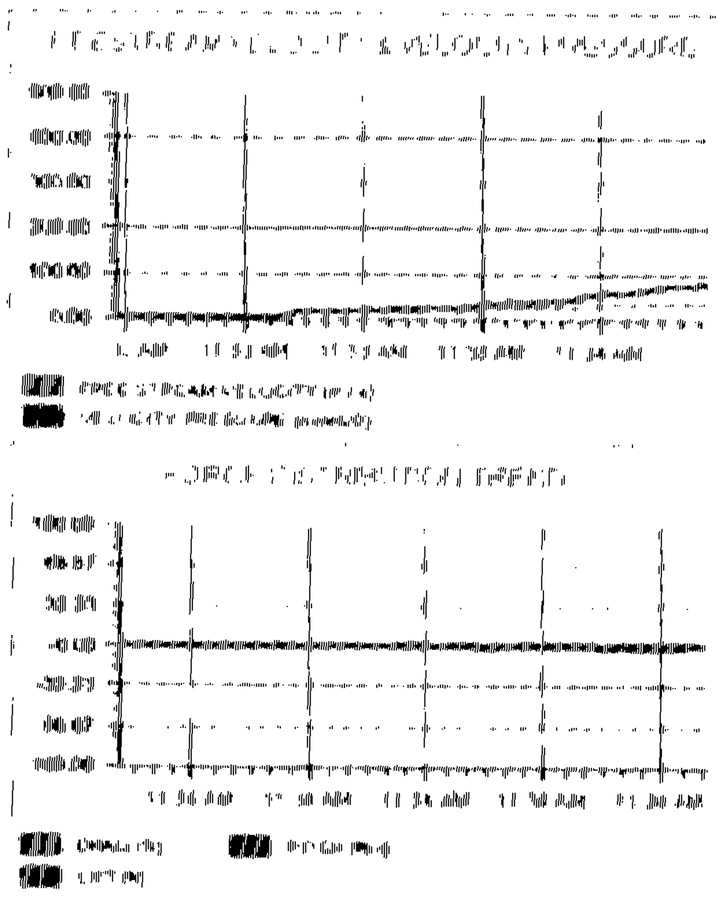
VELOCITY MEASUREMENT
FREESTREAM VELOCITY
mph
DRAG
lb
VELOCITY PRESSURE
mmHG
LIFT FORCE
lb
FAN SPEED
RPM
PITCH MOMENT
ft-lb
MAIN
CONTROL
VELOCITY
STATIC PT

Run 2

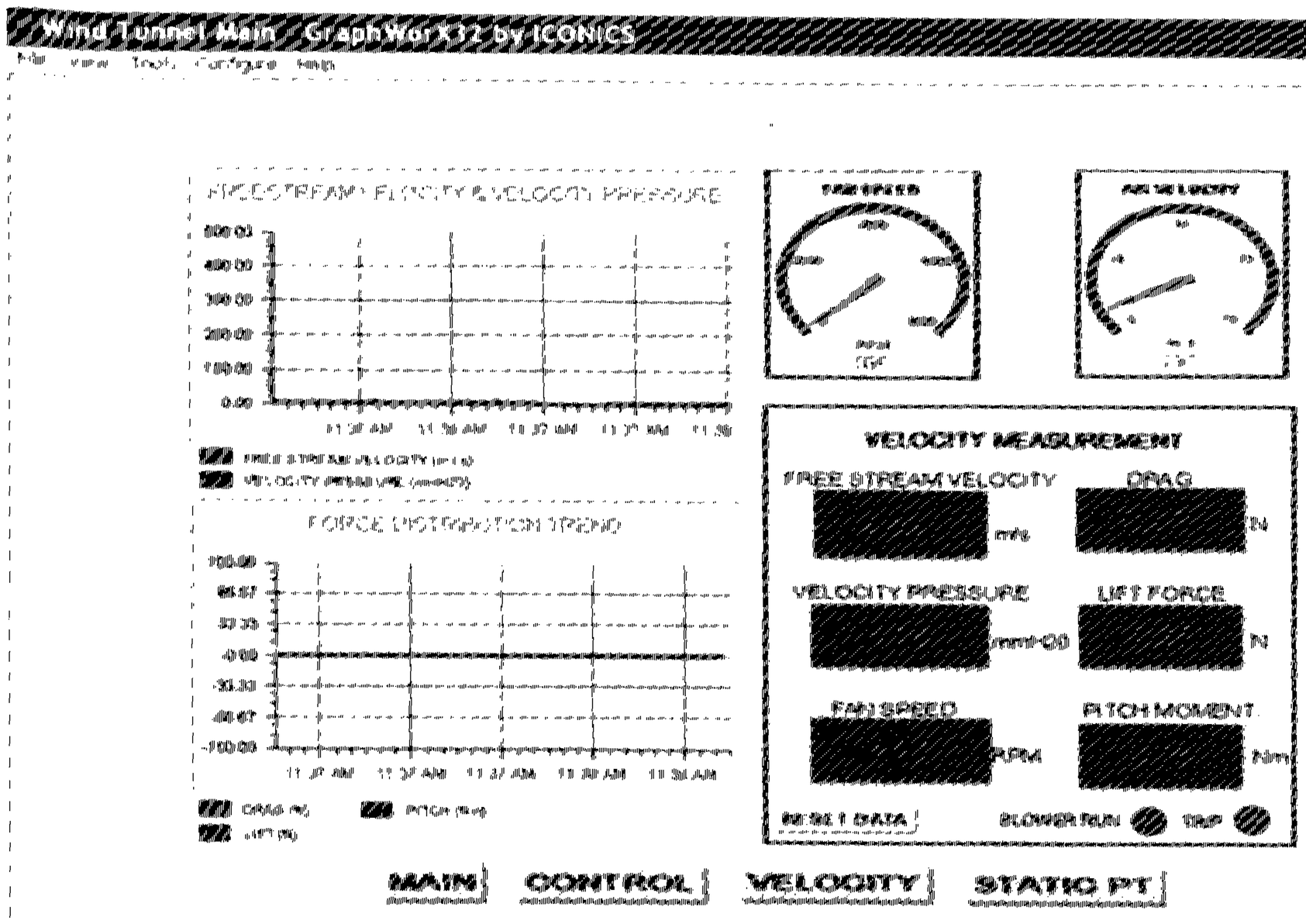
Wind Tunnel Main / GraphWorX32 by ICONICS
PRESSURE/VELOCITY PROFILE
FORCE DISTRIBUTION TREND
VELOCITY MEASUREMENT
FREE STREAM VELOCITY
DRAG
VELOCITY PRESSURE
LIFT FORCE
FAN SPEED
PITCH MOMENT
MAIN
CONTROL
VELOCITY
STATIC PT

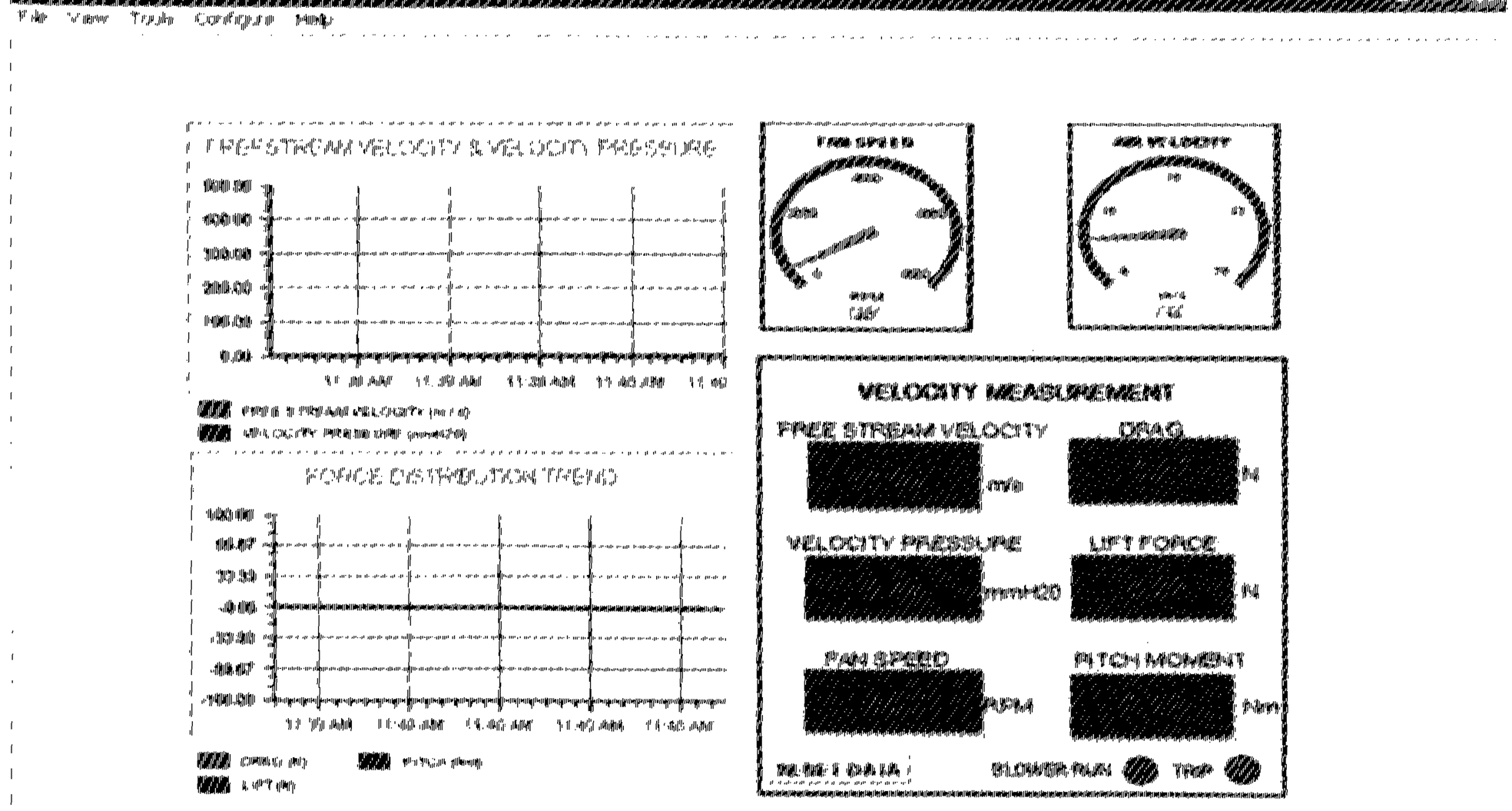
Wind Tunnel Main / GraphWorX32 by ICONICS
PRESSURE/VELOCITY PROFILE
FORCE DISTRIBUTION TREND
VELOCITY MEASUREMENT
FREE STREAM VELOCITY
DRAG
VELOCITY PRESSURE
LIFT FORCE
FAN SPEED
PITCH MOMENT
MAIN
CONTROL
VELOCITY
STATIC PT

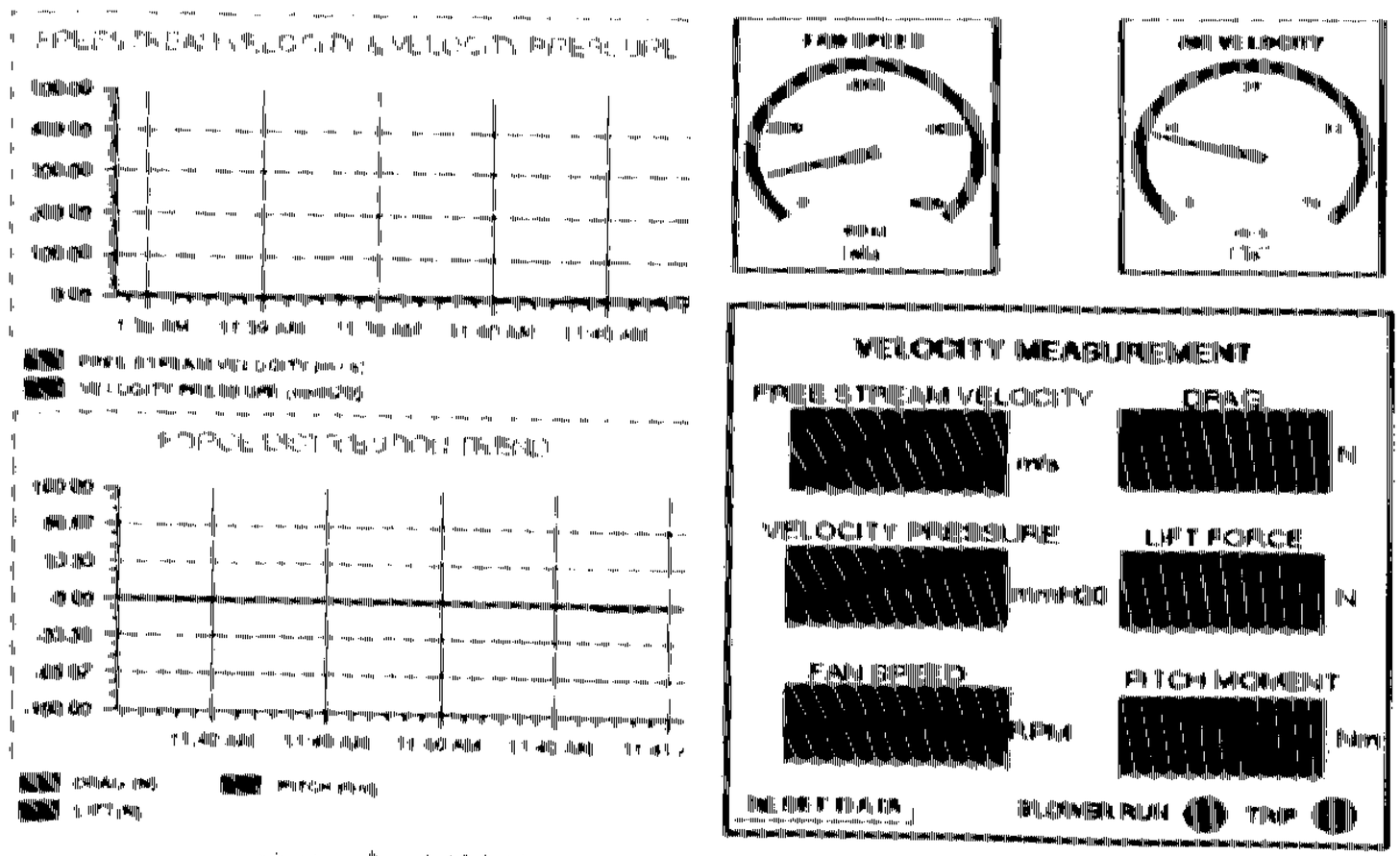
Wind Tunnel Main GraphWorX32 by ICONICS
File View Tools Configure Help
FREESTREAM VELOCITY & VELOCITY PRESSURE
FORCE DISTRIBUTION TREND
FAN SPEED
VELOCITY
VELOCITY MEASUREMENT
FREE STREAM VELOCITY
DRAG
VELOCITY PRESSURE
LIFT FORCE
FAN SPEED
PITCH MOMENT
RESET DATA
BLOWER RUN
TRIP
MAIN
CONTROL
VELOCITY
STATIC PT

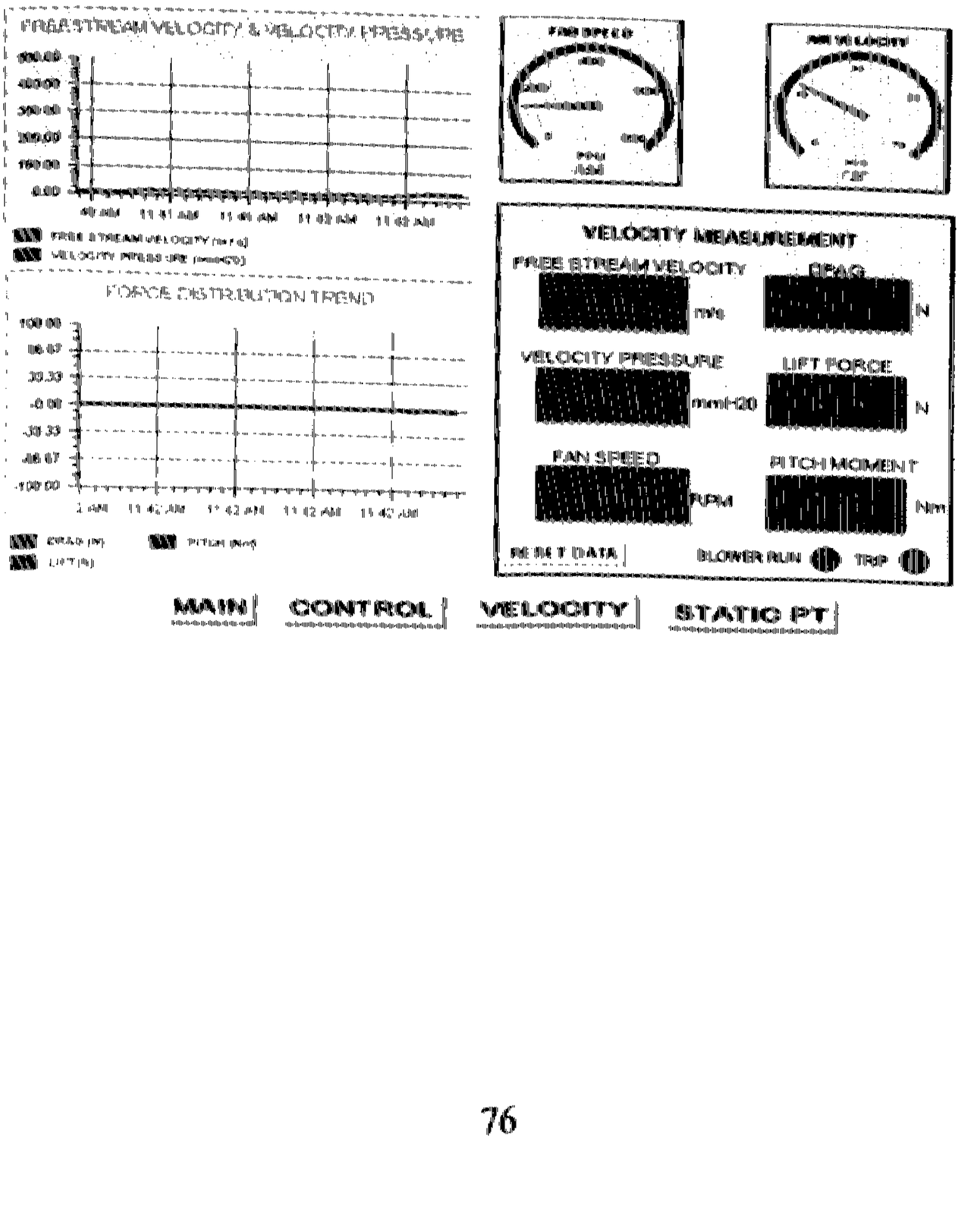
Wind Tunnel Main GraphWorX32 by ICONICS
File View Tools Configure Help
FREESTREAM VELOCITY & VELOCITY PRESSURE
FORCE DISTRIBUTION TREND
FAN SPEED
VELOCITY
VELOCITY MEASUREMENT
FREE STREAM VELOCITY
DRAG
VELOCITY PRESSURE
LIFT FORCE
FAN SPEED
PITCH MOMENT
RESET DATA
BLOWER RUN
TRIP
MAIN
CONTROL
VELOCITY
STATIC PT

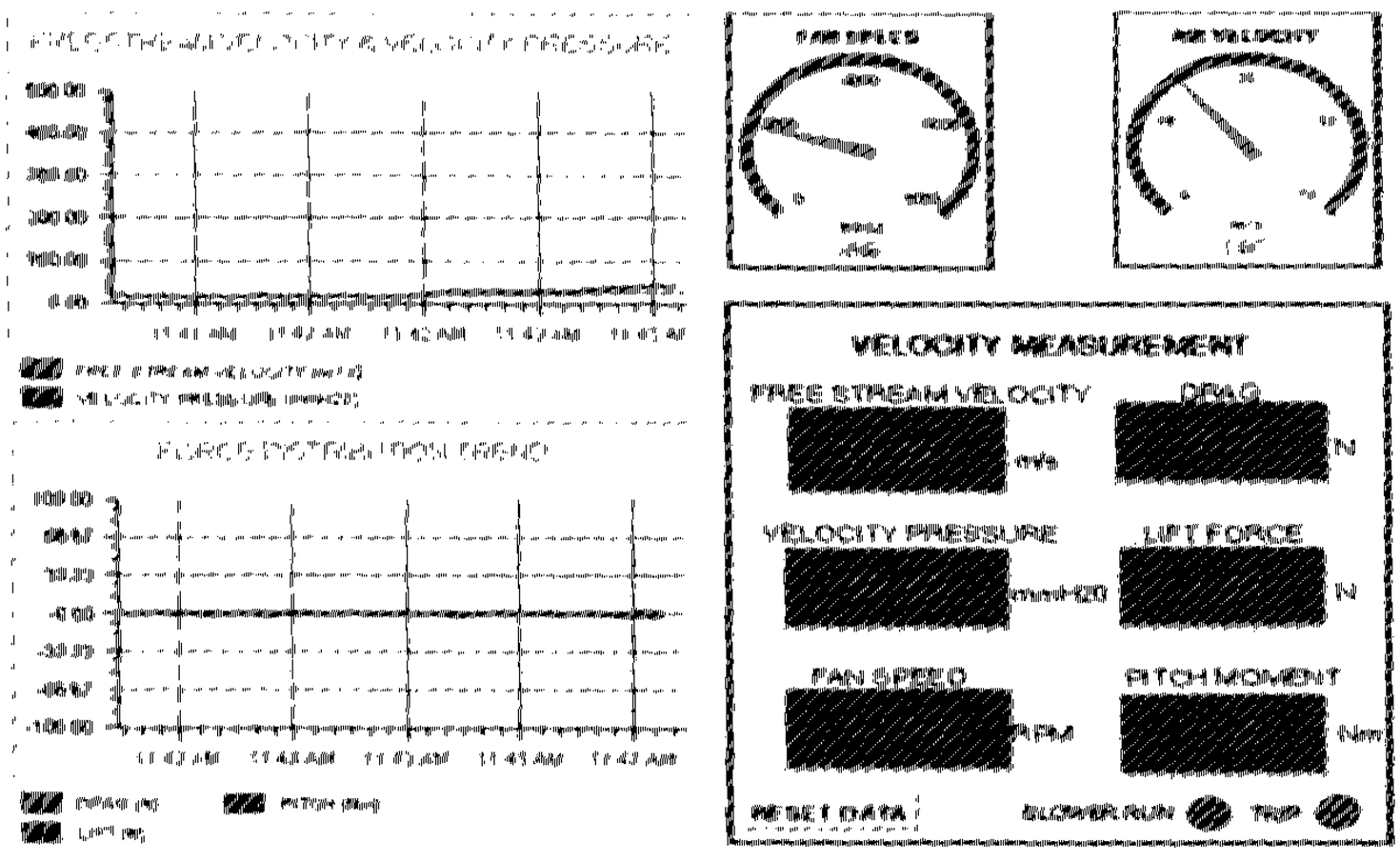
VELOCITY MEASUREMENT
FREE STREAM VELOCITY
DRAG
VELOCITY PRESSURE
LIFT FORCE
FAN SPEED
PITCH MOMENT
RESET DATA
BLOWER RUN
TEST
MAIN
CONTROL
VELOCITY
STATIC PT

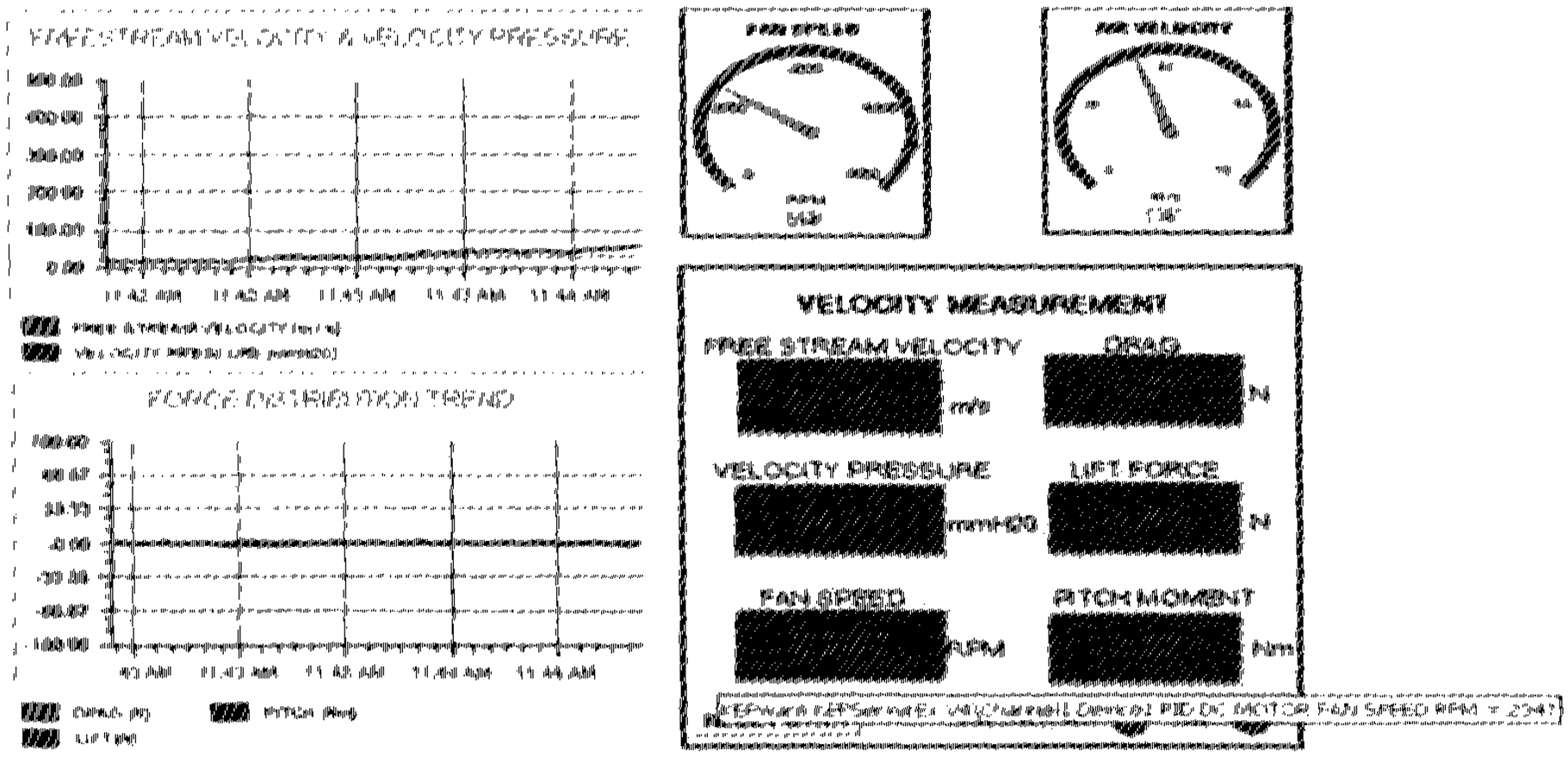
VELOCITY MEASUREMENT
FREE STREAM VELOCITY
DRAG
VELOCITY PRESSURE
LIFT FORCE
FAN SPEED
PITCH MOMENT
MAIN
CONTROL
VELOCITY
STATIC PT

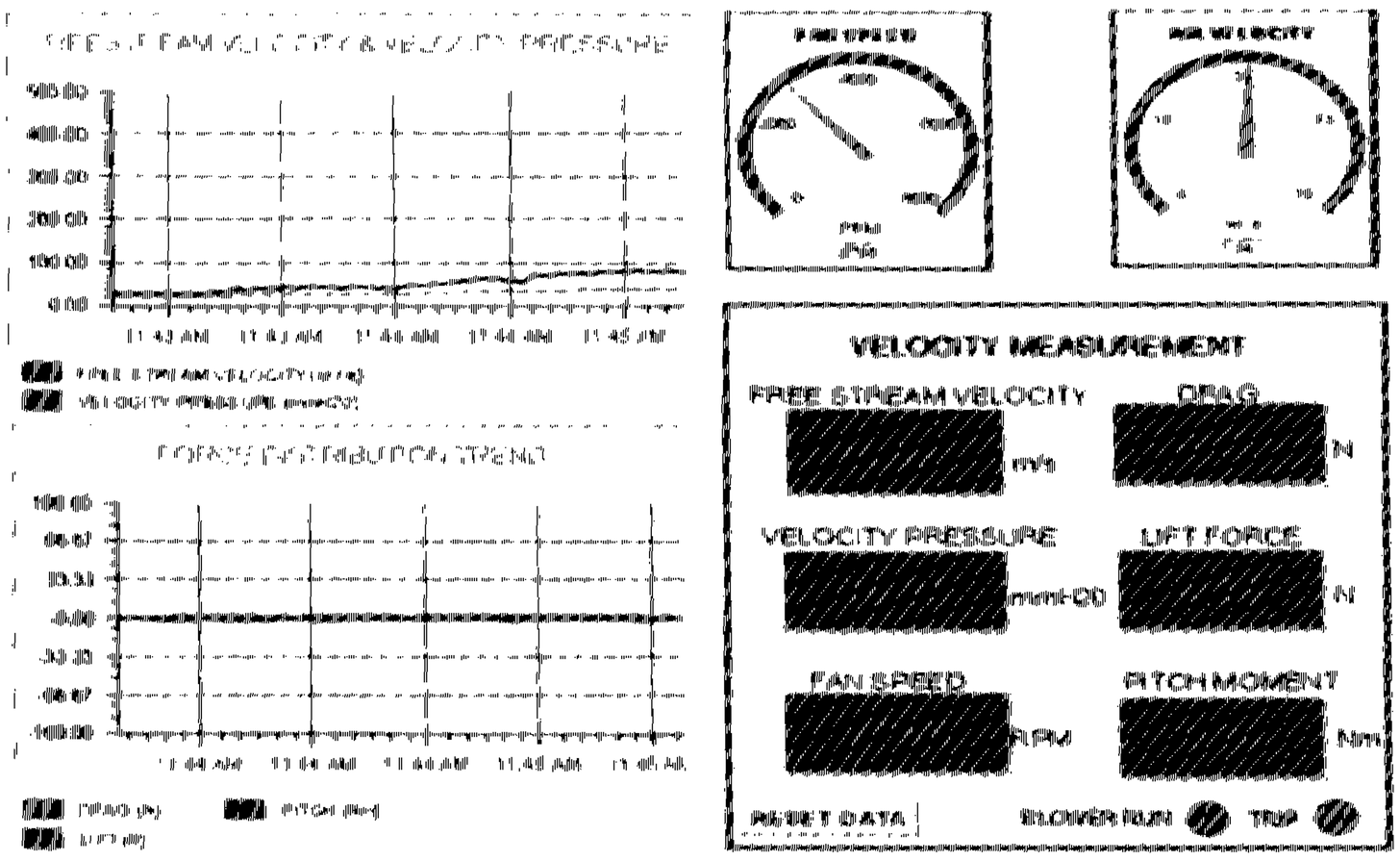
VELOCITY MEASUREMENT
FREE STREAM VELOCITY
m/s
DRAG
N
VELOCITY PRESSURE
mmH2O
LIFT FORCE
N
FAN SPEED
RPM
PITCH MOMENT
N/m
RESET DATA
BLOWER RUN
TRIP
MAIN
CONTROL
VELOCITY
STATIC PT

Run 3

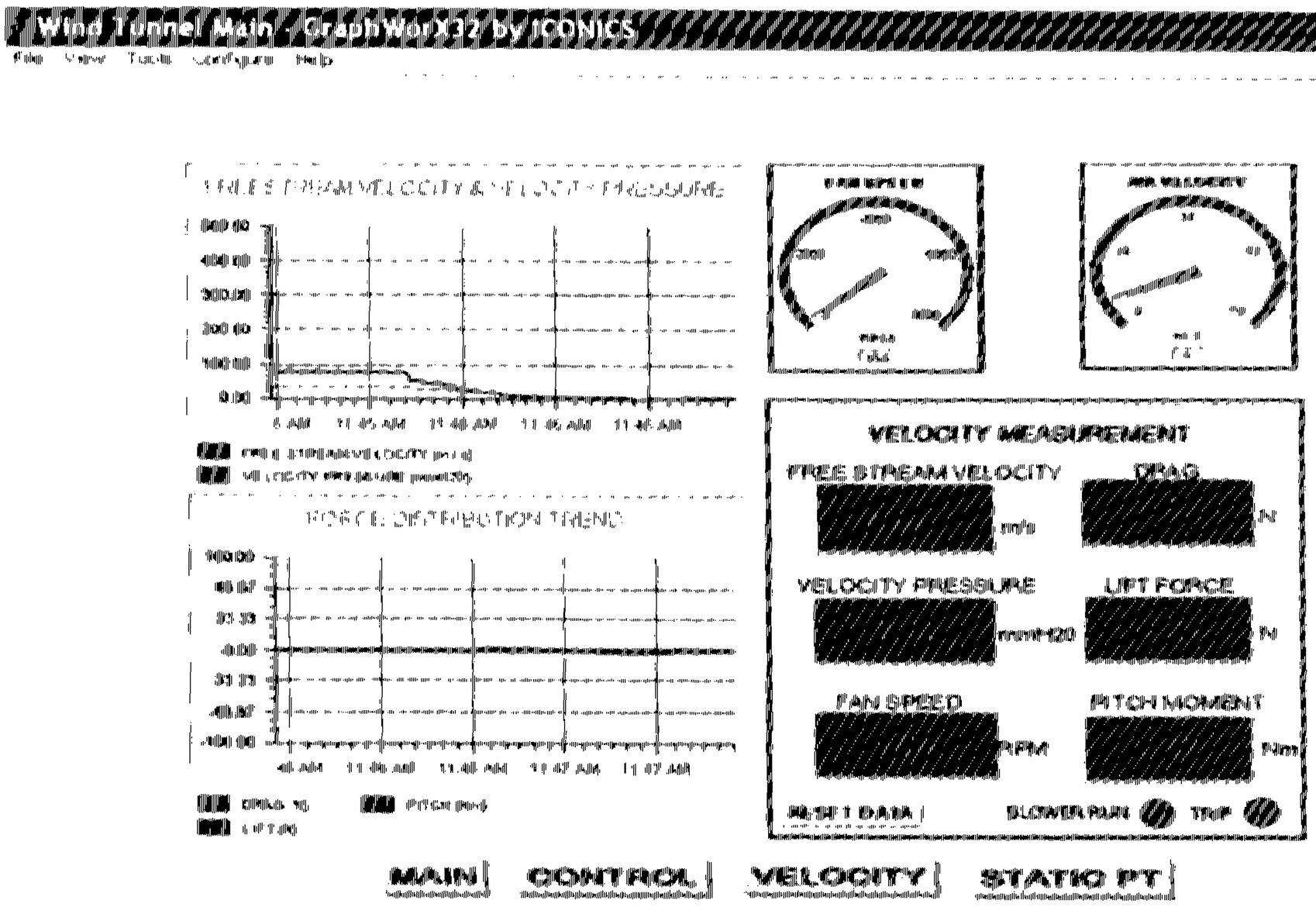
Wind Tunnel Main - GraphWorX32 by ICONICS
VELOCITY MEASUREMENT
FREE STREAM VELOCITY
DRAG
VELOCITY PRESSURE
LIFT FORCE
FAN SPEED
PITCH MOMENT
MAIN
CONTROL
VELOCITY
STATIC PT

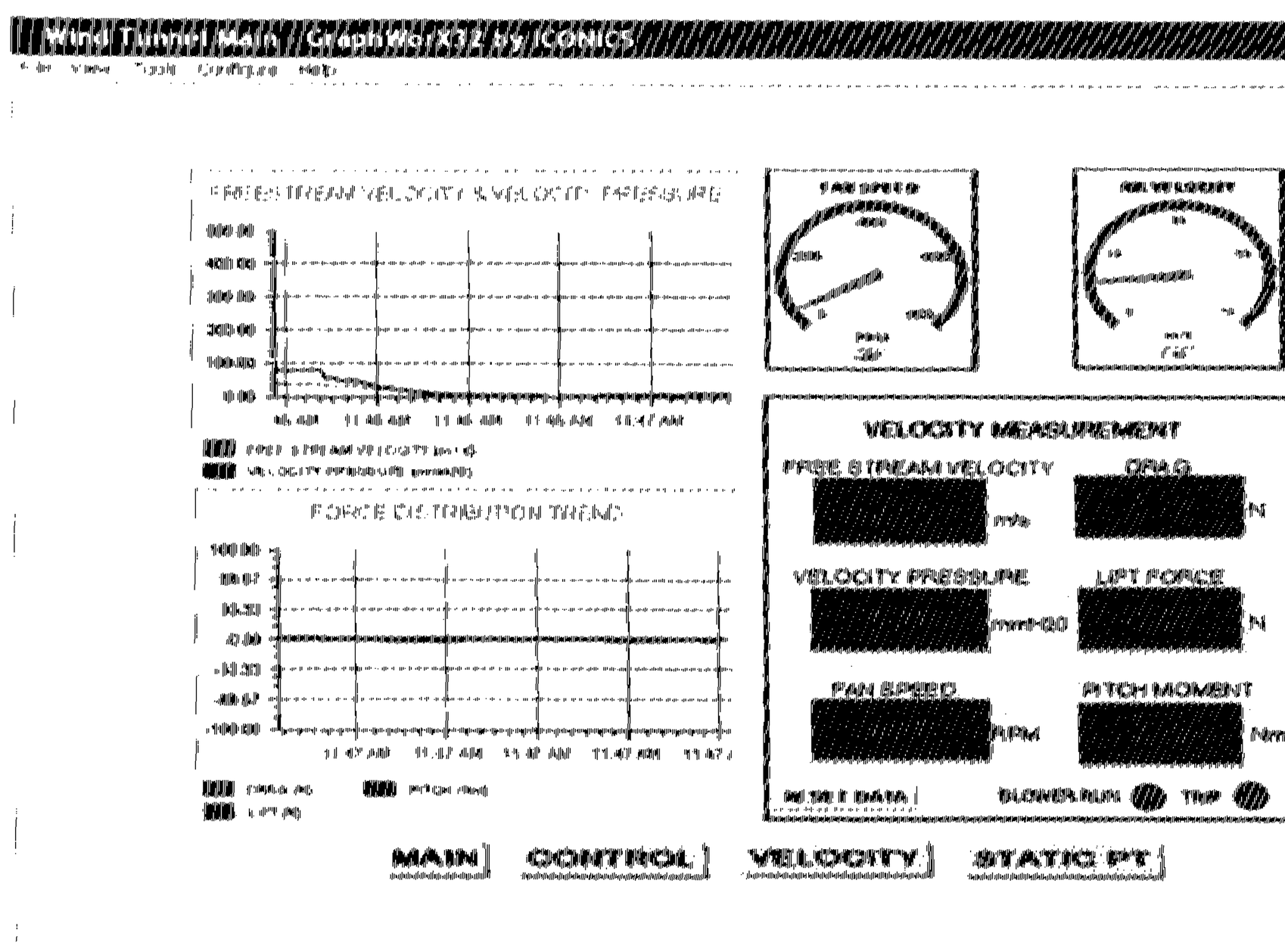
Wind Tunnel Main - GraphWorX32 by ICONICS
VELOCITY MEASUREMENT
FREE STREAM VELOCITY
DRAG
VELOCITY PRESSURE
LIFT FORCE
FAN SPEED
PITCH MOMENT
MAIN
CONTROL
VELOCITY
STATIC PT

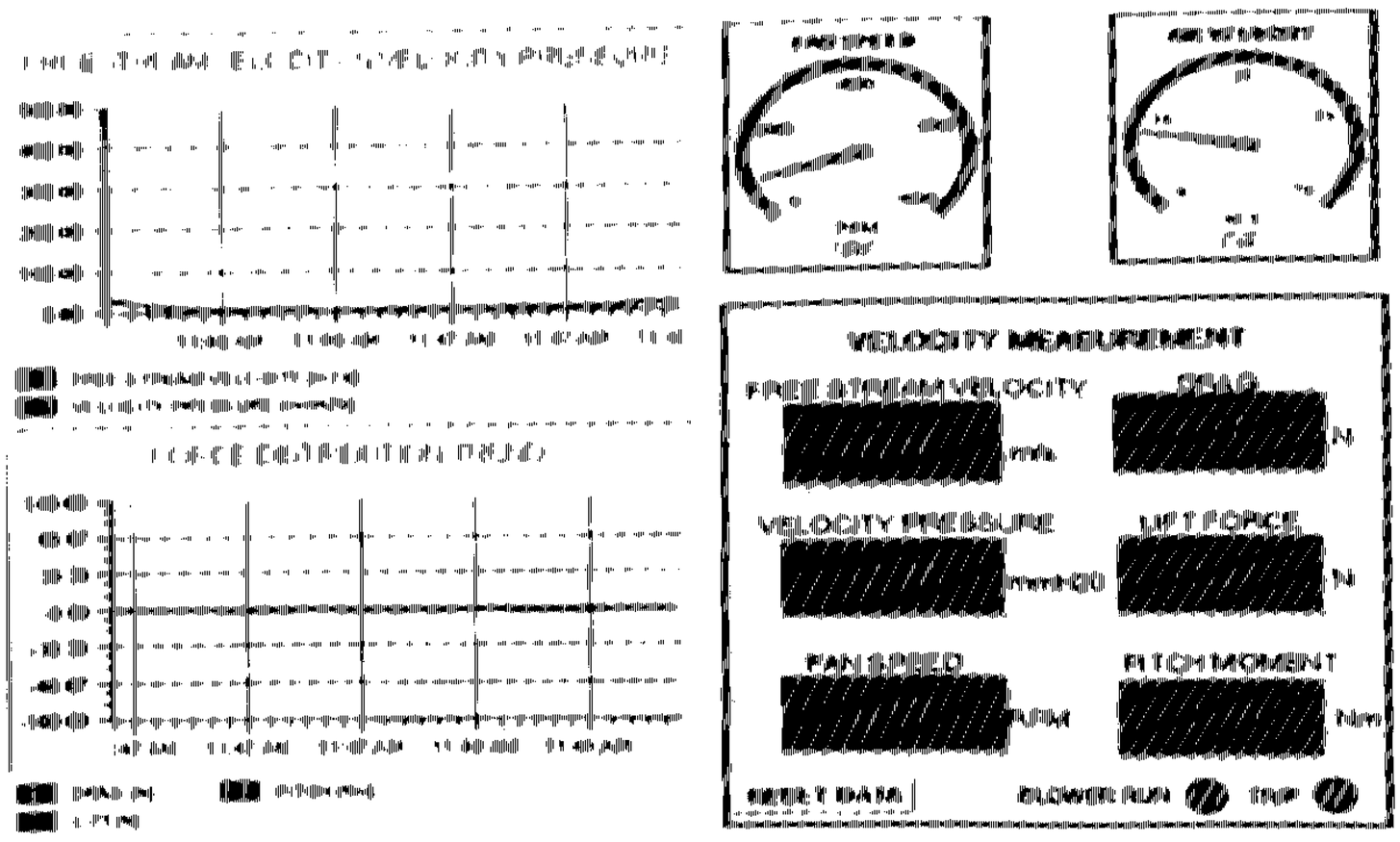
VELOCITY MEASUREMENT
FREE STREAM VELOCITY
DRAG
VELOCITY PROFILE
LIFT FORCE
FAN SPEED
PITCH MOMENT
MAIN CONTROL VELOCITY STATIC PT

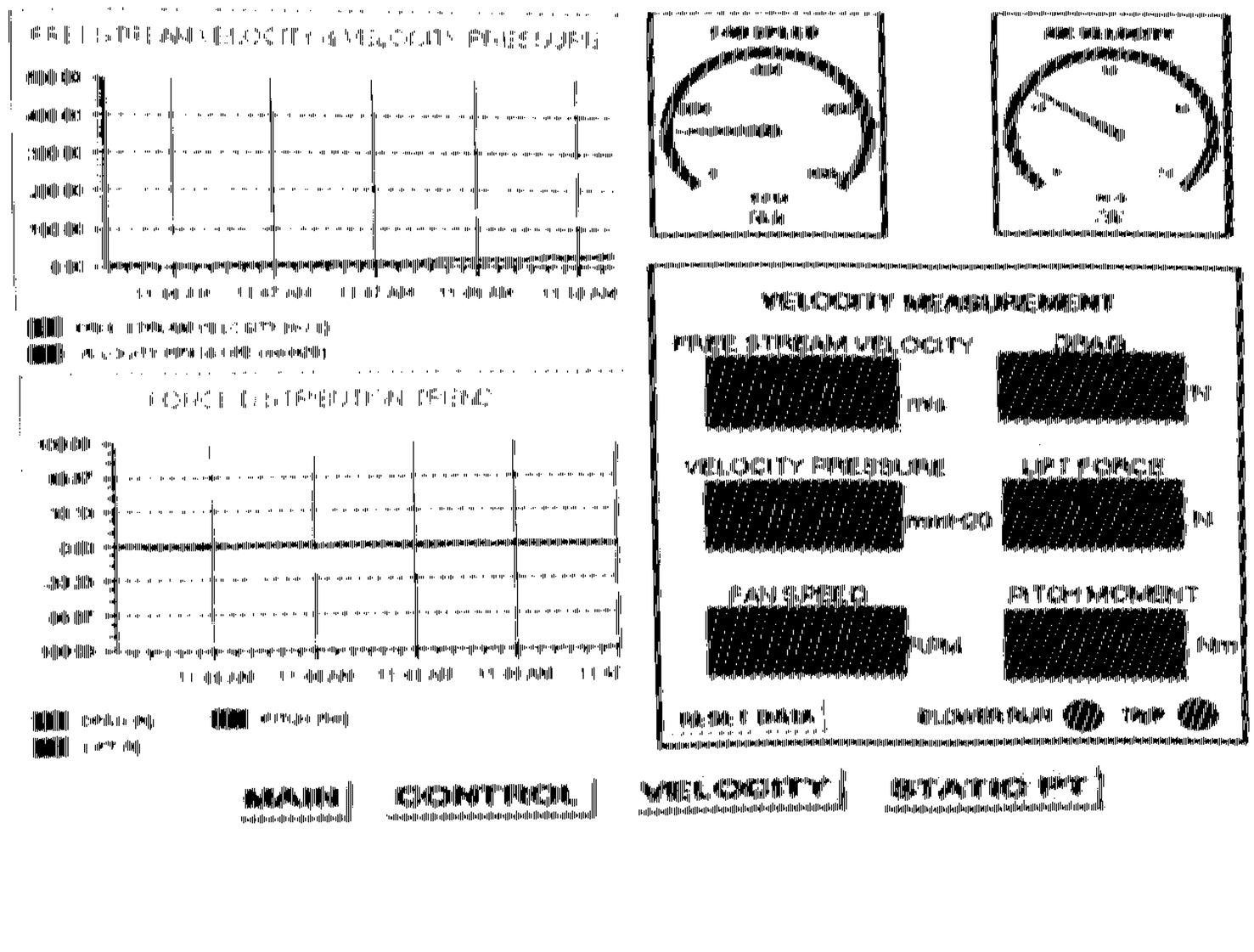
VELOCITY MEASUREMENT
FREE STREAM VELOCITY
DRAG
VELOCITY PROFILE
LIFT FORCE
FAN SPEED
PITCH MOMENT
MAIN CONTROL VELOCITY STATIC PT

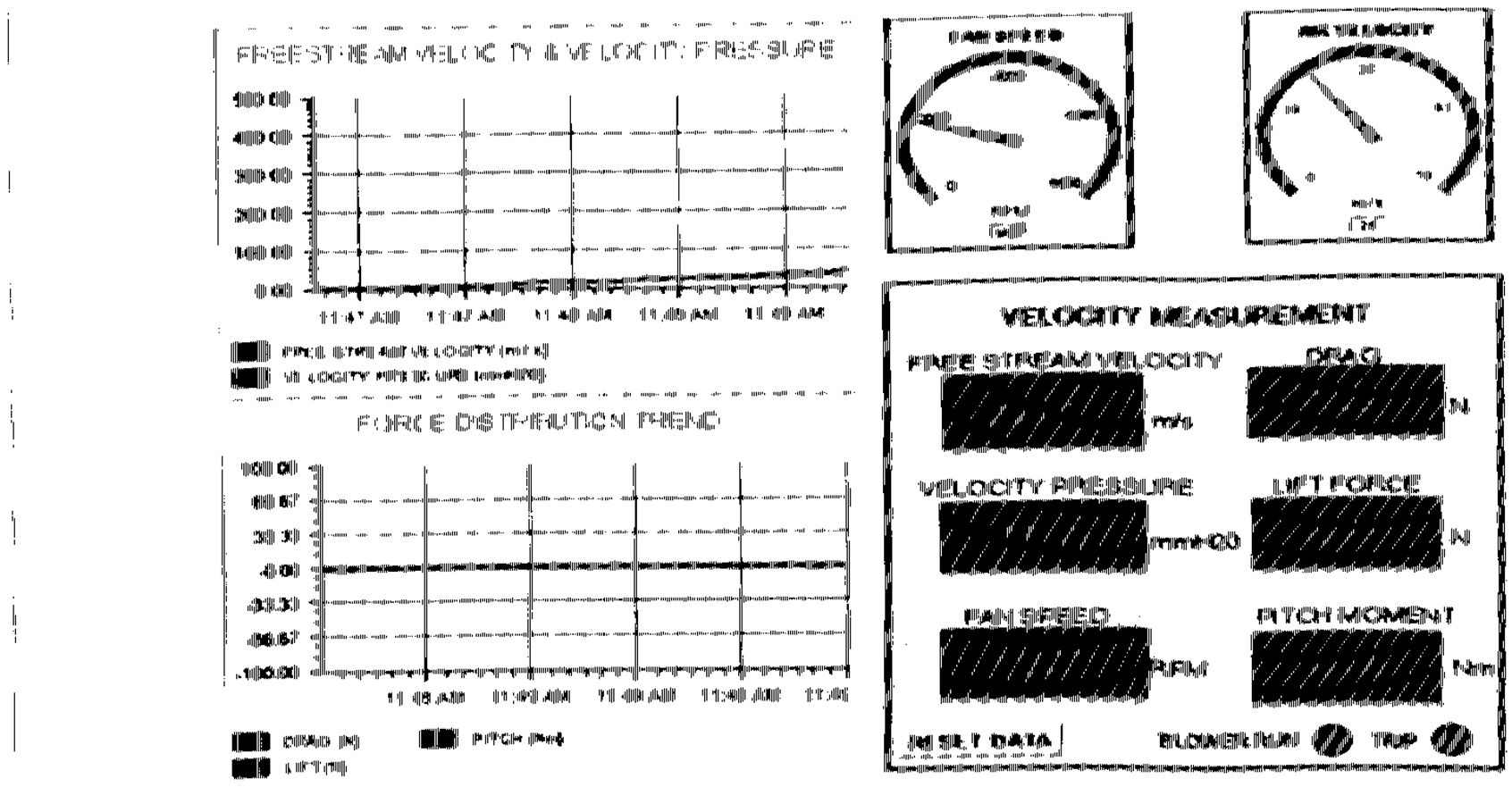
Wind Tunnel Main - GraphWorX32 by ICONICS
File View Tools Configure Help
FREESTREAM VELOCITY/VELOCITY PRESSURE
FORCE DISTRIBUTION TREND
VELOCITY MEASUREMENT
FREE STREAM VELOCITY
DRAG
VELOCITY PRESSURE
LIFT FORCE
FAN SPEED
PITCH MOMENT
RESET DATA
BLOWER RUN
TRIP
MAIN
CONTROL
VELOCITY
STATIC PT

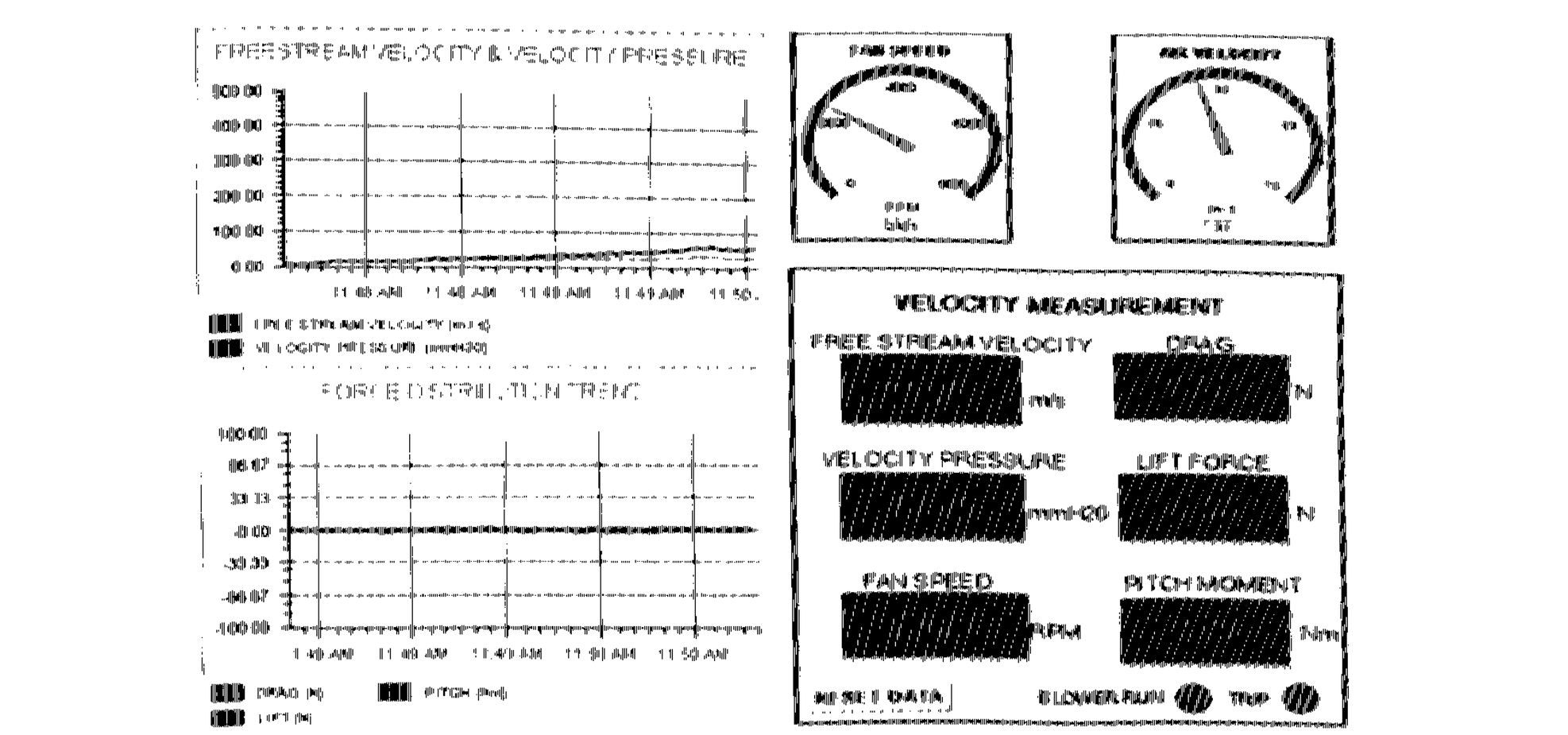
Wind Tunnel Main - GraphWorX32 by ICONICS
File View Tools Configure Help
FREESTREAM VELOCITY/VELOCITY PRESSURE
FORCE DISTRIBUTION TREND
VELOCITY MEASUREMENT
FREE STREAM VELOCITY
DRAG
VELOCITY PRESSURE
LIFT FORCE
FAN SPEED
PITCH MOMENT
RESET DATA
BLOWER RUN
TRIP
MAIN
CONTROL
VELOCITY
STATIC PT

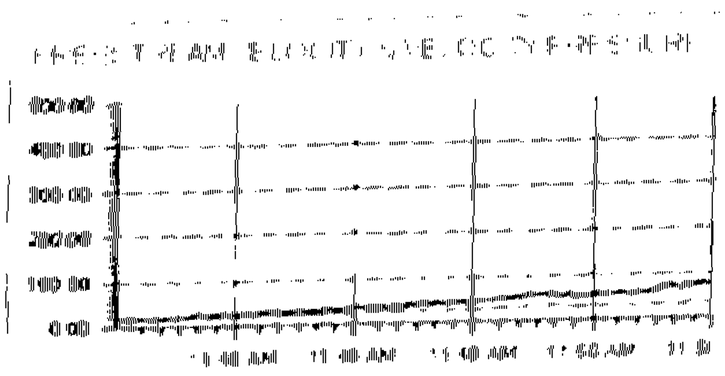

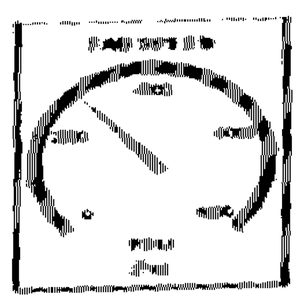

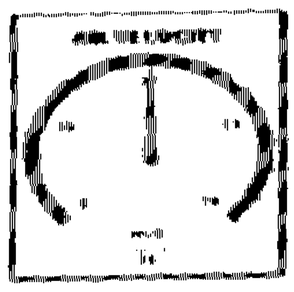

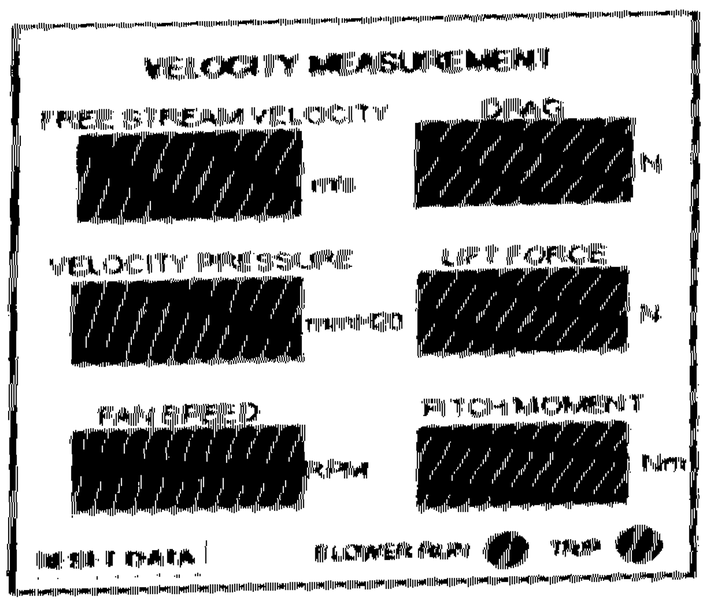
VELOCITY MEASUREMENT
FREE STREAM VELOCITY
m/s
DRAG
N
VELOCITY PRESSURE
mm-H2O
LIFT FORCE
N
FAN SPEED
RPM
PITCH MOMENT
N-m
MOTOR DATA
BLOWER RUN
TRIP